CONFORMAL PROPELLANT TANKS AND VANE DESIGN

by

Robert Beggs

A Thesis

Submitted to the Faculty of Purdue University

In Partial Fulfillment of the Requirements for the degree of

Master of Science in Aeronautics and Astronautics

School of Aeronautics and Astronautics

West Lafayette, Indiana

May 2022

THE PURDUE UNIVERSITY GRADUATE SCHOOL
STATEMENT OF COMMITTEE APPROVAL

Dr. Steven Collicott, Chair

School of Aeronautics and Astronautics

Dr. Stephen Heister

School of Aeronautics and Astronautics

Dr. Timothee Pourpoint

School of Aeronautics and Astronautics

Approved by:

Dr. Gregory Blaisdell

Dedicated to my parents, John and Linda, for their continual support

ACKNOWLEDGMENTS

This research was funded by the grant "Small-Sat Propellant Management Technology" from Flight Opportunity Program of Spaceflight Technology Mission Directorate of NASA (NASA grant numbers: 80NSSC18K1287 and 80NSSC20K1811). This research also features contributions from the Purdue students taking AAE 418: Zero-Gravity Flight Experiment.

Dr. Collicott's assistance and expertise throughout this project has been priceless and very much appreciated. I am very grateful to have had the opportunity to work on this important research project.

TABLE OF CONTENTS

LIST OF TABLES

LIST OF FIGURES

ABSTRACT

Current small satellite propellant tank design is driven by three factors: volume optimization, manufacturing capability, and propellant management. Conformal propellant tanks offer solutions to the design challenges of optimizing satellite volume and manufacturing costs. Conformal propellant tank designs that meet these challenges have unknown effects on propellant management. Compounding this uncertainty is the industry shift towards new green propellants with large contact angles. Improper propellant management can deliver gas to a thruster or leave propellant trapped away from the tank outlet while draining. Both scenarios reduce the lifespan of satellites.

Stamping is one manufacturing process that can produce tanks that optimize volume and are relatively easy to manufacture. The effects of the stamping process on tank shape and propellant management is evaluated through testing four different tank geometries. The stamping process sometimes leaves behind a seam where two sides of a tank are joined together. A total of six tank and vane combinations are tested. One set of traditional tanks serve as a control. Three tanks tested share vane geometry and have different interiors to evaluate the effects of the stamping process on propellant management. The first tank has a smooth interior, the second has a seam at the joints and the third tank has a seam and ridges for increased stiffness. The last two tanks have an interior in the shape of an arc and have different vanes. The experiment is flown on the ZeroG airplane to test the tank and vane designs in a weightless environment.

The experiment consists of a payload rack, eleven experimental pods and one power distribution pod. Each experimental pod is designed to be modular and independent from all other experimental pods. Each experimental pod hosts a camera, electrical box, second containment and fluid system with four tanks.

The results of this study show no discernible difference could be observed between tanks with or without a seam from the stamping process. When ridges are added to a tank that are parallel to the contact line, liquid may not wick into the ridge if it is dry. If the ridge is wet the liquid spreads out on the surface of the tank further. The differences between propellant positioning for zero and nonzero contact angle fluids are discussed.

1. INTRODUCTION

Traditional fuel tanks in large satellites are designed to minimize weight, and are typically in the shape of a cylinder with hemispherical end caps. Current design considerations for small satellite fuel tank design or construction are tank volume optimization, manufacturing capability, and propellant management. Historically weight minimization has been the main driver of propellant tank design. Some designs have moved away from this line of thought in an effort to minimize spacecraft volume. One example is a toroidal propellant tank proposed for the length limited space transportation system [1]. As new small satellites are designed, weight minimization is of less concern. Traditional fuel tank wall thickness and weight do not scale down as much as the overall satellite volume, especially at the sizes small satellites are being produced. Some traditional fuel tanks have reduced weight so much that they are only strong enough to support their weight while pressurized. Small satellite manufacturers are moving to low pressure pump driven propulsion systems because pressurized minimum weight tanks are infeasible at this scale. Creating conformal propellant tanks that optimize the tank and satellite volume is a driving design factor in design for many small satellites.

Another factor in small satellite tank design is manufacturing lead time. For instance, the current fast-paced market does not encourage the use of the traditional extreme minimal-weight tank designs which can require years to manufacture. This lead time is much too long for any satellite manufacturer looking to produce a secondary payload or multiple satellites in a cost effective manner. The stamping process is a method that could reduce manufacturing lead times and produce conformal tanks more economically. Stamping can also be used with a variety of metals including titanium, steel, and aluminum. Throughout the design process shifting from a cheap material for prototyping and creating a final part with a more expensive material could be very attractive in industry. Using the stamping process to produce tanks also offers tank designers options to increase mechanical strength of tanks through the implementation of bends and ridges. Research focused on several tank shapes that could be made by the stamping process and applicable to general satellite design, including blended, stamped, stiffened, and arcs.

Propellant management is another design consideration in fuel tank design. In weightlessness capillary effects dominate liquids behavior, since body effects are no longer present. Capillary effects are driven by surface tension of the liquid. Surface tension of a liquid can be considered the amount of energy per unit area of a liquid. To increase the surface area of the liquid, energy must be added to the liquid. In an environment where there is no external energy source, surface tension will drive the liquid to the minimum energy state and thus minimum surface area. In a void, this behavior results in a spherical drop.

The capillary effects in conformal tanks creates several challenges compared to the traditional smooth walled axisymmetric design. In a rectangular tank, propellant will naturally wick into the corners of the tank to a minimum energy state. If there are several corners in a tank, liquid will generally be held last in the tightest corner during tank depletion. If propellant is trapped away from the tank outlet, the satellite lifespan is effectively reduced and can cause disruptions in orbital maneuvers if gas is delivered to the engine. To combat this, propellant management devices (PMDs) are employed to control the position of the propellant in the tank and ensure gas free flow to the engine [2]. Traditionally propellant management has been accomplished through the use of pressurized bladders that push propellant out of the tank as the fill fraction is decreased. New small satellite propellant tanks are designed to be low pressure, and have increasingly complex geometry so bladders are no longer a viable option. Other types of PMDs are vanes, traps, sumps, sponges, galleries, and screens [2], [3], [4], [5]. According to Jaekle "vane PMDs are the simplest, least costly and most reliable PMDs" for these reasons only vanes are considered for propellant management in this thesis [2]. Vanes manage propellant location in the tank by creating the smallest corner near the outlet of the tank, so the liquid will naturally wick towards the outlet. In lieu of other PMDs, vane design is the limiting factor in propellant flow rate during high acceleration maneuvers and are critical to satellite performance.

Wicking performance is also effected by the contact angle of the liquid. Contact angle is defined as "the angle measured within the liquid between the solid and the tangent to the liquid-gas interface at the three-phase line" and is a result of the liquids surface tension [6]. Contact angle is essentially an external measure of the liquids surface tension. Liquids with a contact angle near zero will wick much easier than liquids with a nonzero contact

angle because they have lower energy per unit area or surface tension. Since surface tension drives the liquid to the minimum energy state, decreasing surface tension allows the liquid to spread across solid surfaces more. Figure 1.1 shows a representation of this phenomenon for different fill fractions in a spherical tank. The red liquid is silicon oil which has a contact angle near zero, and the blue liquid is propylene glycol which has a nonzero contact angle. Since large contact angle liquids like new green propellants do not wick as well as those with a low contact angle keeping the propellant at the outlet is a greater challenge. A traditional propellant tank with silicon oil is used as a control group. Each conformal tank design is evaluated with propylene glycol as a propellant simulant. The position of silicon oil and propylene glycol in an arc tank is compared.

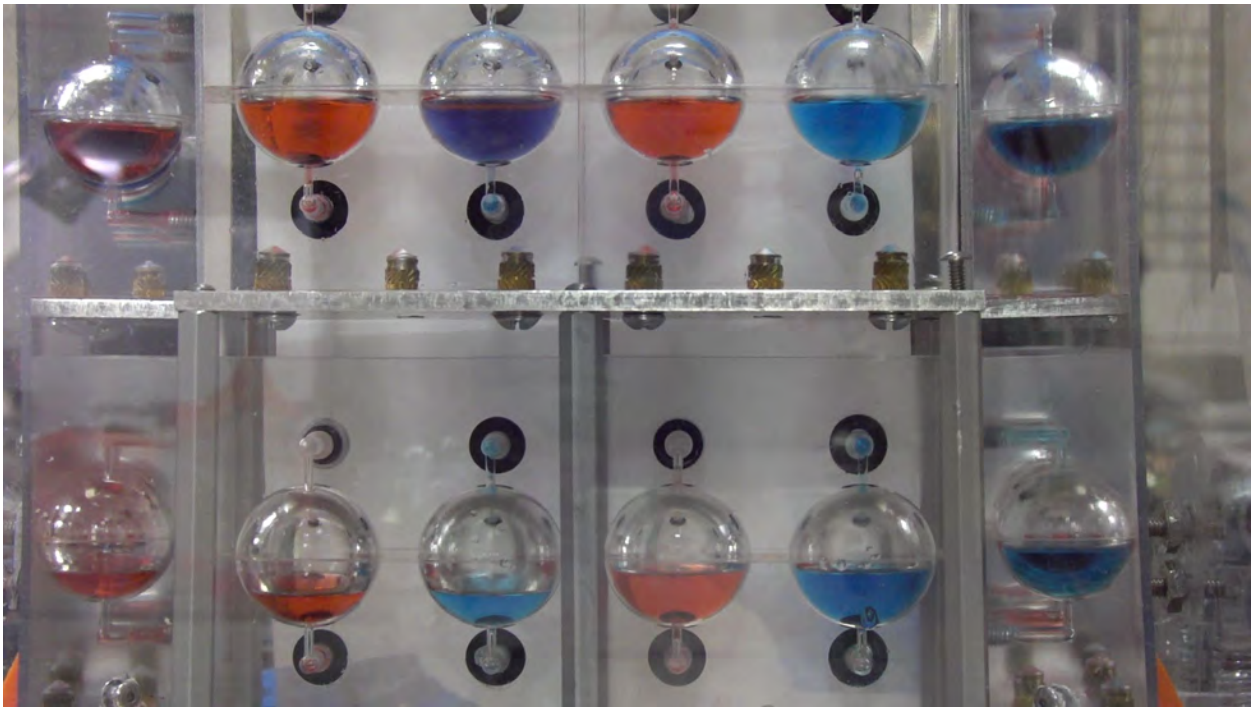

(a) 1G Flight

(b) Weightless Flight

Figure 1.1. Contact Angle and Propellant Wicking

2. CONFORMAL TANKS EXPERIMENT OVERVIEW AND DESIGN

The experiment sits on an an aluminum T-slot frame built with 1500-series parts from the 80-20 company which is referred to as the payload rack. The payload rack measures 53 inches long, 18 inches wide and 39 inches tall, which fits well within the maximum allowable dimensions of 96 inches long, 60 inches wide and 60 inches tall for an experiment on the ZeroG airplane [7]. The experiment is designed to use a half section in the airplane which is approximately 5 ft by 10 ft when researchers are included in the space [8].

Another constraint imposed on the experiment is weight. In the event of an emergency, all experiments must survive 88.38 m/s^2 acceleration in all 6 degrees of freedom on the airplane [7]. The payload rack when loaded weighs 330 lbs. The payload rack is secured to mounting points located on the floor of the aircraft to feet located in each corner of the frame with four 3/8-24 bolts. Figure 2.1 shows the payload racks mounting feet.

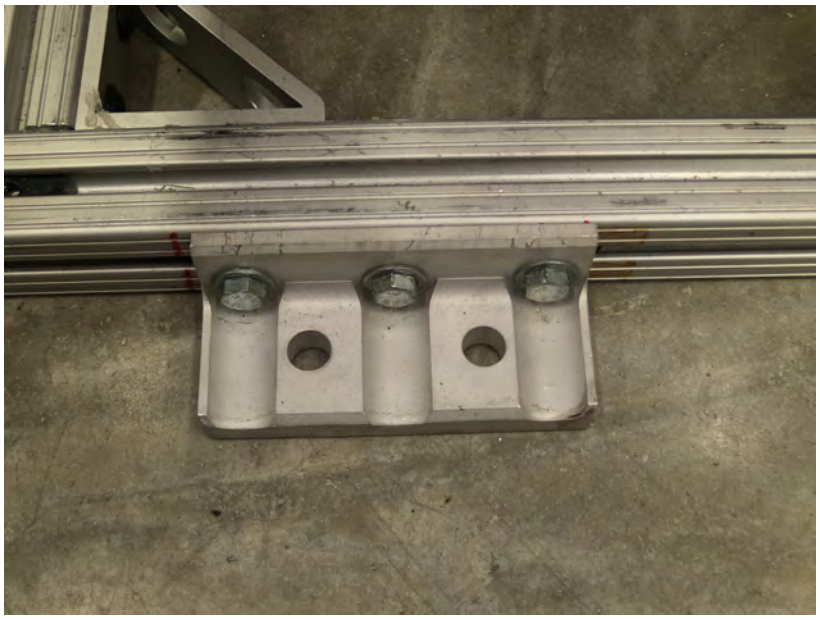

Figure 2.1. Payload Rack Feet

The payload rack is designed to accommodate 12 "pods". A pod is a common framework, plug-n-play structure that holds components required for performing the experiment. A pod may contain power supply components or experimental test component with data collection

equipment as required. This design allows pods to be configured as desired to meet endless experiment requirements. This experiment will use one power distribution pod and 11 experimental pods.

The power distribution pod hosts an AC-DC converter connected to terminal blocks that distribute power to each experimental pod and a power strip that charges cameras in flight. The experimental pods contain an independent electrical system with electrical connectors, camera, and fluid system with one set (two pairs) of tanks. The experimental pods are designed so that they can be assembled and maintained independently of the payload rack. Before a flight, each experimental pod is mounted to the payload rack and tested. Figure 2.2 shows the payload rack installed on the ZeroG airplane.

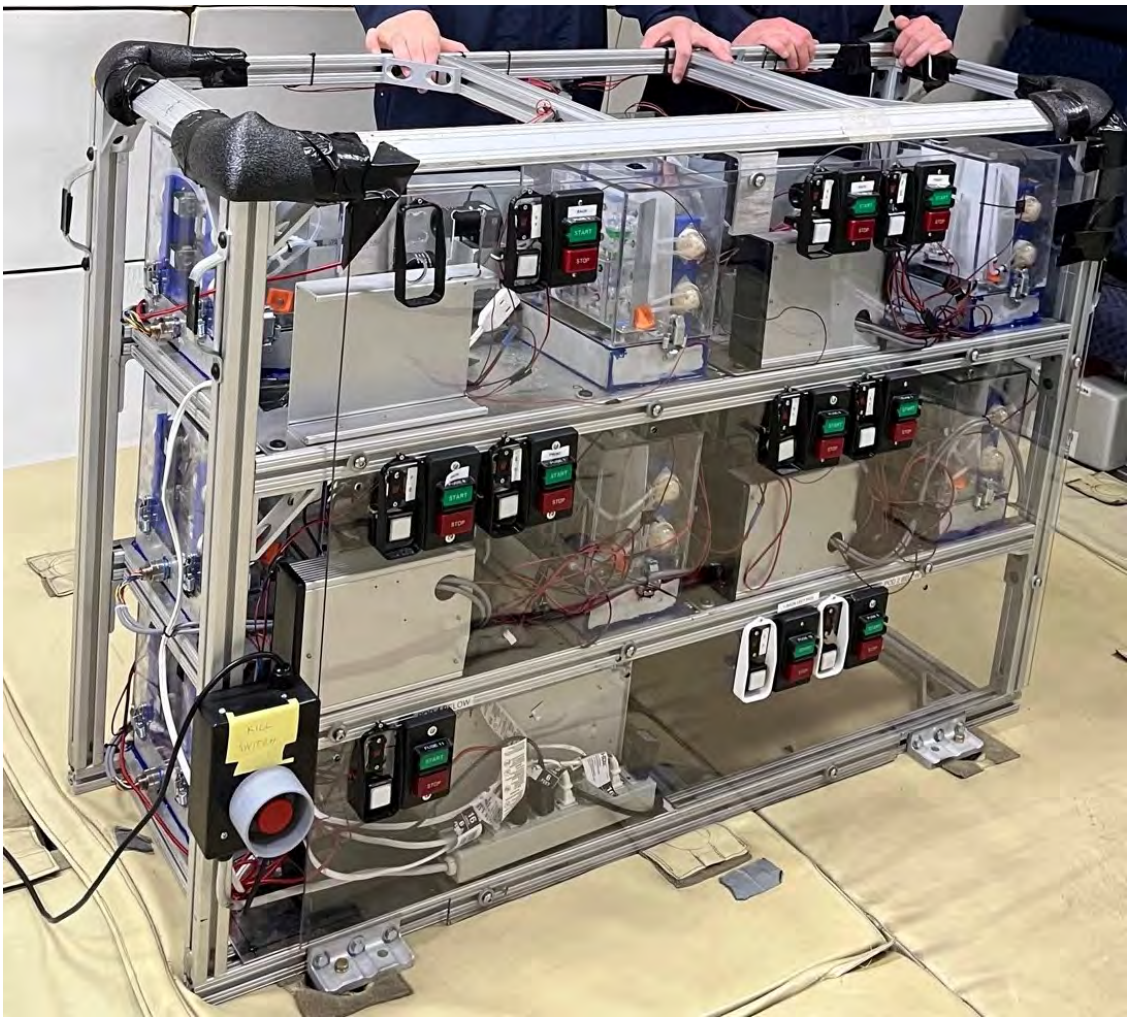

Figure 2.2. Payload Rack Installed in the ZeroG Airplane

The electrical system on each experimental pod includes electrical connectors, a micro controller, LED, four motor speed controllers, and pumps to move liquid through the tanks. Figure 2.3 shows the electrical system of one experimental pod. The fluid system includes media bags, air bags, tanks, and second containment which is used to capture any leaks. There are several tank shapes tested including traditional, blended, stamped, arcs, and stiffened. Each tank offers slightly different vane and interior designs.

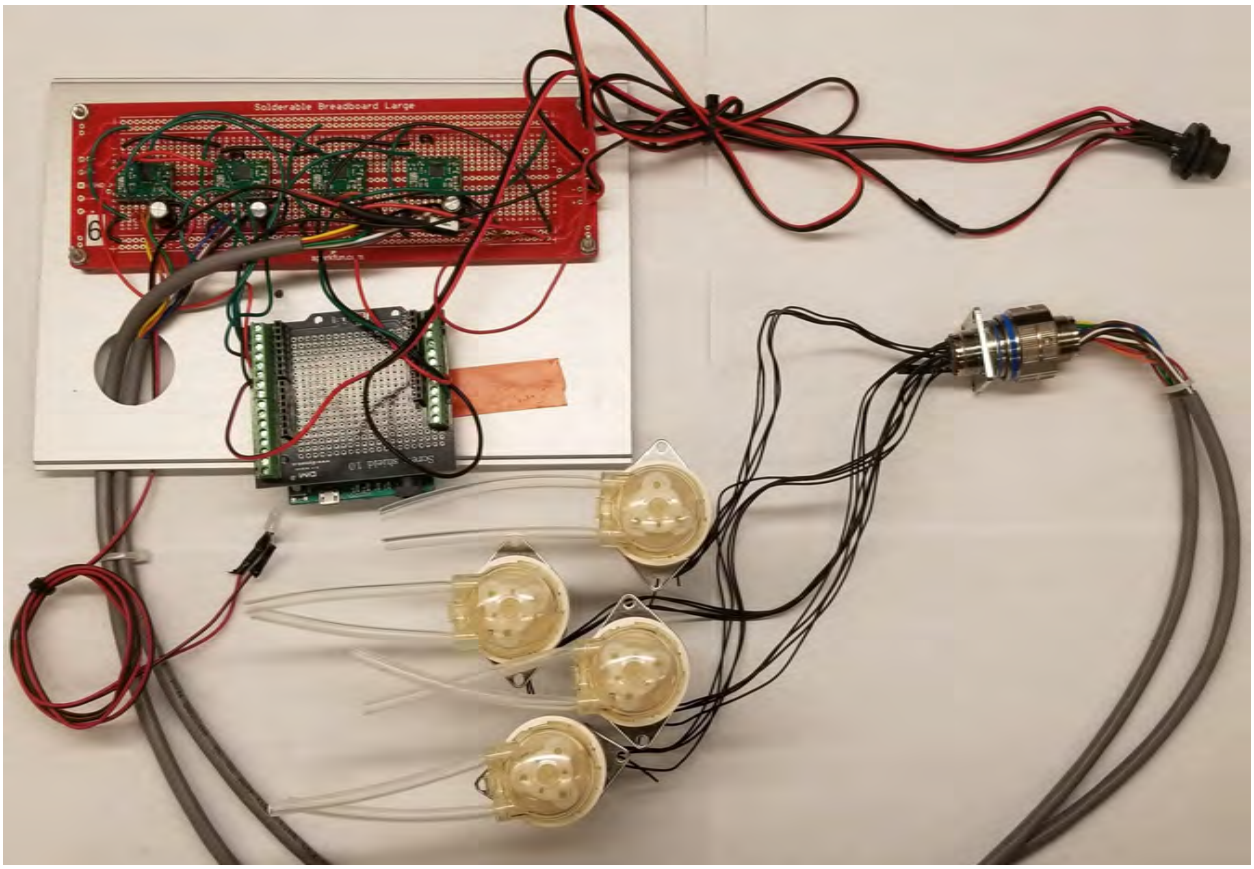

Figure 2.3. Experimental Pod Electrical System

2.1 Experimental Facility

2.1.1 Capabilities

The experiment is conducted on a modified Boeing 727 operated by the ZeroG corporation. The test campaign was accomplished over the course of four flights. Two flights each were done in May and December 2021. During the course of a flight, 25-30 weightless

parabolas are performed. Each weightless parabola lasts 20-25 seconds and over the course of a flight approximately 9 minutes and 30 seconds of weightlessness is experienced. This offers an advantage over drop towers and suborbital rocket flights, because the volume of liquid in the tanks can vary each parabola, and the total time in weightlessness is longer. However, two downsides compared to suborbital flight are the short periods of weightlessness and relatively higher perturbations experienced on the airplane. The short periods of weightlessness do not allow for proper true liquid trapping analysis. After each period of weightlessness the tank settles in 1 G and it is not feasible to drain the whole tank in one parabola. This means that it is impossible to determine whether liquid will get trapped at the top of the tank as it is draining. The perturbations from turbulence during the experiment can also be thought of as a spacecraft pointing maneuver, and thus the performance of the tank design during maneuvers can also be evaluated. Using the ZeroG airplane also offers a larger experimental volume and quantity of experimental cases compared to drop towers and suborbital rocket flights. Researchers are also able to interact with the experiment throughout the flight because of the large internal volume on the airplane. Further more, because of the disparity between cost per flight and volume of uses cases per flight, parabolic flight is more cost effective compared to suborbital flight. Parabolic flight also has much less stringent operational weather requirements, and the time from experiment conception to the flight date is shorter than suborbital flight.

2.1.2 Operations

At the start of the flight approximately 15 minutes is given to the researchers to move into the cabin and prepare the experiments for the subsequent parabolas. During this time, the researchers fill the tanks to approximately 80% full. Previous flights have started with 2 Lunar and 3 Martian gravity parabolas which are not used for data. Once the airplane begins weightless parabolas, the tanks have 5% of their volume drained per parabola. This repeats for 10 parabolas until a 1 to 2 minute break is given at 1 G. At this point, if the tanks are drained, the researchers will once again fill them to 80% full. This process is repeated

through the flight as needed. After the flight the tanks are drained. Table 2.1 also describes this process.

Table 2.1. Experiment Operations

Time	Tank Fill Level Start	Tank Fill Level End	Operation
Pre-Parabola	0%	80%	Fill
10 Parabolas	80%	30%	Drain
1G Break	30%	80%	Fill
Repeat Every 10 Parabolas			
Post Flight	80%	0%	Drain

2.2 Mechanical and Fluid System

2.2.1 Mechanical Components

The payload rack has space for 12 trapezoidal pods measuring 24 inches in length, 6 inches and 12 inches wide at opposite ends. Each pod is designed so that they can be removed from the payload rack by taking out four short 5/16-18 bolts and an electrical connector. This allows for assembly of each pod to take place outside of the payload rack and building the pods becomes a non factor in experiment assembly. On each pod is a set of four tanks, four pumps, two media bags, two air bags, two tank plates, a back plate, an electrical box, and a camera mount. To catch any leaks from the fluid system which acts as first containment, second containment surrounds the fluid system. Figure 2.4 shows an assembled experimental pod.

Figure 2.4. Experimental Pod Setup for the Experiment

Second Containment

Second containment is constructed of a transparent polycarbonate box and a two inch aluminum U channel base. The bottom base is made out of four aluminum U channel pieces: a front, left, right, and back side. The front piece is cut down on the top side to 5/8 of an inch to increase the area available to reach into the base. The left and right sides are machined to fit into the front and back pieces. The sides of the base also have tapped holes in them to mount the tank plates and back plate. The back piece is cut to length and has holes to mount stands for the pumps. The back plate also has a 22 pin electrical connector mounted to it. The connector is used to pass power from the electrical box to the pumps in a waterproof manner. A heavy duty absorbent pad is placed into the bottom of the base

to collect any leaked liquid during periods of 1 G. Weatherstripping gasket material is laid down along the outside perimeter of the base to provide a seal with the polycarbonate lid. There are also latch strike plates mounted to the side and back pieces of the base. Between all mounting holes and joints in the base, silicon sealant is used to fill any cracks and keep second containment watertight. Figure 2.5 shows the pod base, with the front side being at the bottom of the image.

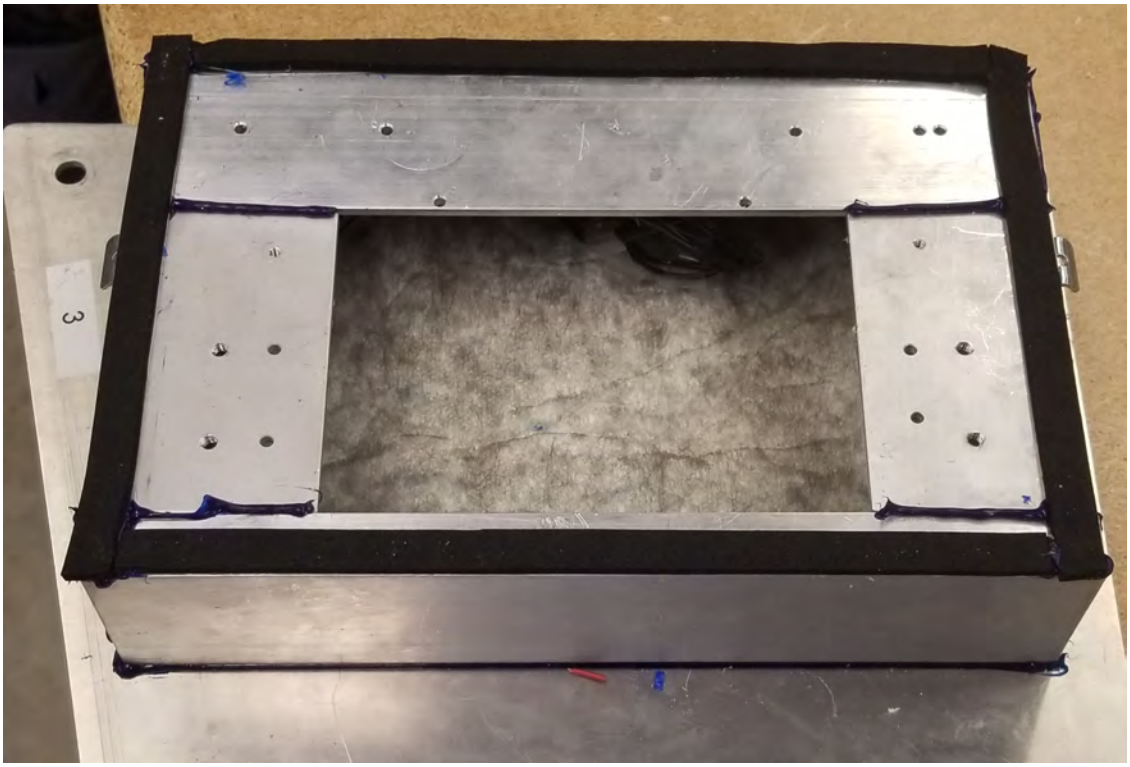

Figure 2.5. Pod Base with Absorbent Pad

The lid of second containment is made from a 3/16 inch thick polycarbonate sheet bonded with methylacrylate solvent to hold the joints together. The overall dimensions are 9 inches wide by 6 inches deep by 7 & 3/4 inches tall. Corresponding latches were added to the sides and back of the lid to secure it to the base. Latches were not put on the front face of second containment so the view of tanks would not be obscured.

Inside of second containment the tanks are mounted to aluminum plates. An upper and lower plate hold two tanks each, to see into the side of the tanks mirrors are pointed at the tank sides. The lower tank plate sits on top of four 5/8 inch hex stand offs that are

fastened to the base. Each lower tank plate has mounting holes cut out for the tanks, mirror mounts and threaded holes for 3 inch long hex stand offs fastened to the upper tank plate. Behind the tanks is a back plate spray painted white to add a flat background and minimize distractions in the data. Figure 2.6 shows the tank plates, hex stand offs, mirrors, tanks, and back plate in second containment.

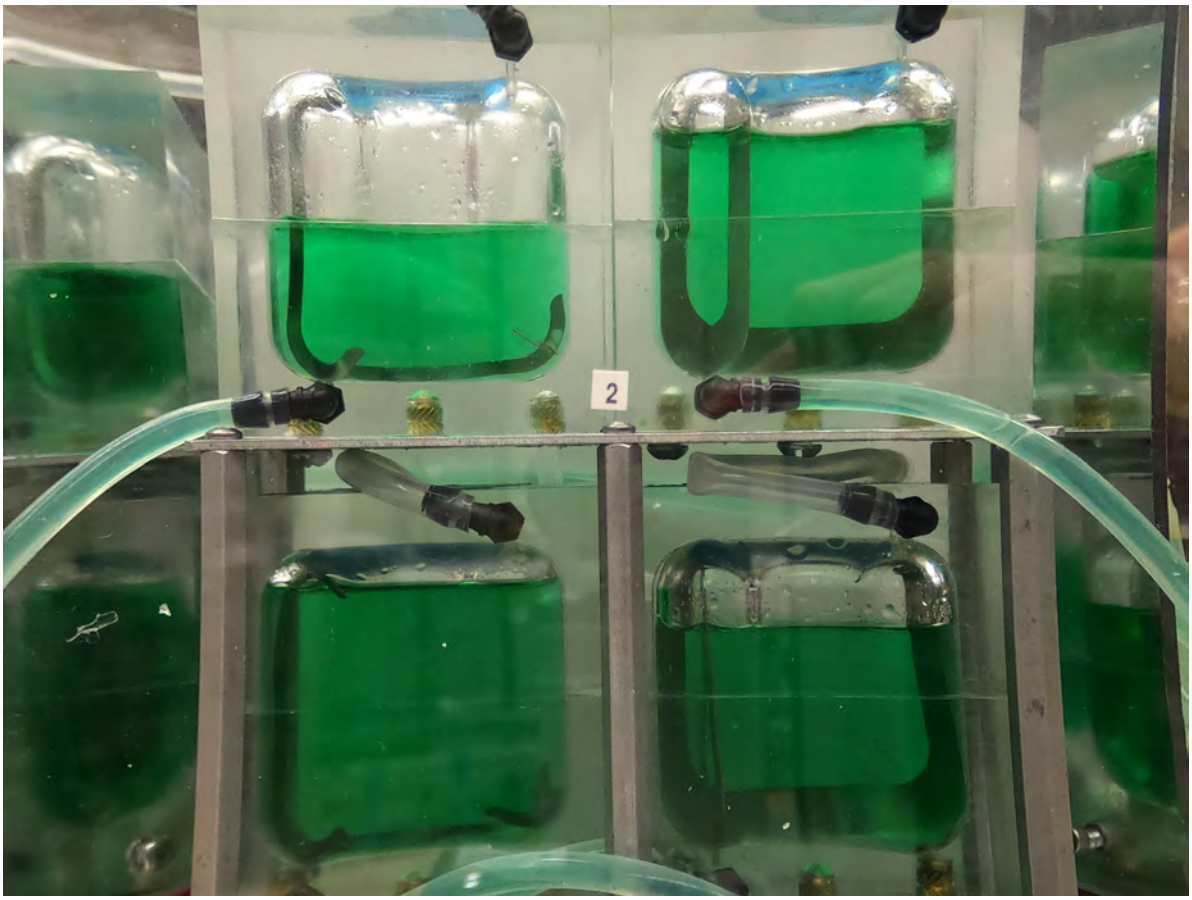

Figure 2.6. Camera View of Tanks

Behind the back plate are 3D printed pump stands. The pump stands allow for all the pumps inlet and outlet tubes to be between the back plate and sides of the lid which helps to minimize kinks in the tubing. Figure 2.7 shows the pump mounts and the pods tubing.

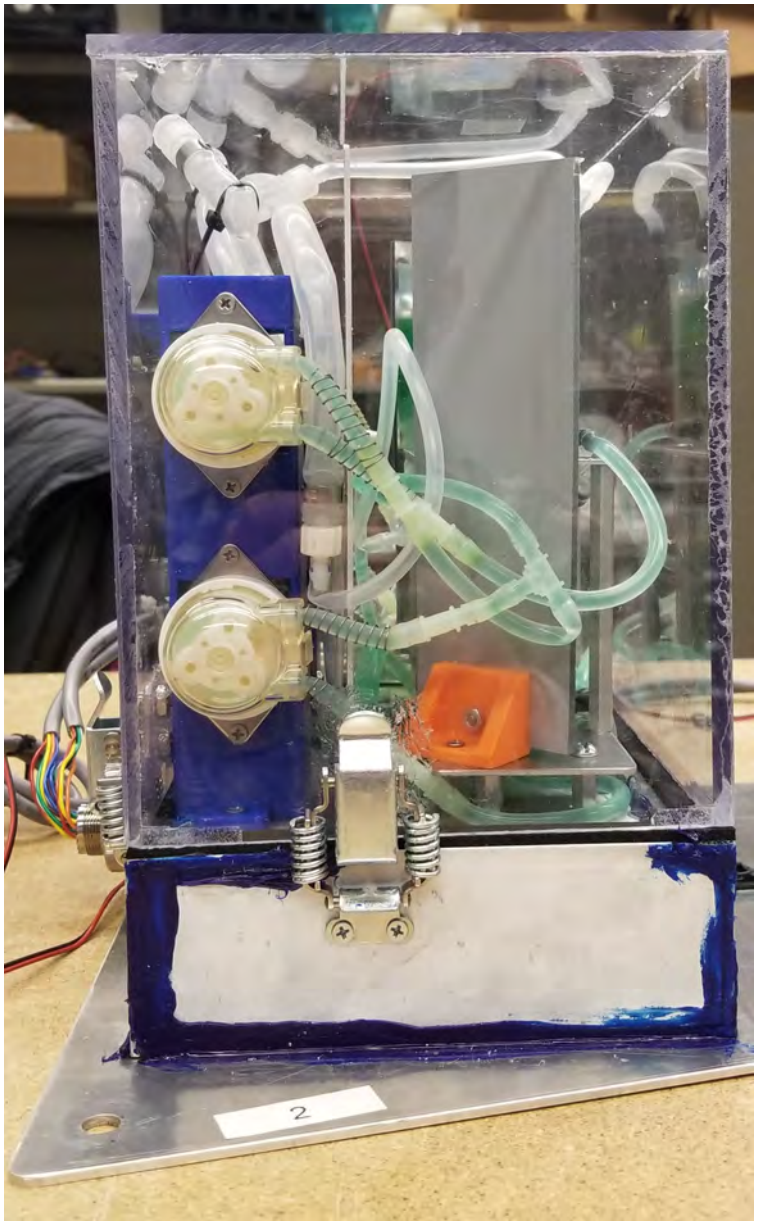

Figure 2.7. Second Containment Side View

In the base of second containment, two media bags are stored with their fill ports tucked between the lower tank plate and second containment base. Two air bags are tucked behind the back plate near the pumps. Figure 2.8 shows the air bags and 22 pin electrical connector for the pod.

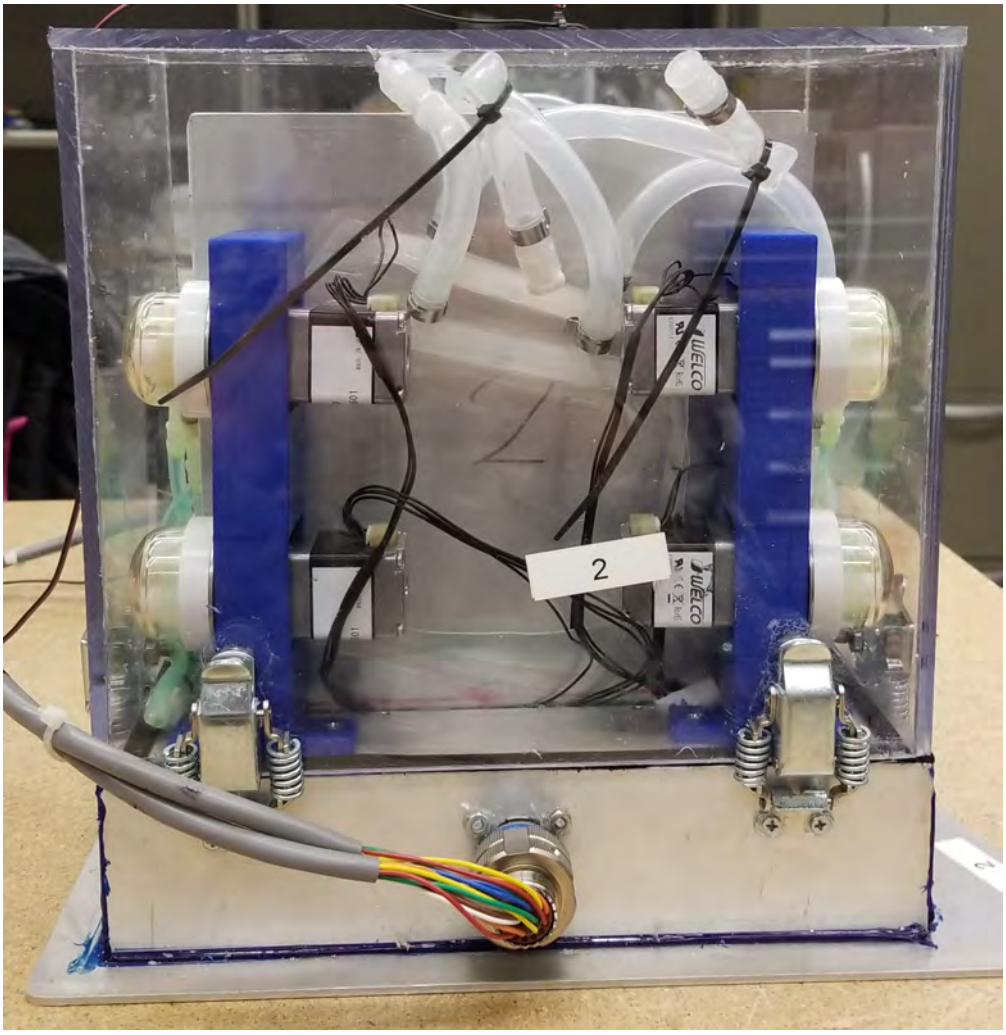

Figure 2.8. Second Containment Back View

Experimental Pod Electrical Box

The electrical box has a shell in the shape of a U, with the open side of the U being a panel that can slide in and out. On the ends of the shell and panel are two plastic side pieces that screw onto the side. The electrical box is mounted on its side in line with the camera so it is not in the field of view of the tanks. This also allows for the panel to be easily taken off the pod by removing the screws on the side pieces. On the side piece closest to second containment the electrical systems power and human interactive controls are passed through an eight pin electrical connector. On the panel a 1.5 inch diameter hole allows for the wires powering the pumps to reach the 22 pin connector on the back of second containment.

The front side panel has a notch cut out so the pump wires don't get pinched between the polycarbonate switch panel and the electrical box when mounted on the payload rack. The bread board is mounted to the panel so each electrical system can be worked on separate from each pod. Figure 2.9 shows the electrical box with the side piece removed.

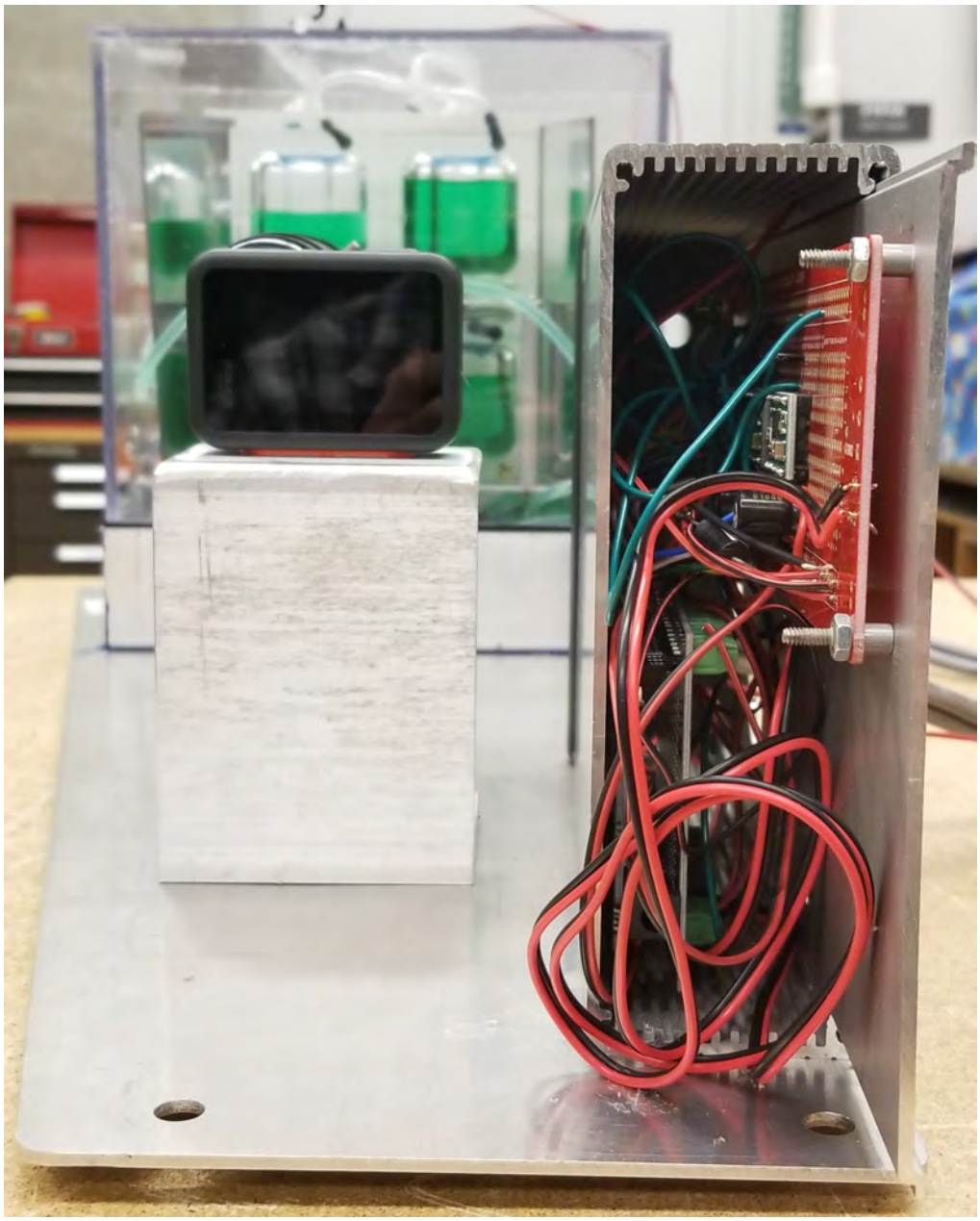

(a)

Figure 2.9. Electrical Box With Side Plate Removed

Figure 2.9. continued

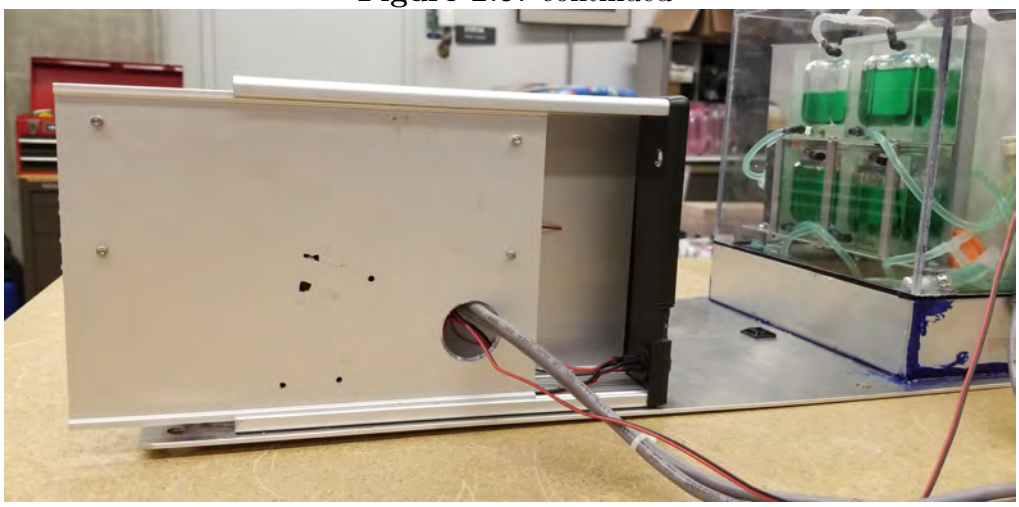

(b)

2.2.2 Tank Design

There are five different tank geometries that are of interest to this thesis. Those being traditional, blended, stamped, stiffened, and arcs. The traditional tank is used as a control case. The blended, stamped, and stiffened tanks share the same vane design. The arc tanks have the same tank shape, but different vanes. The traditional, blended, and arc tanks are made from two halves with a horizontal seam bonded together with methylacrylate. The stiffened and stamped tanks are made from two halves with a bonded vertical seam. The tank outlet is not between the two halves of the stamped and stiffened tanks, the outlet is offset to one half. The outlet for the blended tank is in the same location as the stamped and stiffened tanks so comparisons among the three can be made. All vanes are made from 0.01 inch thick stainless steel sheet. The vanes were laser cut with slots at their intersections for assembly. Section A has images of the vanes before they are assembled.

The traditional tank is like the shape described previously with a cylindrical body and hemispherical end caps. The vanes for this design are two symmetric vanes that go from the bottom to the top of the tank with a hole cut out in the middle that intersect orthogonally. The outlet of the tank is beneath the point the two vanes intersect, in the center of the tank. Each section seen in figure 2.10 is independent from each other and should be considered

one tank. Since the width of each tank is small two tanks can be fit into a single block of acrylic that for example one blended tank is made from. This design allows for increased test cases without impacting overall experiment volume or material cost.

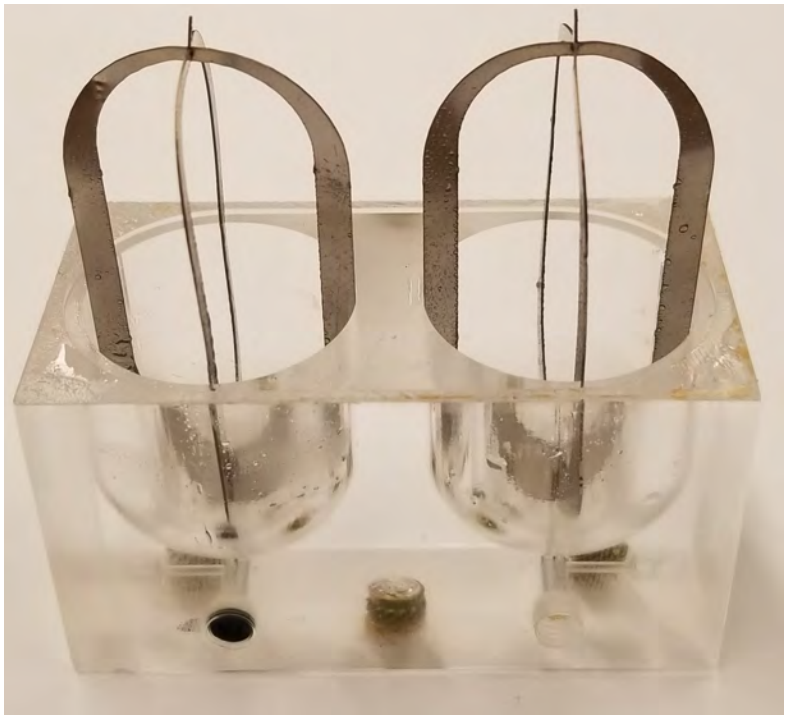

(a) Traditional Tank Front View

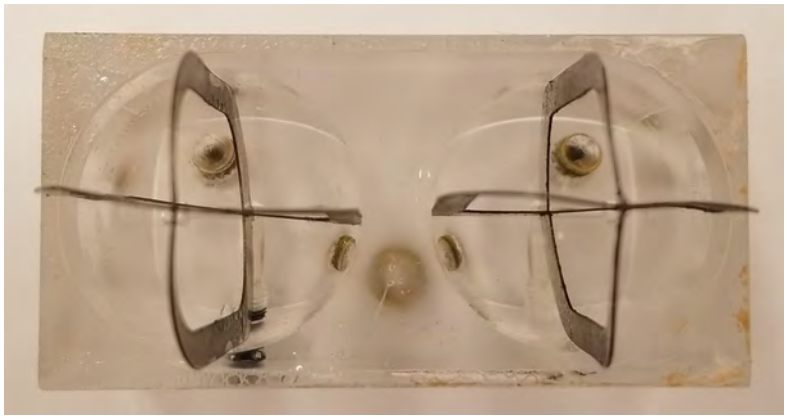

(b) Traditional Tank Top View

Figure 2.10. Traditional Tank Configuration

The blended tank shape is similar to the design of a typical propellant tank used in large satellites with a cylindrical body and hemispherical end caps. Except, the blended tank is stretched in the radial direction. The blended tank is a rectangular prism with fillets on all

edges that are the same radius as the depth of the tank. The blended tanks have a lateral vane along the perimeter of the tank, and connected to the lateral vane are two radial vanes that stretch out from the outlet of the tank. The lateral vane is offset so it goes directly over the tank outlet. Both the radial and lateral vanes get narrower as they move away from the tank outlet. Figure 2.16 shows the bottom half of the blended tank design and the vanes. Figure 2.12 shows a close up of the vanes. The top half of the tank interior is symmetric to the bottom half of the tank interior. In each figure of this section the outlet of the tank is in the bottom left corner. The blended, stamped, and stiffened tanks interior measure 2 inches wide, 1 inch deep and 2 inches tall. Every interior edge has a .5 inch radius fillet. Drawings of each tank design can be found in section B of the appendix.

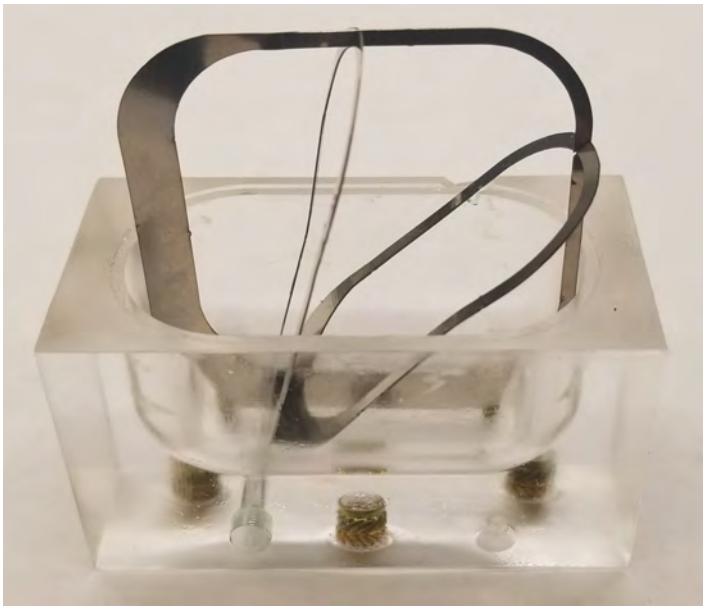

(a) Blended Tank Front View

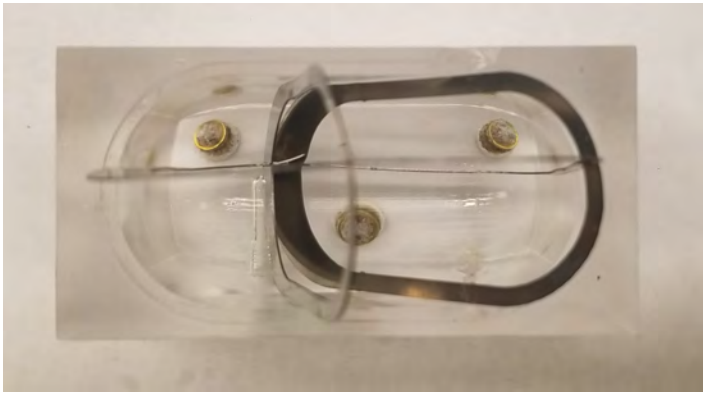

(b) Blended Tank Top View

Figure 2.11. Blended Tank Design

Figure 2.12. Blended, Stamped, and Stiffened Tank Vanes

The stamped tank takes on the same general shape as the blended version but has a small lip modeled as a rounded-off edge measuring .05 inches radially where the two tank halves come together. Figure 2.13 shows the stamped tank cross section.

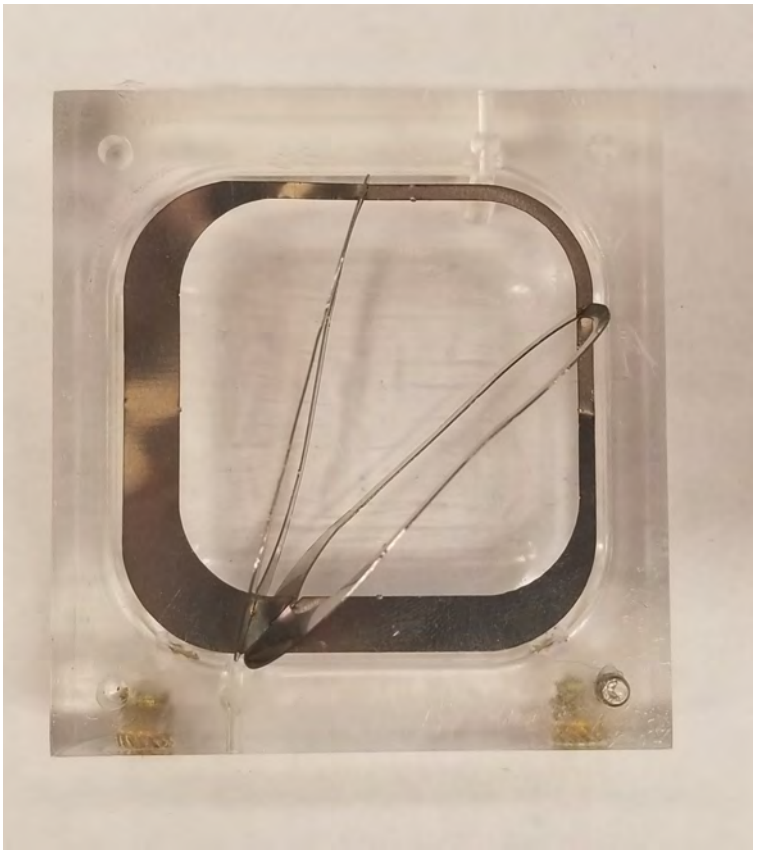

Figure 2.13. Stamped Tank Cross Section

This tank is designed to model a smooth walled tank that is made through the stamping process. To create a mating surface for the two halves each half of the tank is individually stamped with a flange on the exterior. Bending the flange to the exterior is what results in the rounded-off edge on the interior of the tank. In assembly the flange of one halve is bent around the other to provide a seal. Figure 2.14 shows a blown up image of the rounded-off edge on the interior of the tank and the bent flange from tank assembly.

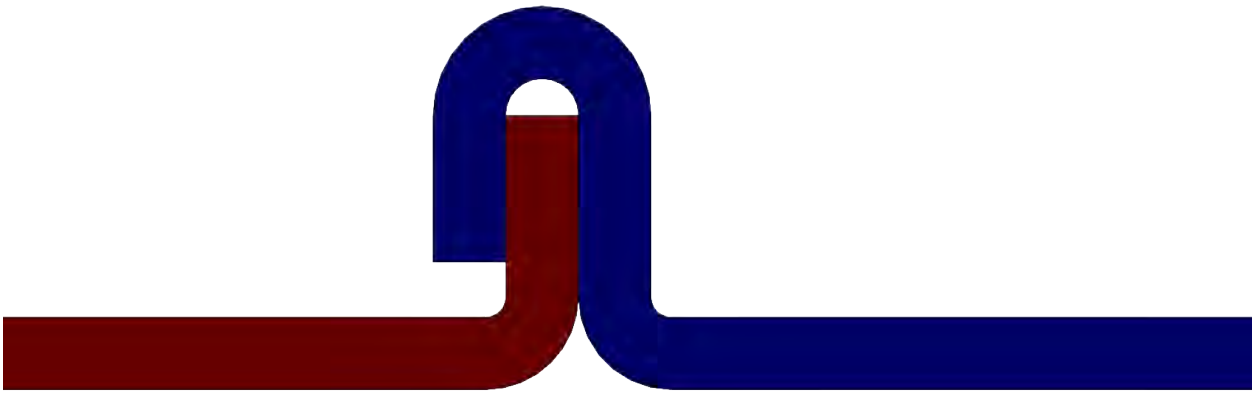

Figure 2.14. Detailed View of Stamped Tank Assembly, the Tank Interior is Below the Colored Pieces

The stiffened tank is another variation of the blended tank. This tank has the same small lip included like the stamped tank, but it also has five ridges on the flat tank faces. Each ridge measures 1 inch long, .029 inches deep and 3/32 of an inch wide with a 3/32 inch diameter fillet at the ends. This tank is designed to model a tank made through the stamped machining process with ridges added for increased mechanical stiffness. Figure 2.15 shows the stiffened tank cross section.

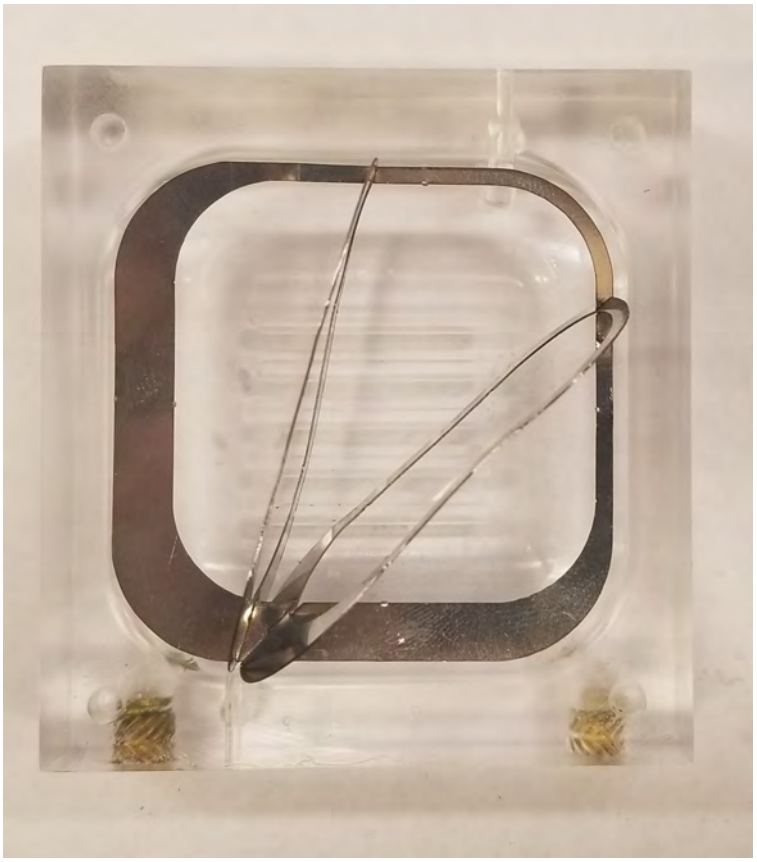

Figure 2.15. Stiffened Tank Cross Section

The arc tanks are again similar to the blended tanks, except they are "bent" along the flat face of the tanks in the vertical direction. These tanks are designed to behave like a tank wrapped around some other member of the satellite structure, in an effort to optimize satellite volume. There are two different vane configurations for the arc tanks. One version, referred to as V1 has vanes in the filleted section, or perimeter of the tank along the top, bottom and sides similar to the tanks discussed above. This version has a vertical vane in line with the outlet connecting the top and bottom of the tank, and this puts the tightest corner above the outlet of the tank at low fill fractions. Another version, referred to as V2 has vanes along the filleted section with an x at a termination point on the lateral vane in the the bottom corner away from the outlet, an x at a termination point at the top of the tank above the outlet and another x in the corner directly above the outlet. The x at the termination point away from the outlet is elevated slightly higher than the x directly above

the tank outlet, so they should not conflict at low fill fractions. The V2 vane design weighs less than the V1 design, but manufacturing this design would be more complicated.

(a) Arcs Front View, V1 Left & V2 Right

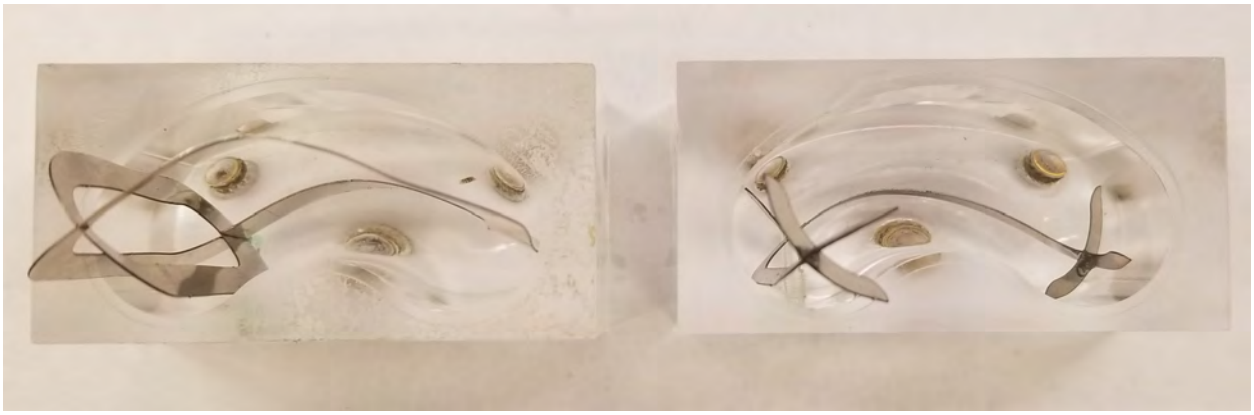

(b) Arcs Top View, V1 Left & V2 Right

Figure 2.16. Arc Tank Configurations

2.2.3 Fluid System

Each pod has a dedicated fluid system. Using one fluid system per pod allows for easy removal from the payload rack, and simplifies second containment design and testing of liquids with different contact angles. Each pod contains four 50 ml biological processing bags, four EA Series peristaltic pumps from Welco, four tanks, and 1/8 inch ID tubing

between all components. Two of the bio processing bags are used to hold the liquid media, and the other two serve as air bags. To prepare the experiment 50 ml of liquid media is injected into the media bags through the fill port. Then the pumps are run to fill the tanks completely with the bleed port open. Next the fill port is closed and a syringe is used to remove any excess air from the air bag through the bleed port. Then a valve on the bleed port between the syringe and air bag is closed so no air can get back into the system. The tanks are then drained before loading the experiment onto the airplane. To run the pumps we use a push button and to control the direction the pumps spin, we use a switch connected to the electrical system. Figure 2.17 shows a diagram of the liquid system of a single pod.

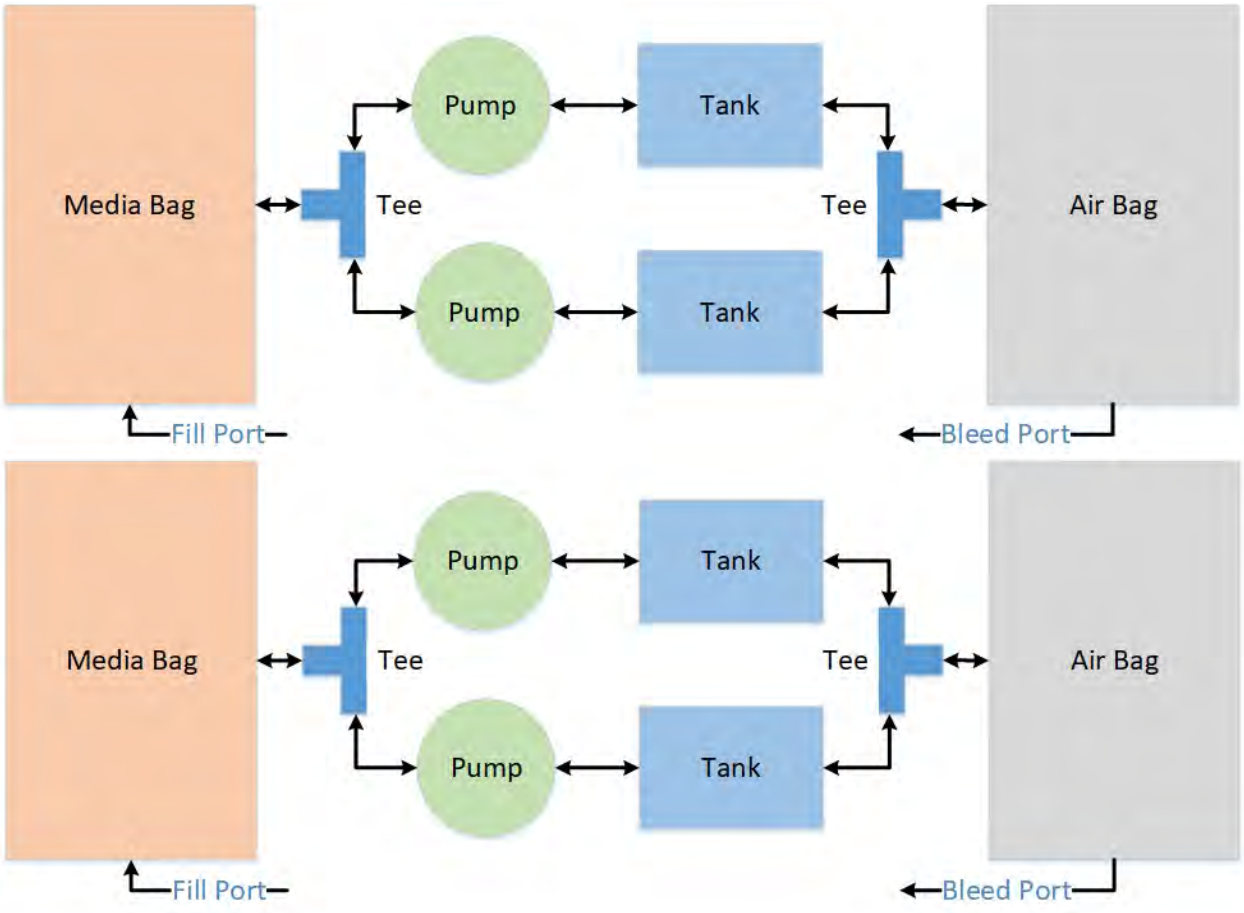

Figure 2.17. Pod Liquid System

Analogues of propellants are used in this experiment for safety and environmental considerations. Silicon oil is a well known liquid with 0° contact angle making it exceptional at

wicking and has minimum adverse health effects. Silicon oil is an analog to hydrazine and cryogenic propellants. To model propellants with a non-zero contact angle propylene glycol is used. Propellants with a non zero contact angle include hydrogen peroxide and other new green propellants. During the experiment silicon oil was dyed red, and propylene glycol was dyed blue or green.

2.3 Electrical System

The electrical system consists of the pumping components, cameras, and human interface. The airplane provides 115 Volt alternating current electrical power to the payload rack through a Nema 5-20R receptacle [7]. To cut off all power to the experiment, there is an emergency stop switch mounted on the front of the payload rack. The emergency stop also splits the electrical system into the camera circuit and pump system circuit through a double pole single throw connection. Each pumping system of the pod is powered through an alternating current to direct current converter that reduces 115 Volts to 12 Volts. The cameras are charged directly by a 115 V alternating current power strip during flight. To control each pod on the front of the payload rack, there is a switch to energize the electrical system, a push button to run the pumps and a sliding switch to control the direction the pumps rotate.

2.3.1 Experimental Pod Electrical System

This experiment will be powered through a Nema 5-20R connector to the 115 Volt single phase power supply [7]. The current limit on each connector is 20 Amps, which is well above the experiments current draw of 4 Amps [7]. Two terminal blocks are used to connect the positive and neutral connections on the AC to DC converter to each pod. For sake of brevity, the wiring of only one pod will be discussed. The positively charged terminal block is wired to a 2 amp automotive fuse and a power switch. The other terminal of the switch is wired to an eight-pin connector. The ground terminal block is wired directly to the eight pin connector. This side of the eight pin connector is also wired to the pump push button and direction switch. Dividing the pods electrical system this way allows for the switches

to be mounted to the payload rack, and pods are easily swapped out once the connector is undone from the pod.

On the male side of the connector, power is distributed to a Large SparkFun Solder-able Breadboard. To control the pumps, a button and switch are wired through the eight-pin connector to an Arduino Leonardo which measures a voltage change across digital pins and the ground pin to start the pumps and switch their direction. The breadboard power is distributed to four Polulu A4988 stepper motor drivers through four 100 μF capacitors, which together run four pumps. An LED is also connected to the positive and negative sides of the bread board through a Dyna Ohm 4006-20 constant current resistor to provide extra light for filming on the lower levels of the payload rack. The bread board also provides power to the Arduino Leonardo through the Vin pin.

The Arduino provides power to the Polulu A4988 stepper motor drivers logic from the 5 Volt pin. Pin 4 on the Arduino Leonardo provides a signal to the stepper motor drivers that controls what direction the pumps spin. Pins 0 to 3 on the Arduino Leonardo interacts with the stepper motor drivers as well, and controls how fast the pumps run. This setup allows for each pump to run at different speeds. Sections C and D in the appendix have the Arduino Leonardo code and pump flow rate calibration.

From each stepper motor driver four wires are connected to a Amphenol 26FC35PN 22 pin connector, with 16 total positions filled on the connector. This connector serves as a bridge from second containment to the electrical board, and allows for the breadboards and Arduinos to be easily swapped out. The connector mounted to second containment, an Amphenol 20FC35SN type connector is wired directly to the stepper motors that drive the pumps.

Figure 2.18 shows a detailed diagram of the pod electrical system discussed above and table 2.2 provides a key to the labeling. The red wires represent the positive side, and the blue wires represent the neutral side. Black wires are connected to the Arduino and pump controls. Green wires control the pump rotation direction. Orange wires control the stepper motor speed. Pink wires connect the stepper motor drivers and the stepper motors. An electrical schematic can be found in section E.

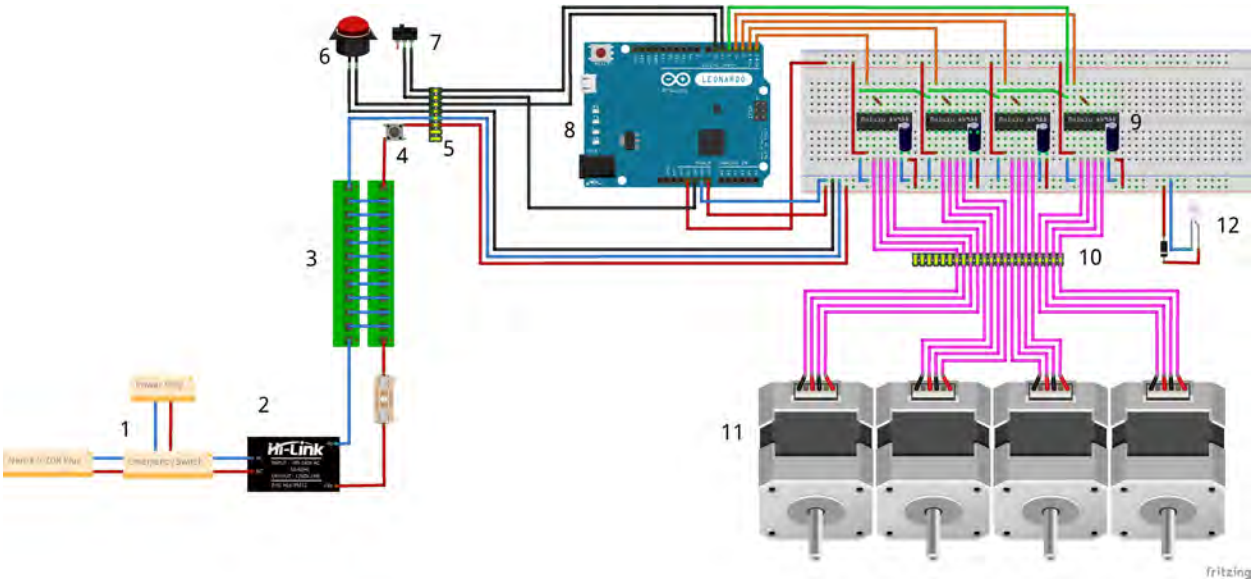

Figure 2.18. Pod Electrical System

Table 2.2. Pod Electrical System Key

Label Number	Item
1	Nema 5-20R Receptacle
2	Ac-DC Converter
3	Terminal Blocks
4	Pod Power Switch
5	8 Pin Connector
6	Pump Run Button
7	Pump Direction Switch
8	Arduino Leonardo
9	Pump Speed Controller
10	22 Pin Connector
11	WPM EA Series Pump
12	LED

2.3.2 Camera System

Each pod has a single camera that faces the corresponding tank arrangement directly. Sony RX0's with a 1 inch, 16 millimeter focal length, F1.4 20MP lens recorded the pods with two tanks or less and Go Pro Hero 8's with a 1/2.3 4.5-10MM 10MP CS lens recorded the rest of the tanks. The limiting orientation for field of view of the cameras is in the vertical

airplane when shooting in landscape. Since the pods with two tanks have 3 inches less vertical space that needs to be recorded matching them with the larger focal length lens that the Sony RX0's used creates the least dead space in the image. Using linear extrapolation a 10.5 mm focal length lens and 1/4 inch tall spacer on the bottom of the current camera mount would optimize the Sony cameras field of view. To save the data 128 gigabyte micro SD cards were used. To hold the cameras in place during the flight, a mount was machined out of four inch tall U channel. On the top of the U channel a slot and a hole were machined to prevent the cameras from turning, and to hold the camera in place during the flight. Each camera was charged during flight from a power strip connected to the emergency switch to minimize battery drainage issues.

Camera Mounts

The camera mounts are machined from a 4 inch tall and 2 inch wide piece of aluminum U channel. On the top of the camera mount the footprint of the camera is machined out, so during the flight the cameras can't turn from side to side. Each camera mount is fastened to the pod base with two 1/4-20 screws and a hole in the bottom so a screwdriver can be used to tighten the camera screws. The edges of the camera mounts were sanded down to prevent cuts from sharp edges during adjustment. Figure 2.19 shows the Go Pro and Sony RX0 Backbone mounts.

(a) Go Pro Mount

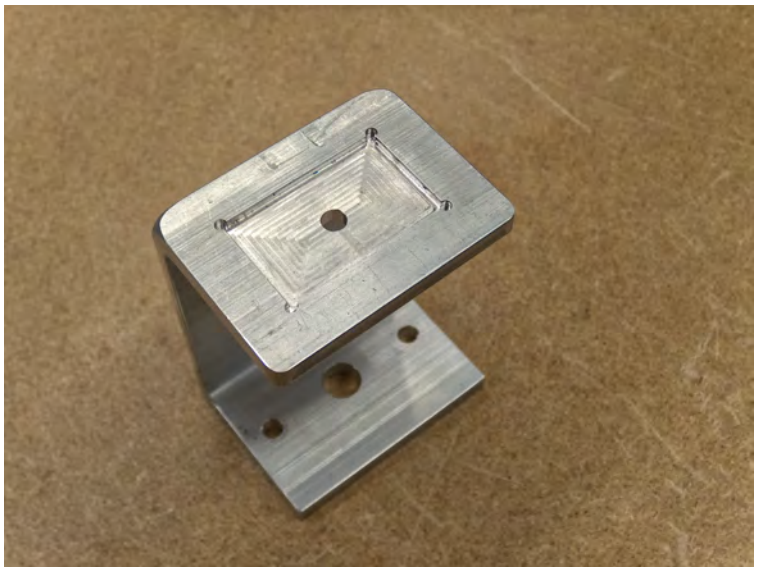

(b) Sony RX0 Backbone Mount

Figure 2.19. Camera Mounts

2.3.3 Human Interface

On one side of the payload rack a 48 inch by 36.5 inch, sheet of 1/8 inch thick transparent polycarbonate has holes cut into it to hold all of the pod controls. Each pod has a separate set of buttons to control power to that specific pod. Each pod also has a push button to run the pumps, and a switch to control which direction that the pumps spin. There is a

3D printed shroud around the button and switch to prevent researchers from accidentally hitting them during flight. Figure 2.20 shows the buttons, switches, and shroud mounted to the polycarbonate on the payload rack. There is also an emergency stop button attached to an 80-20 rail. The emergency stop button cuts all power to the experiment.

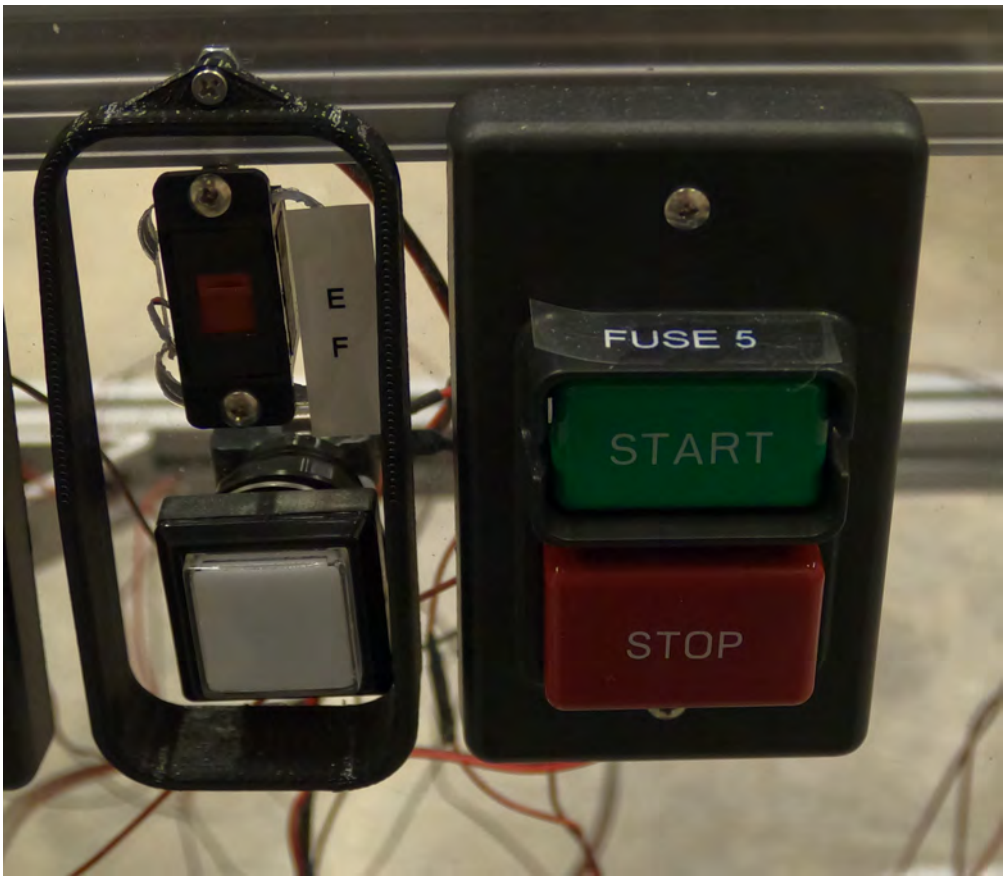

Figure 2.20. Human Interface

3. CONFORMAL TANKS RESULTS

3.1 Experimental Results

Performance of the traditional, blended, stamped, stiffened, and arc tanks with corresponding vane geometries are examined for a range of fill fractions. For each tank design performance of the PMDs at each fill fraction is not possible due to difficulties with leaking tanks, tubing kinking, and bleeding air from the fluid system. In this section a high fill fraction refers to a tank approximately 75-100% full of liquid, medium fill fraction is 25-75% full, low fill fraction is 10-25% full and very low fill fraction is below 10% full.

3.1.1 Traditional Tank Results

The traditional fuel tank comprises an interior geometry in the shape of a cylinder with hemispherical end caps and two symmetric vanes offset 90% from each other that go from the bottom to the top of the tank. The traditional fuel tank with silicon oil is evaluated as a control case to the conformal propellant tanks.

At a medium fill fraction the liquid wicks up the tank different amounts. The variation is seen across parabolas and also throughout the course of a single parabola. In one case shown in figure 3.1, the liquid wicks up the vanes symmetrically to the top of the tank encapsulating the bubble. The area between the vanes is left untouched by the liquid since the vanes are spread far enough apart the liquid does not create a sheet on the tank wall. During some parabolas the liquid oscillated up and down which resulted in more liquid being positioned at the top or the bottom of the tank. When the liquid is at the top of the tank it begins to wick into the air outlet and can fill up the tube leading to the air bag. Figure 3.2 shows an example of the air bag tube (in the middle upper section of the figure) full of silicon oil during a period of 1 G. One possible way to prevent this would be to use a Teflon tube.

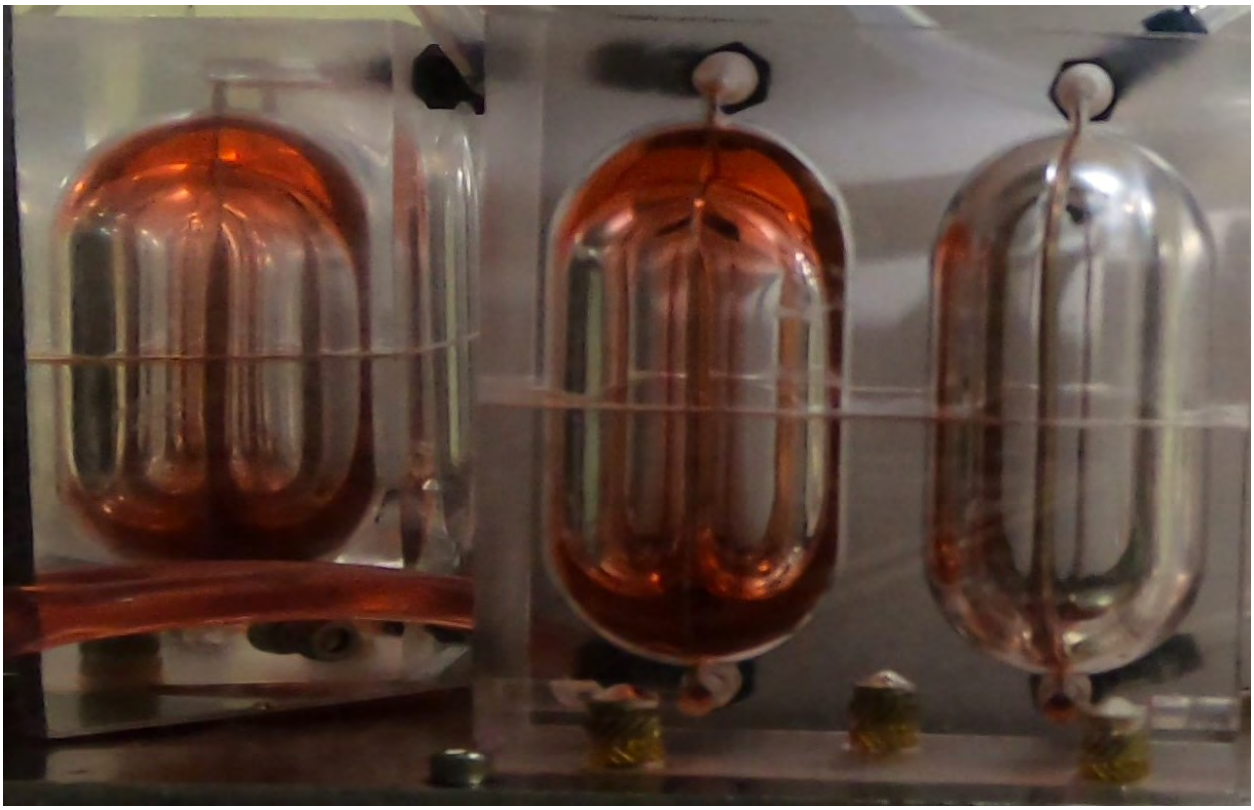

Figure 3.1. Traditional Tank Medium Fill Fraction With Encapsulated Bubble at 0±0.01g, Side View Left

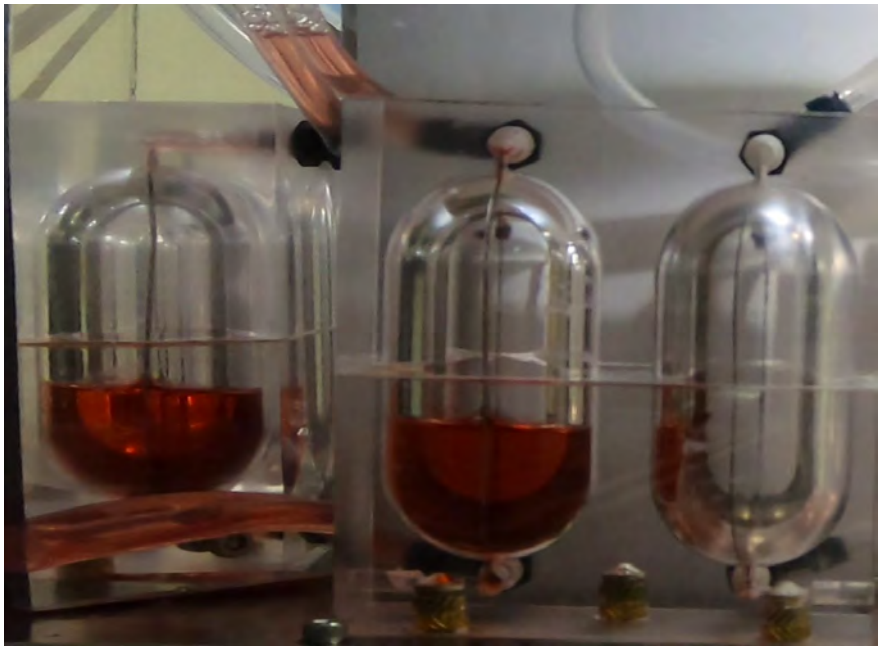

Figure 3.2. Silicon Oil In Air Bag Tubing at 1g, Side View Left

Variations in the liquid position could also be seen across different parabolas. Figure 3.3 shows the liquid position in four different parabolas. In only one parabola shown in figure 3.3a did the liquid encapsulate the bubble like the case seen above in figure 3.1. In three other parabolas the liquid does wick to the top of the tank, and into the air outlet. However, the bubble is not fully encapsulated by the liquid and the amount of liquid on the vanes can vary greatly. This is likely the result of variations in the pilots maneuvers.

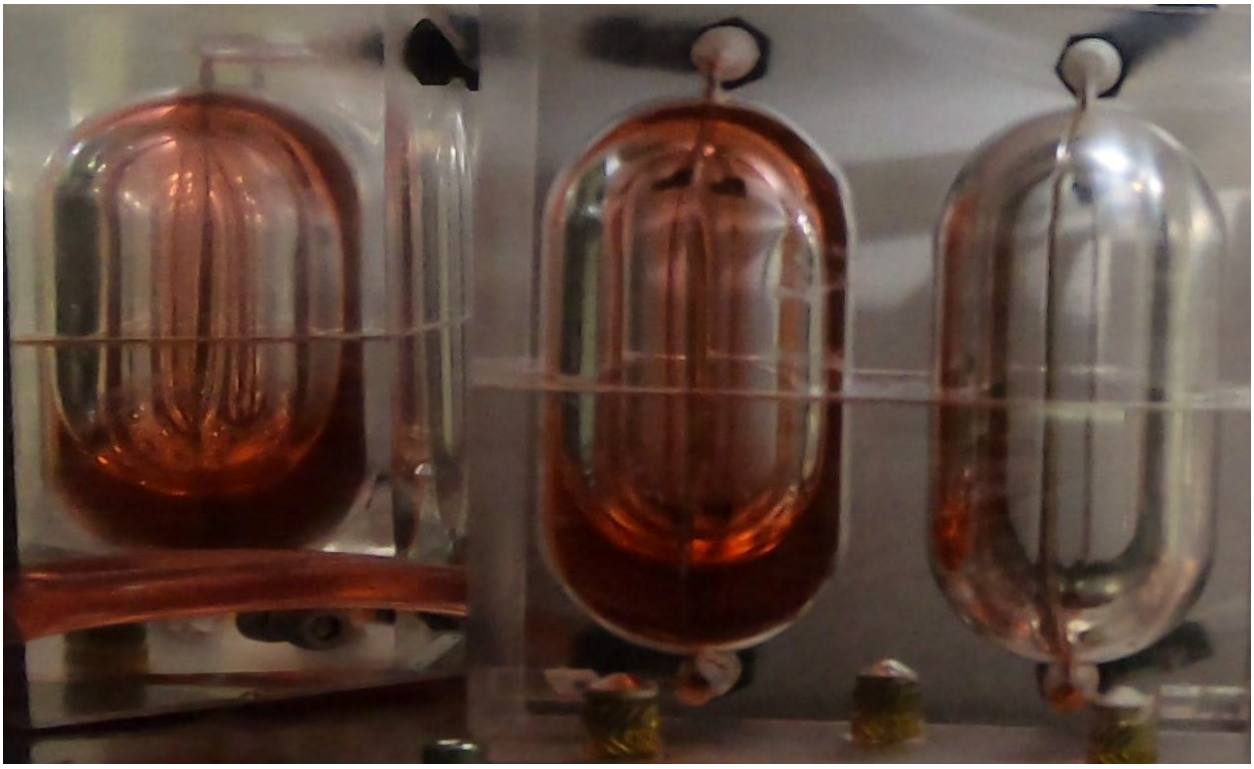

(a)

Figure 3.3. Traditional Tank Medium Fill Fraction at 0±0.01g, Side View Left

Figure 3.3. continued

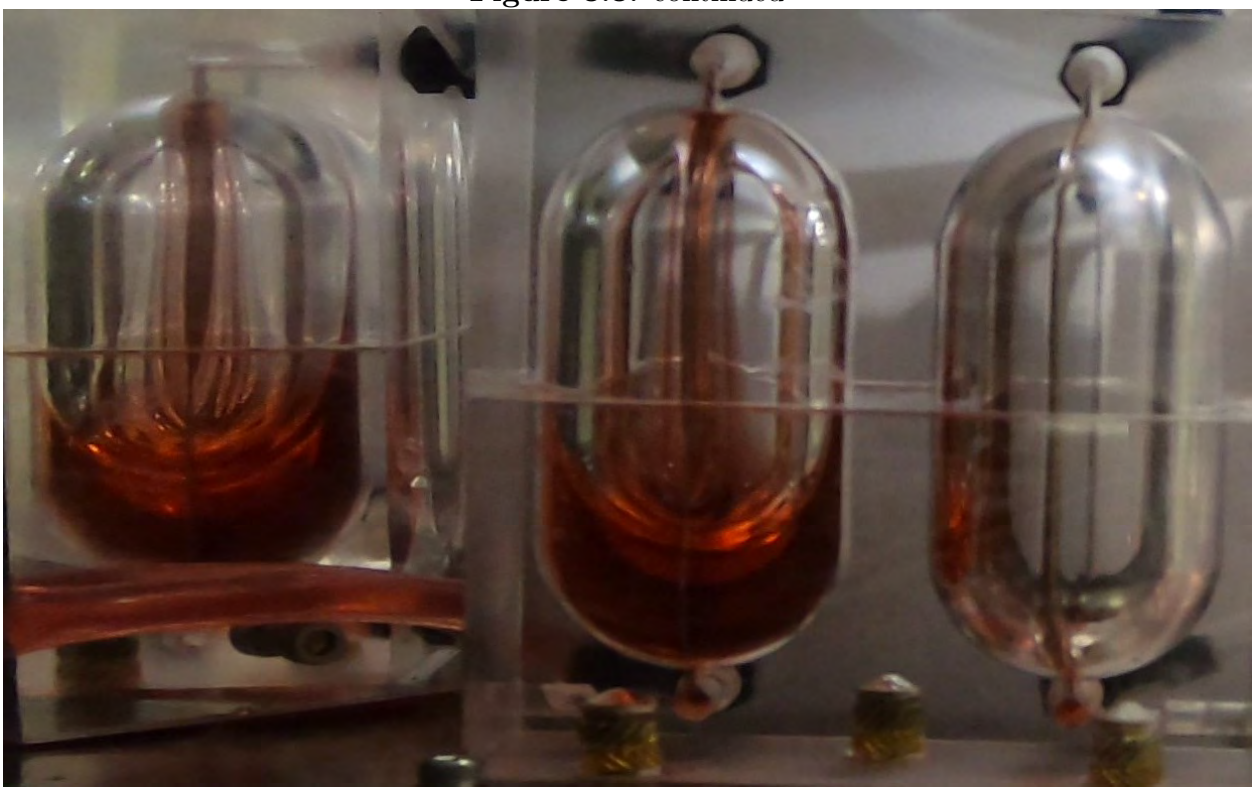

(b)

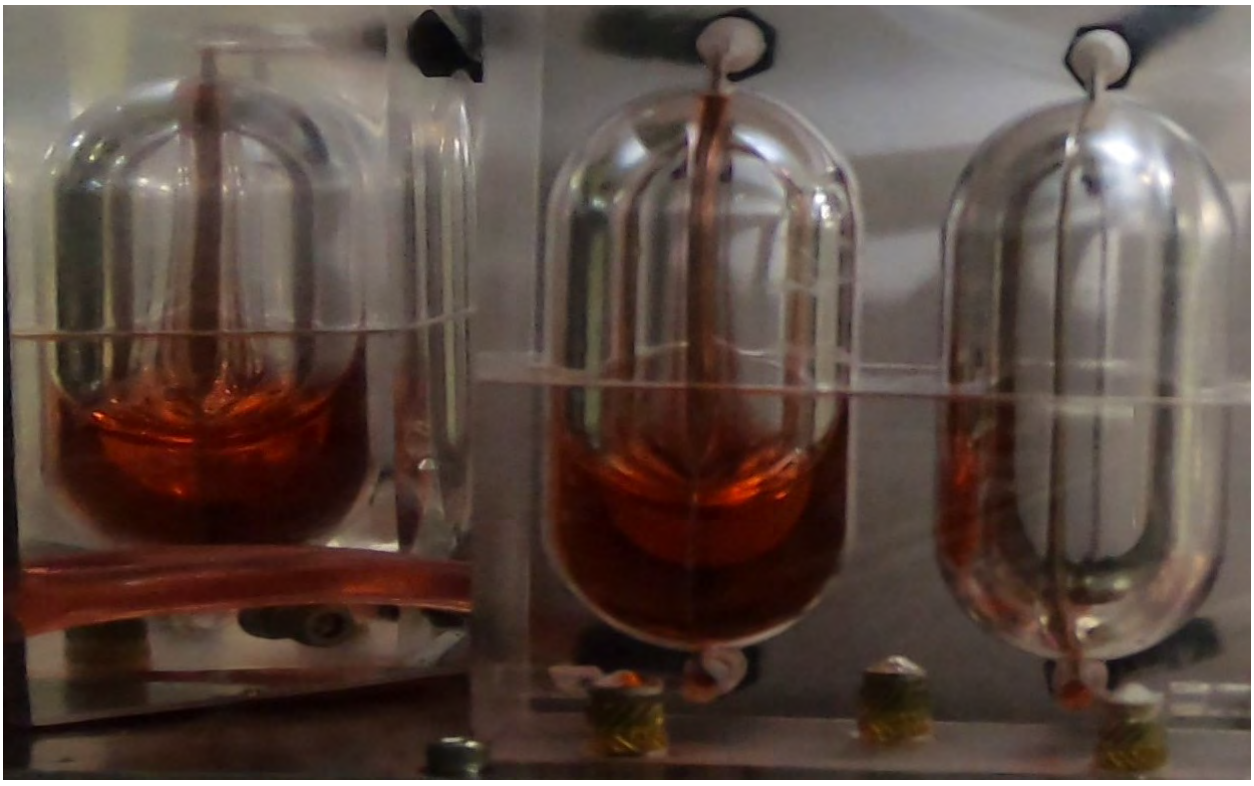

(c)

Figure 3.3. continued

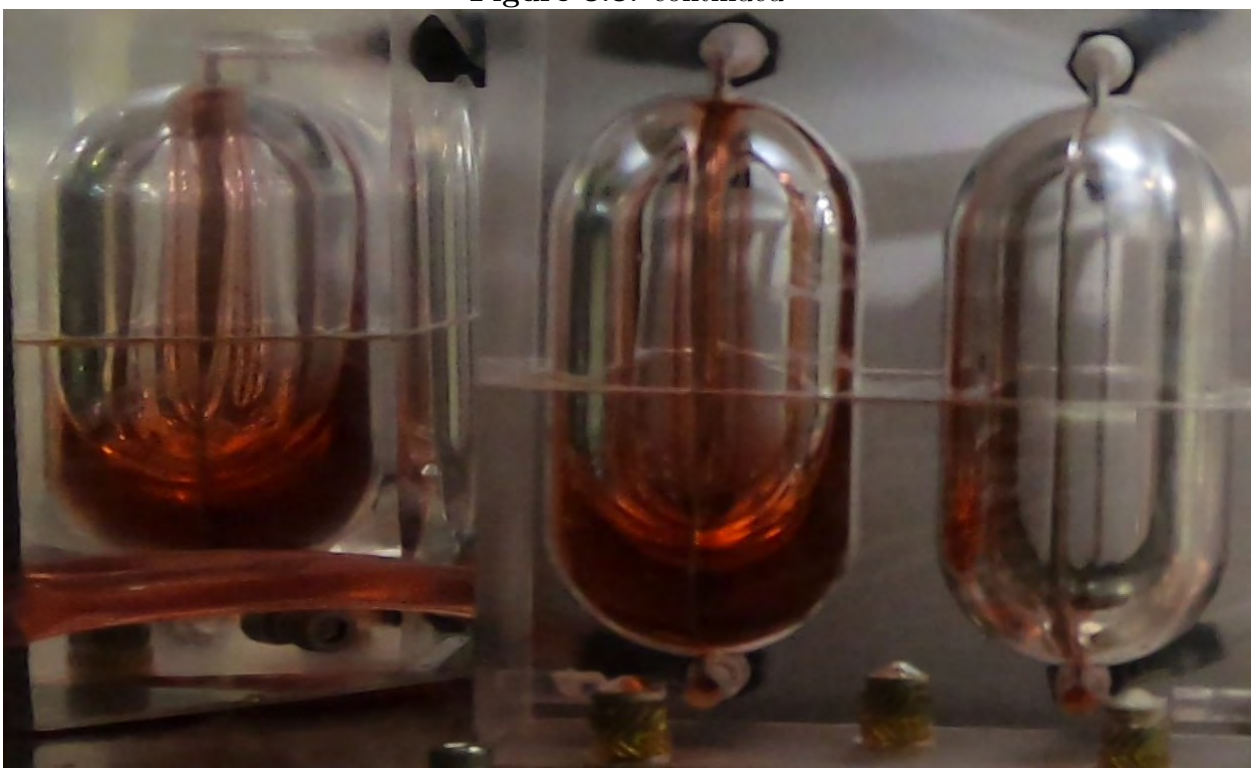

(d)

The liquid position in the tank at a low fill fraction remains similar to the medium fill fraction case. The liquid still wicks to the top of the tank along the vanes and some liquid wicks into the air outlet. The differences between the two fill fractions is the amount of liquid that wicks to the top of the tank and up the vanes in general. In the low fill fraction case, less liquid wicks up the vanes and there are less parabolas where the liquid begins to encapsulate the bubble. Figure 3.4 shows some examples of the traditional tank at a low fraction.

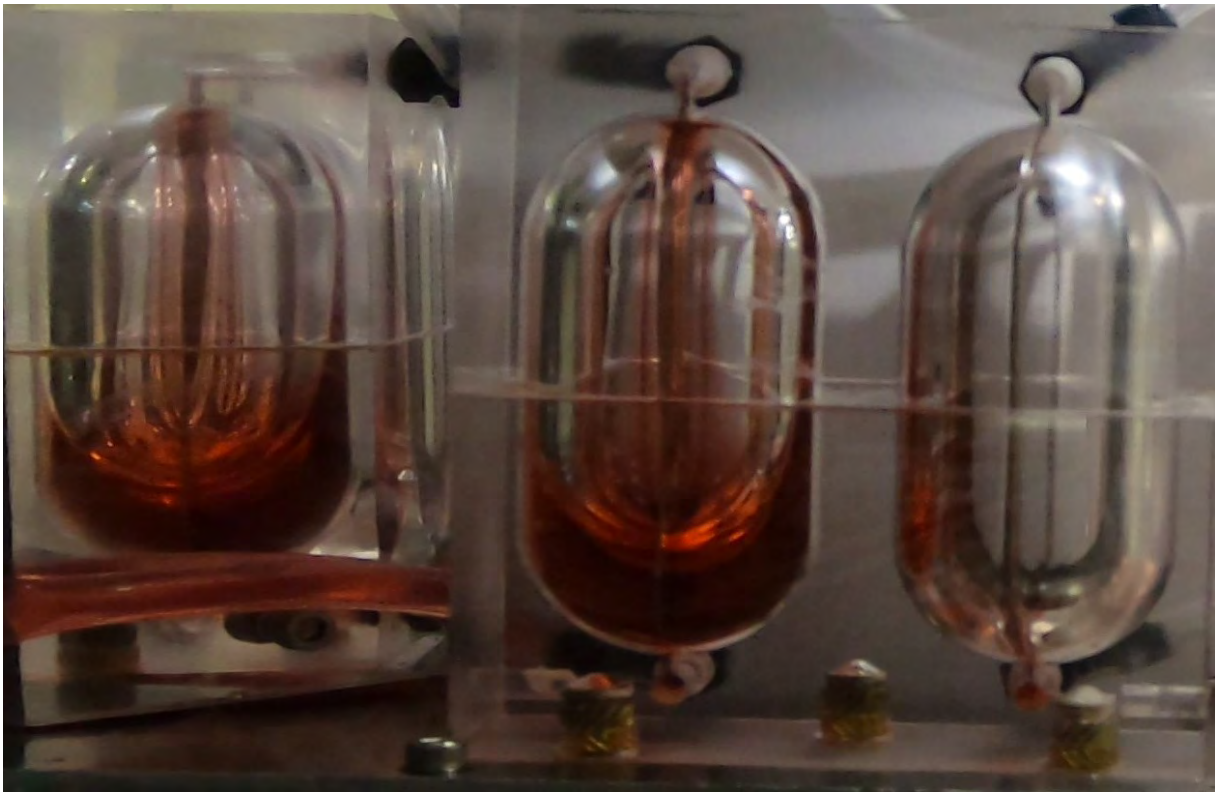

(a)

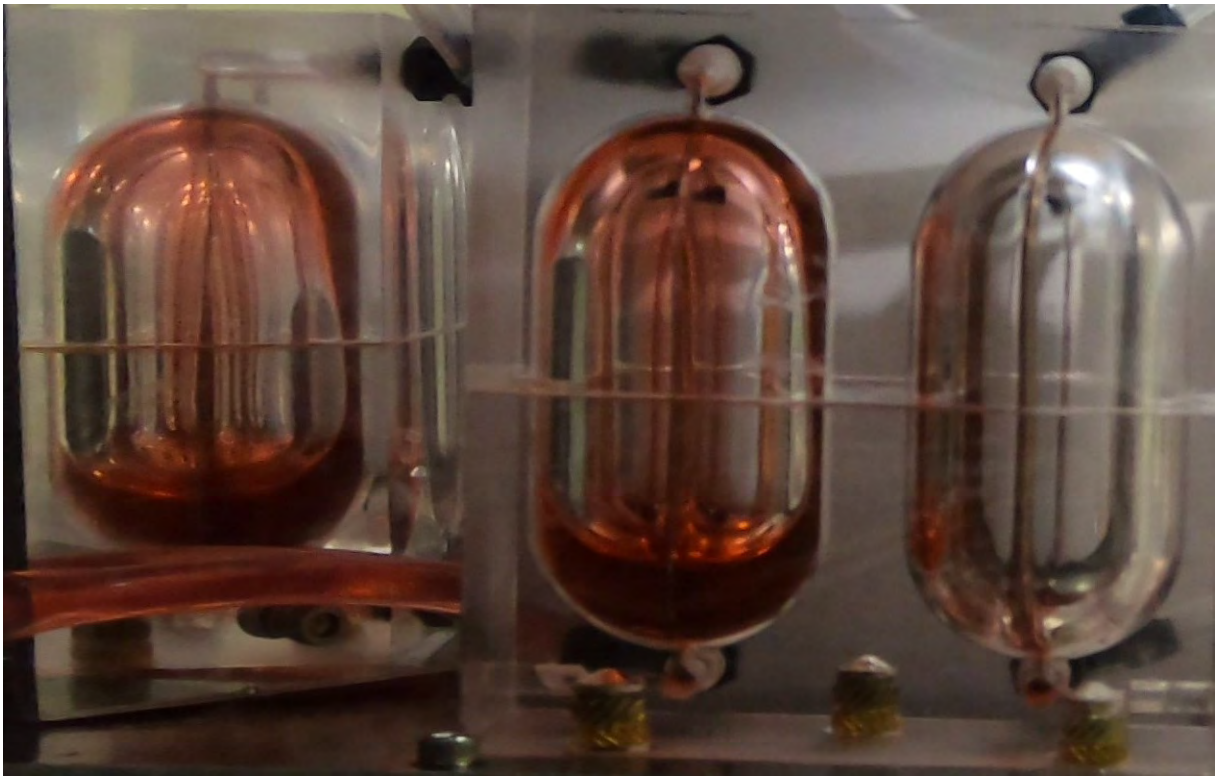

(b)

Figure 3.4. Traditional Tank Low Fill Fraction at 0±0.01g, Side View Left

Figure 3.4. continued

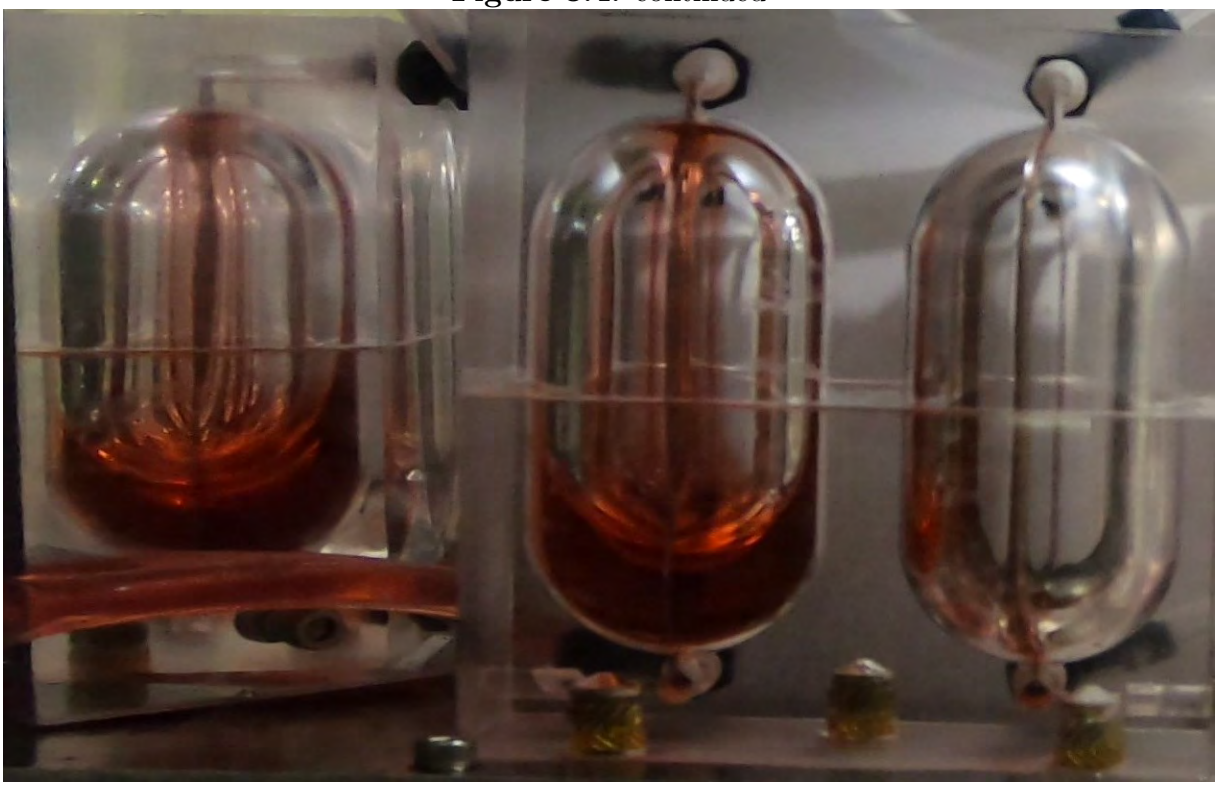

(c)

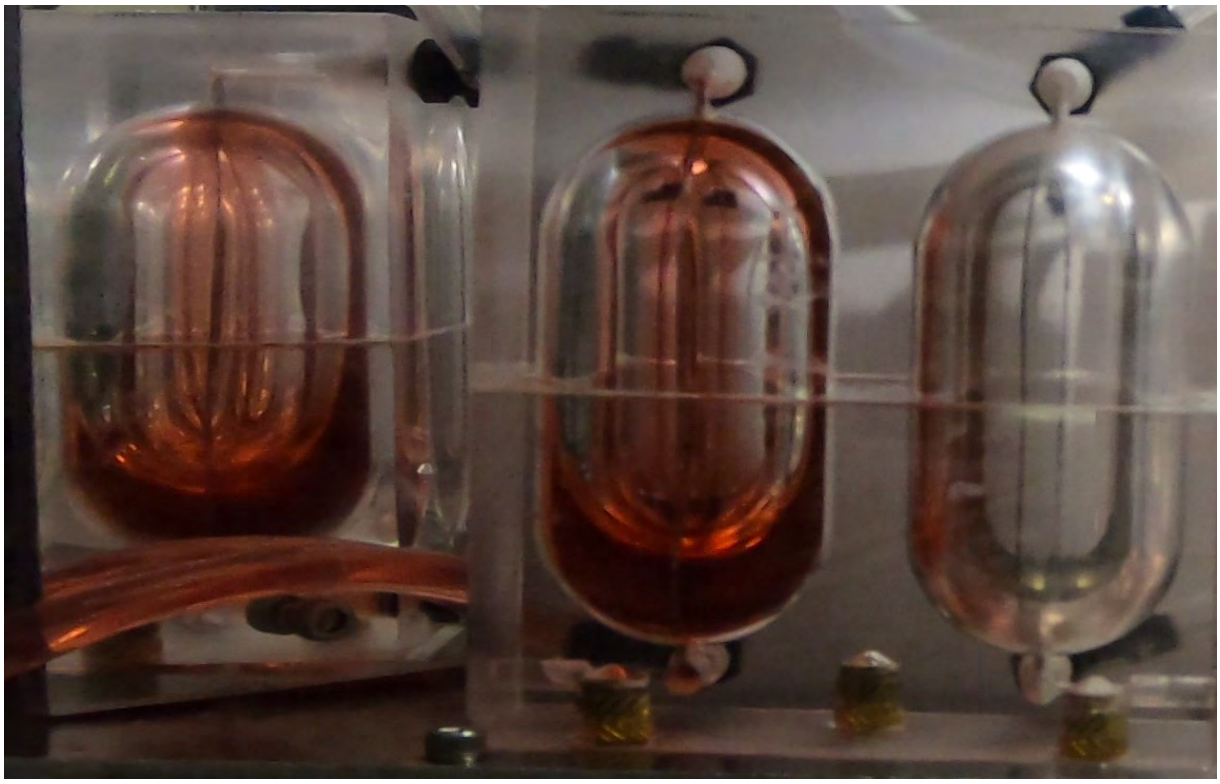

(d)

Even at very low fill fractions the liquid still wicks the vanes to the top of the tank. At this point there is not nearly enough liquid in the tank for the liquid to encapsulate the bubble. Higher fill fractions have also seen relatively consistent widths of the liquid wicking up the vane and at this fill fraction that is no longer the case. As the liquid wicks up the vanes the width of the liquid channel decreases with the largest difference in width near the bottom of the tank. Even with extremely little liquid left in the tank, like that shown in the left tank of figure 3.5b. The reason this occurs is because silicon oils contact angle is near zero, allowing it to wick in almost any circumstance. Figure 3.5 has examples of critical wetting for several very low fill fractions in the traditional tanks.

(a)

Figure 3.5. Traditional Tank Very Low Fill Fraction at 0±0.01g, Side View Left

Figure 3.5. continued

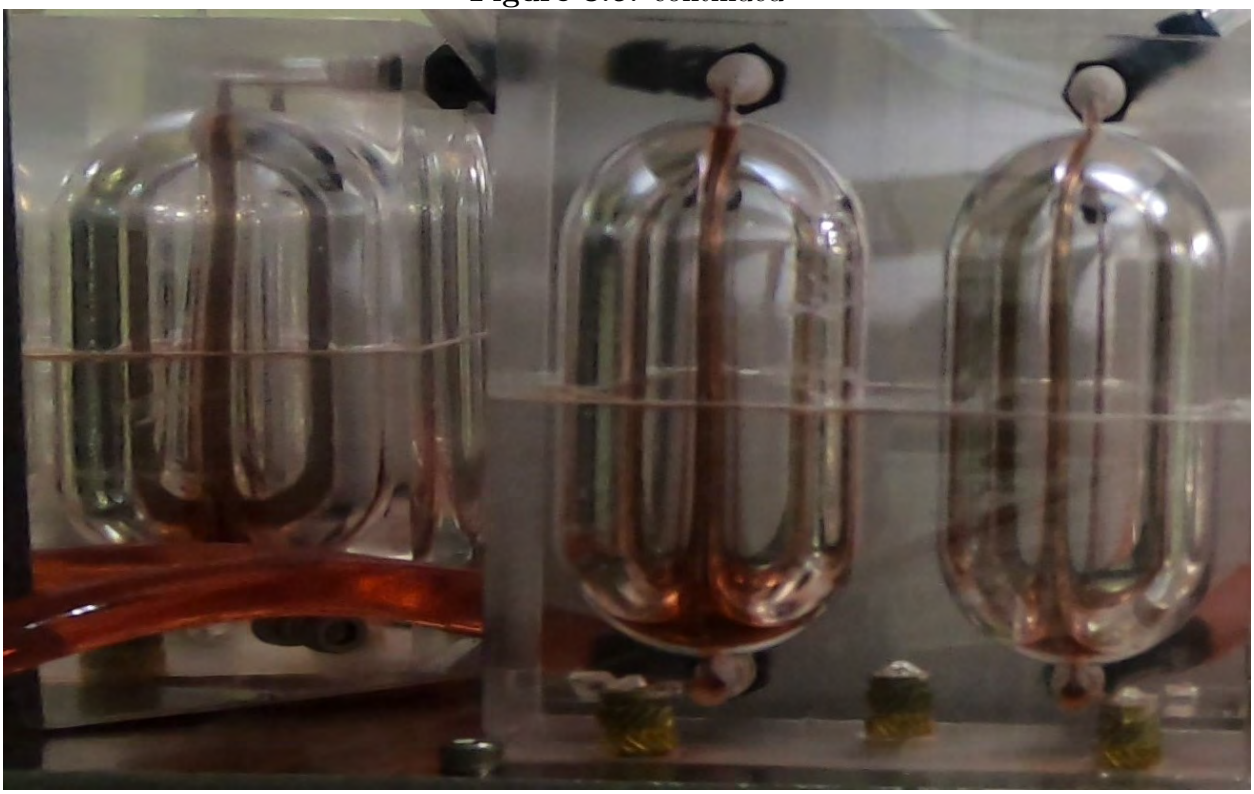

(b)

3.1.2 Blended Tank Results

When the blended tank was assembled the vanes were glued in place improperly and the radial vanes begin on the opposite side of the tank from the outlet. This should only effect the liquid position at low fill fractions where gas can enter the tank outlet. In the blended tanks at a fill fraction of approximately 80 to 90% the bubble remains at the top of tank in weightlessness. Liquid fillets are formed between the vanes which is shown in figure 3.6a. At fill fractions between 70 to 80% the bubble situated itself in the corner closest the tank outlet. In many parabolas, the line between gas and liquid phases would match the vane geometry. In other cases like that shown in figure 3.6b the bubble remains close to the radial vanes, but extends past them.

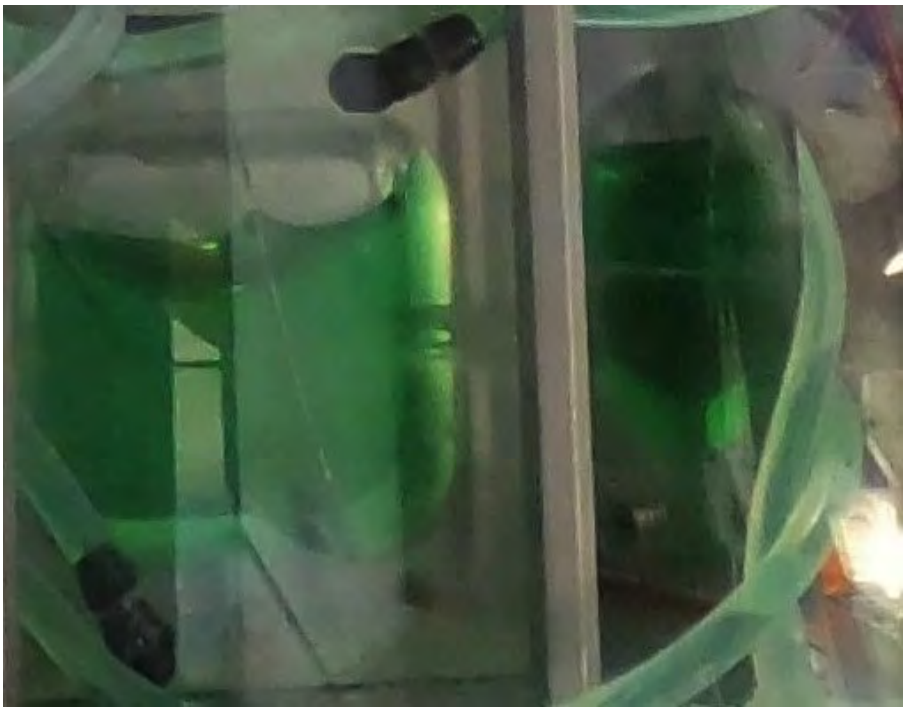

(a)

(b)

Figure 3.6. Blended High Fill Fraction at 0±0.01g, Side View Right

At medium fill fractions the liquid creates a fillet down the length of the tank once again. One interesting feature is how the liquid interacts with the lateral vane. This vane is slightly off centered and the liquid wicks much further up the vane on the side closest to the tank wall. There is a discontinuity in wicking height, and liquid slope across the vane. On the vanes that extend radially from the outlet the liquid begins to wick from the mean liquid gas phase line to the vanes as seen in the first high fill fraction case. The liquid fillet here is exaggerated compared to the high fill fraction case on the lower vane. It can be presumed that the lower vane has a greater effect on the liquid as the fill fraction decreases since it is less steep than the top vane. The liquid fillet between the radial vanes is also more pronounced than at a high fill fraction. Figure 3.7 shows this case, with the tank outlet on the right side. The tank outlet remains on this side for the rest of the blended figures.

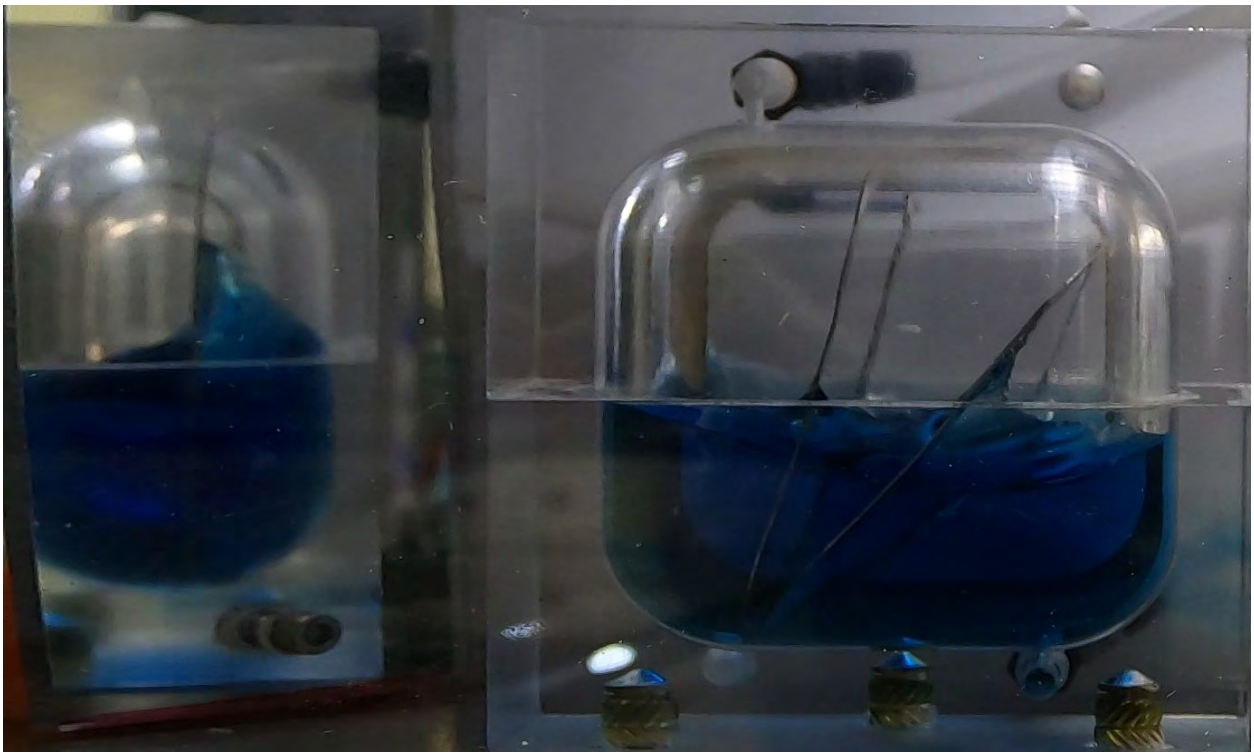

Figure 3.7. Blended Medium Fill Fraction at 0±0.01g, Side View Left

As the fill fraction lowers further the bulk of the liquid is concentrated around the vanes that extend radially from the tank outlet. The liquid fillets across the lateral vane become more continuous. Once the fill fraction reaches 5 to 15% discontinuities in liquid height

across the radial vanes begin to form. Figure 3.8 shows this process from high to low fill fraction.

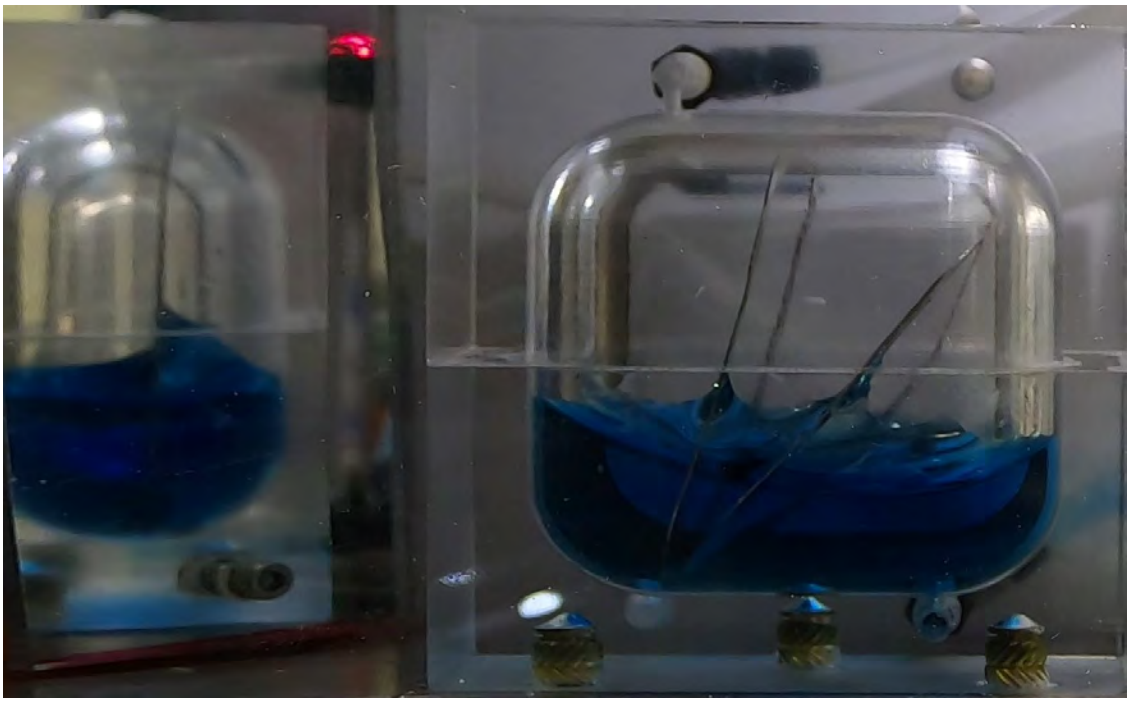

(a)

(b)

Figure 3.8. Blended Low Fill Fraction at 0±0.01g, Side View Left

Figure 3.8. continued

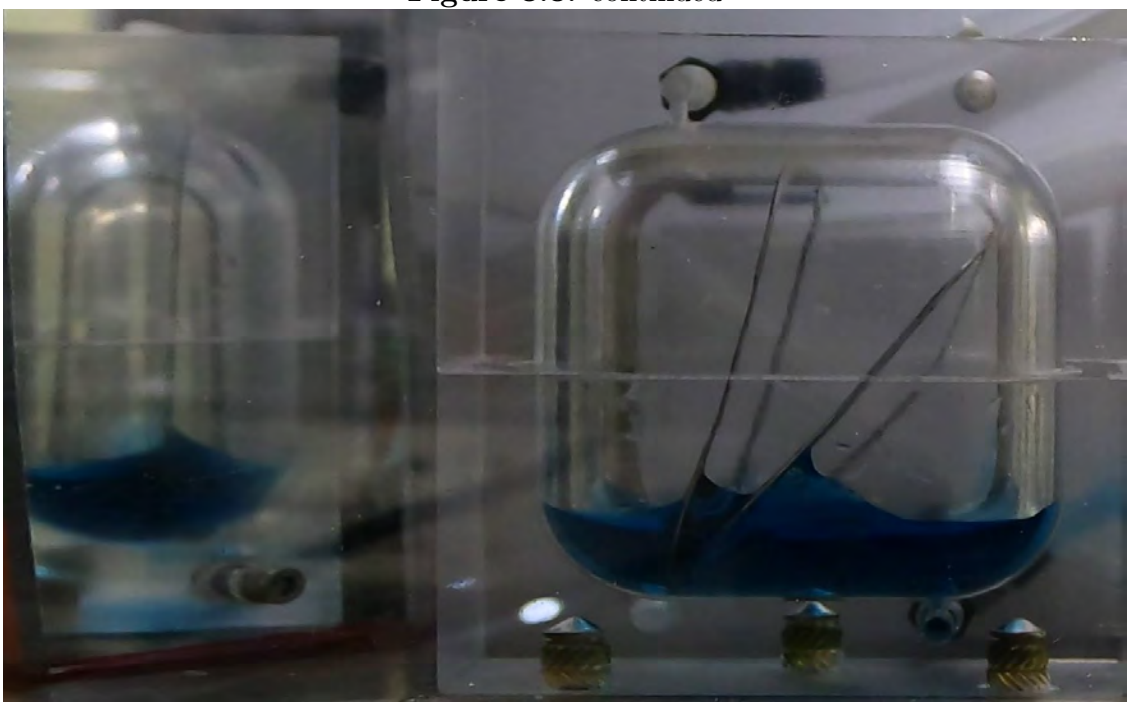

(c)

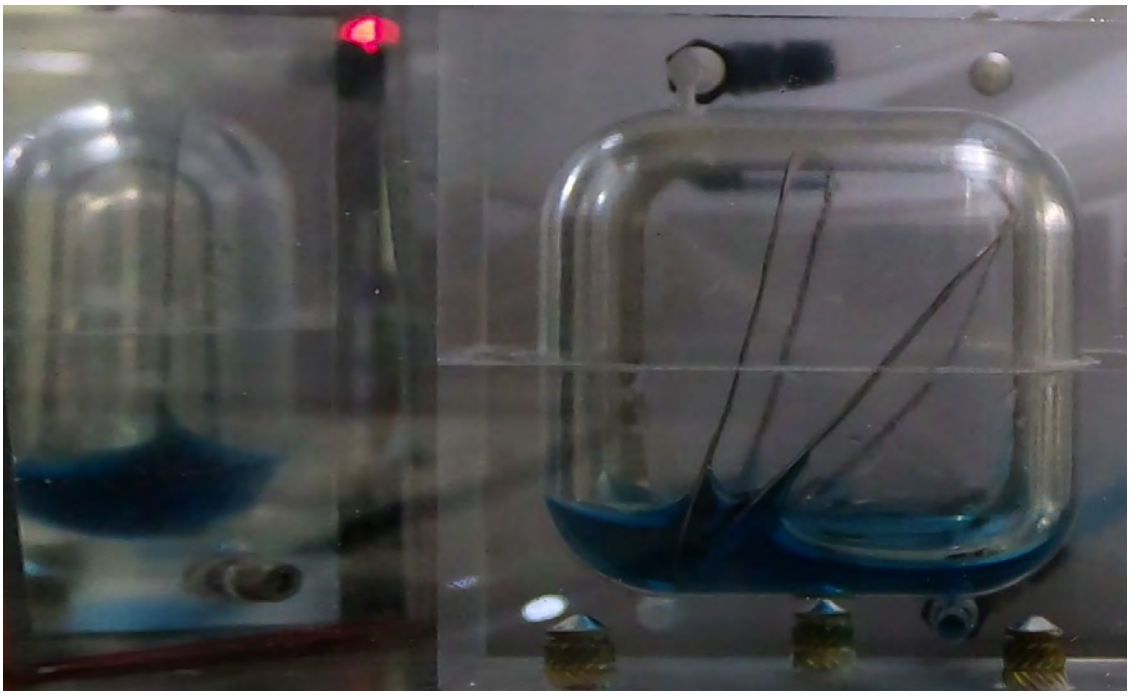

(d)

3.1.3 Stamped Tank Results

The stamped tank has similar geometry to the blended tank, but to simulate a crease from the stamping manufacturing process a rounded-off edge is machined along the mean line of tank in the lateral direction. In figure 3.9 the outlet of the tank is on the left side. Only very low fill fractions of this tank could be evaluated. The liquid appears to be near the same location in the stamped tank at a similar fill fraction of the last blended case. One difference is the absence of a fillet between the wall of the tank and the radial vanes in figure 3.9a. It is difficult to determine whether the liquid is wicking into the slot because of mirror placement and the dark image with dark green liquid. As the fill fraction is lowered the walls of the tank have a smaller effect on the liquid, and the liquid does not create a fillet in the corner away from the outlet in figure 3.9c or figure 3.9d. At very low fill fractions the bulk of the liquid shifts under the less steep radial vane which could lead to propellant trapping, shown in figure 3.9d.

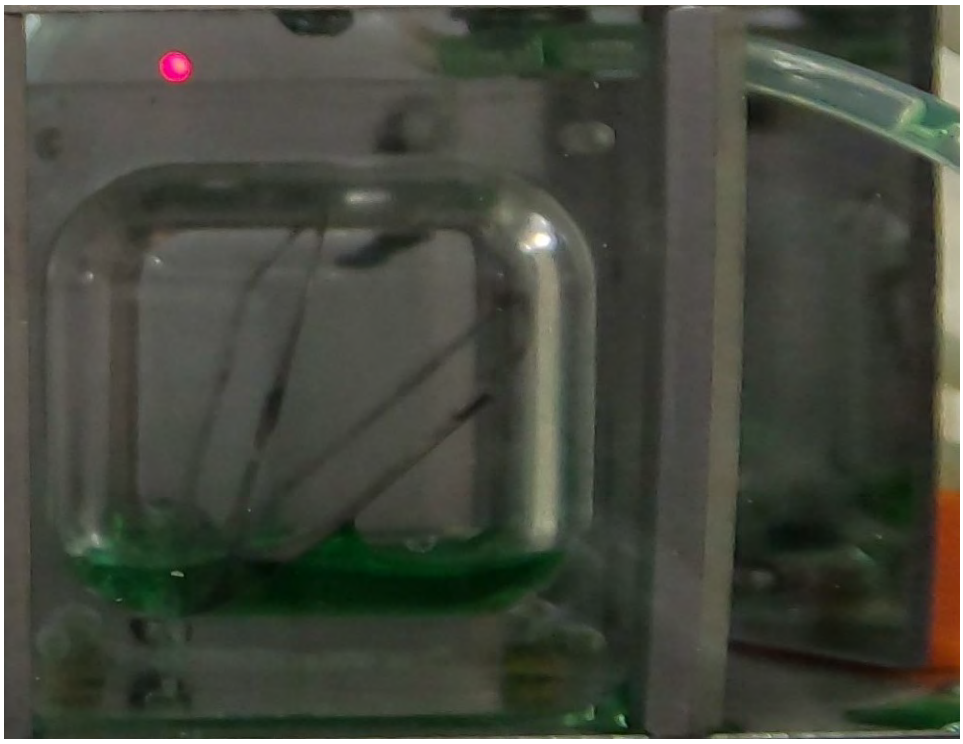

(a)

Figure 3.9. Stamped Very Low Fill Fraction at 0±0.01g, Side View Right

Figure 3.9. continued

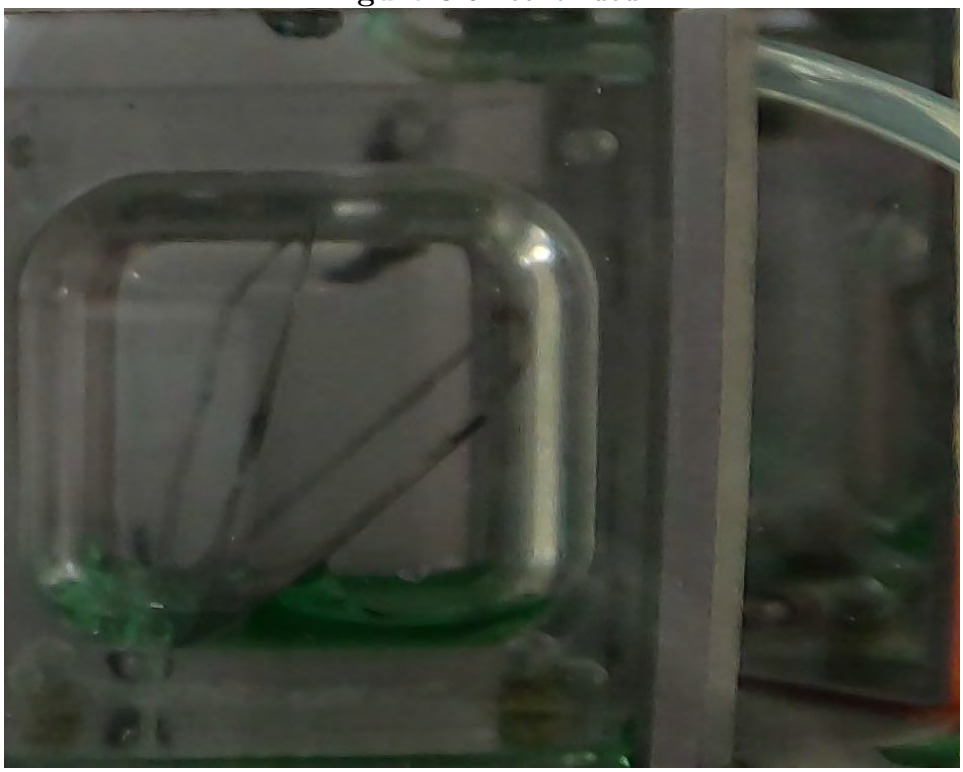

(b)

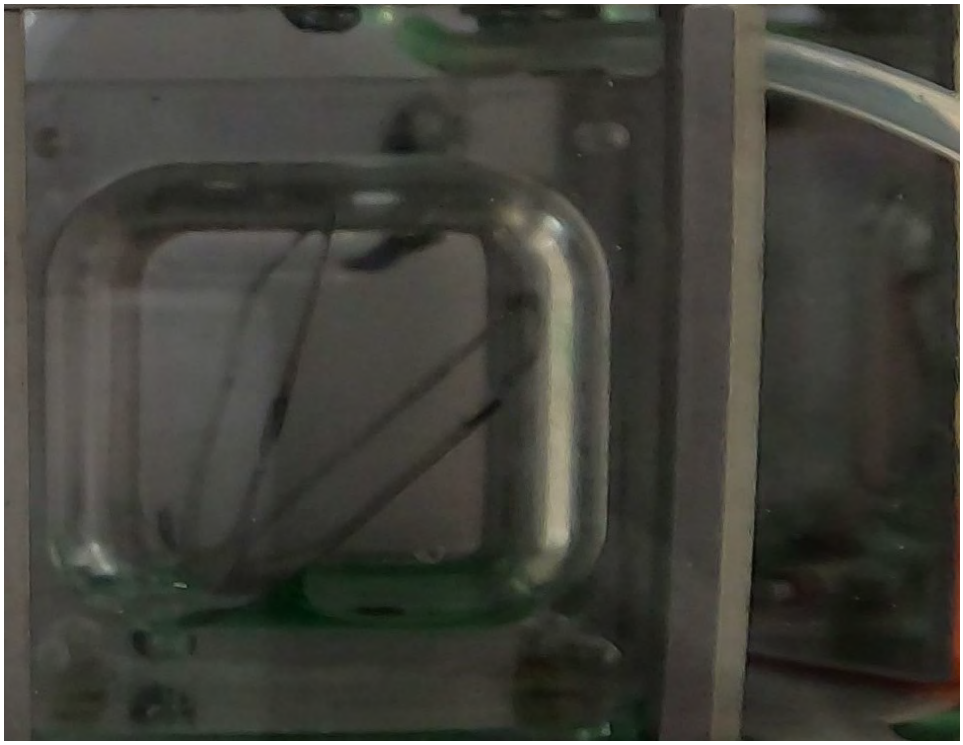

(c)

Figure 3.9. continued

(d)

3.1.4 Stiffened Tank Results

The stiffened tanks take the same features as the blended and stamped tanks, but add in ridges to model a tank with increased stiffness. The ridges are orientated 90° from vertical. For all figures of the stiffened tanks the outlet is on the left side of the tank. The ridges in this orientation can hinder the liquids ability to wick onto the vanes when compared to the blended tank case. Figure 3.10 shows several examples where the liquid is unable to wick past the 4th tank ridge. This causes the bubble to be more flat in nature. Blended tanks with a high to medium fill fraction demonstrated smaller fillet radii with differing radii between vanes, or one large bubble extending from the opposite corner of the outlet to the middle of the tank. For the stiffened tanks multiple fillet radii are replaced with one larger fillet that sweeps into the corners of the tank away from the ridge. One possible explanation for this phenomenon is that this data was recorded while the tank was being filled to this level. So the 4th ridge in the tank was dry, and the liquid may behave differently if the

meniscus was decreasing in height and left the ridge wet. Since the liquid is searching for the minimum energy state, wicking into a wet ridge can effectively reduce the energy of the liquid by decreasing the free surface area. Whereas wicking into a dry ridge will increase the liquids free surface area momentarily. For the medium to high fill fractions of the stiffened tank the same discontinuity from the blended tanks in liquid height across the lateral tank vane on the left side of the tank. The fluid height discontinuity can be seen on the right side of the tank as well, but the effect is complicated by the radial vanes coming from the tank outlet. Figures 3.10d and 3.10c show a small discontinuity across the lateral vane on the right side of the tank. Figures 3.10a and 3.10b show that the liquid has completely filled the gap between the lateral and radial vanes on the side of the tank furthest from the camera. On the side of the tank closest to the camera liquid wicks up the radial vane and creates a small fillet between the radial and lateral vanes. In all cases liquid has wicked up the less steep radial vane. This phenomenon can not be confirmed to occur on the blended tank because the mirrors were only one side of that tank.

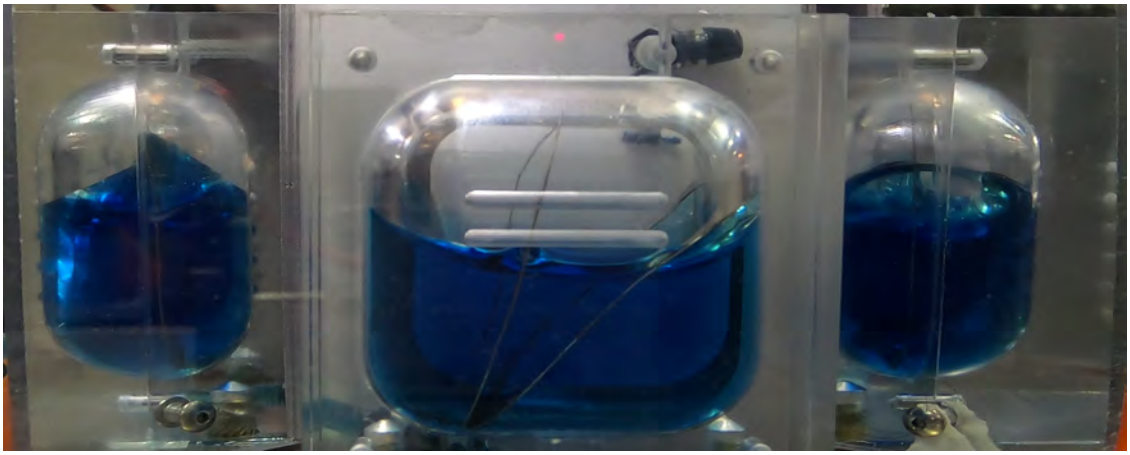

(a)

Figure 3.10. Stiffened Medium to High Fill Fraction at 0±0.01g, Side View Left and Right

Figure 3.10. continued

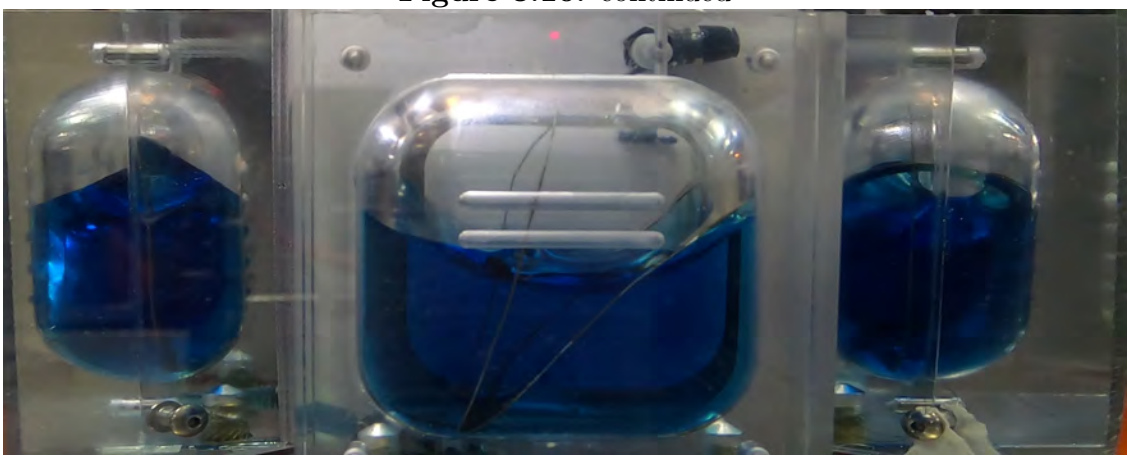

(b)

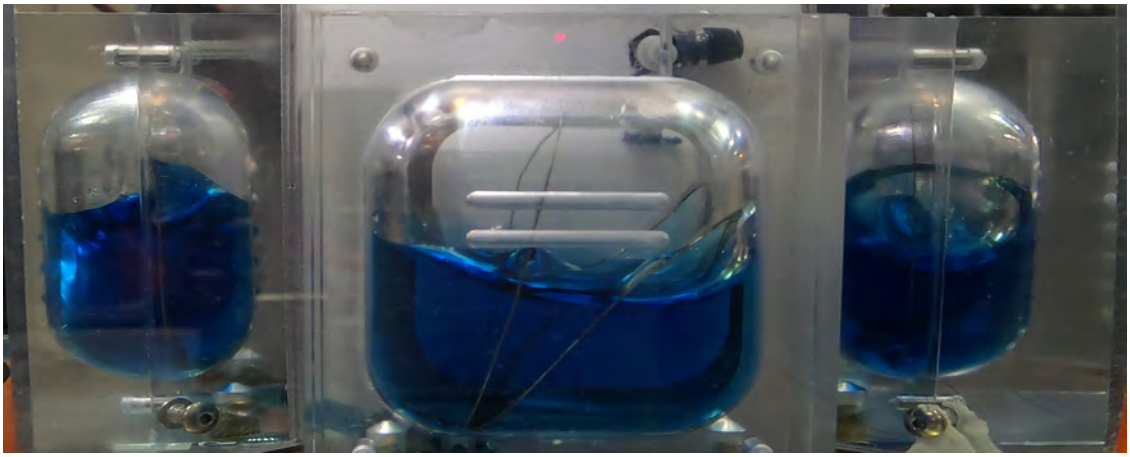

(c)

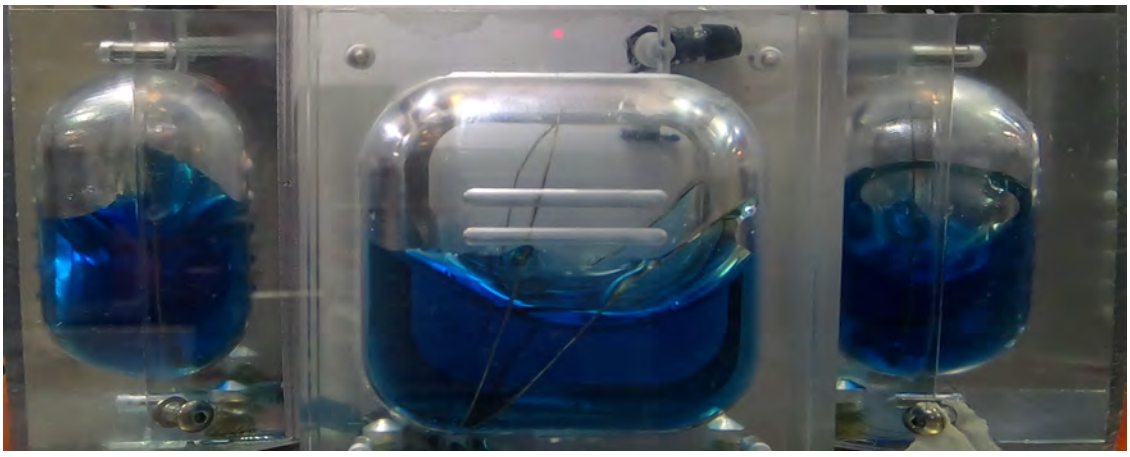

(d)

At low fill fractions the ridges in the tank still play an important role in determining the liquids position. Compared to the blended tanks the liquid creates a more exaggerated fillet in the lateral direction and appears to wick further up the tank in some cases, shown in figure 3.11a. In both figures 3.11a and 3.11b the liquid fillet between the radial vanes appears to be less defined, which is likely caused by the ridges in the tank at this location. These figures also show the same discontinuity in liquid height on the left side of the tank across the lateral vane, but it is absent on the right.

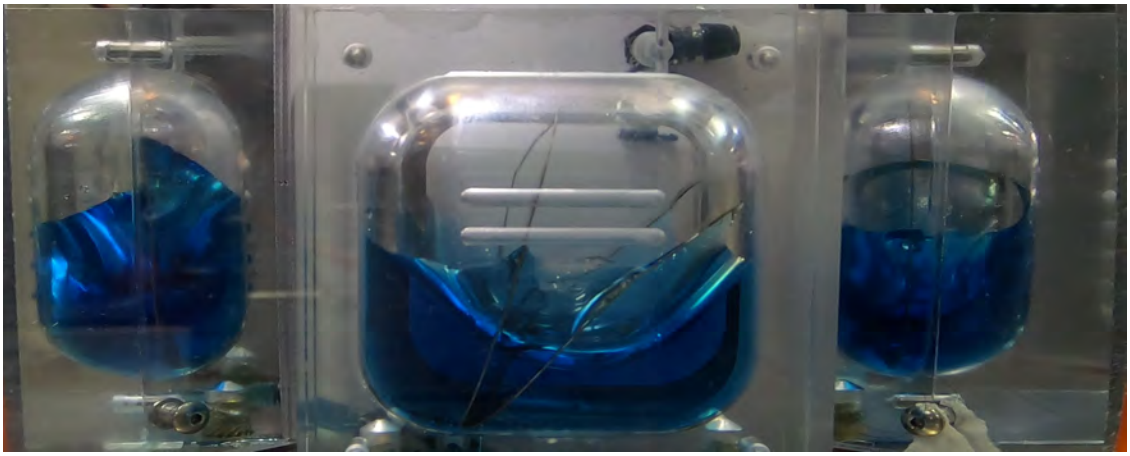

(a)

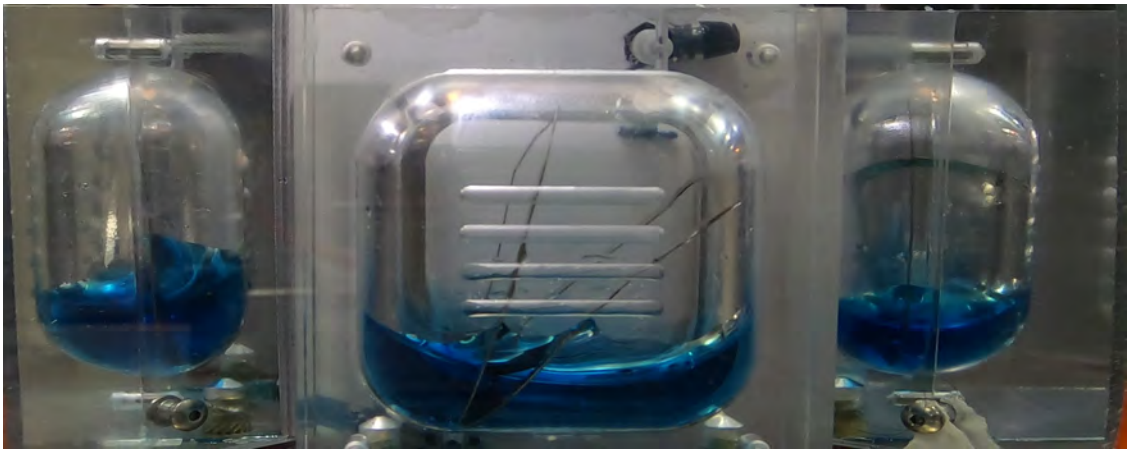

(b)

Figure 3.11. Stiffened Low Fill Fraction at 0±0.01g, Side View Left and Right

As the tanks fill fraction becomes very low the lateral vane plays less of a role in liquid positioning, and the radial vanes become more dominant. Figure 3.12 shows that as the fill fraction decreases the liquid begins to concentrate around the radial vanes and the lateral

vane on the right side of the tank. Figure 3.12a show that the liquid does not wick into the ridge near the steep radial vane, but does wick into the ridge on the shallow vane. As the fill fraction decreases further the liquid stays concentrated on the lateral vane on the side away from the camera and the radial vanes. There is potential that the remaining liquid gets trapped under the shallow radial vane.

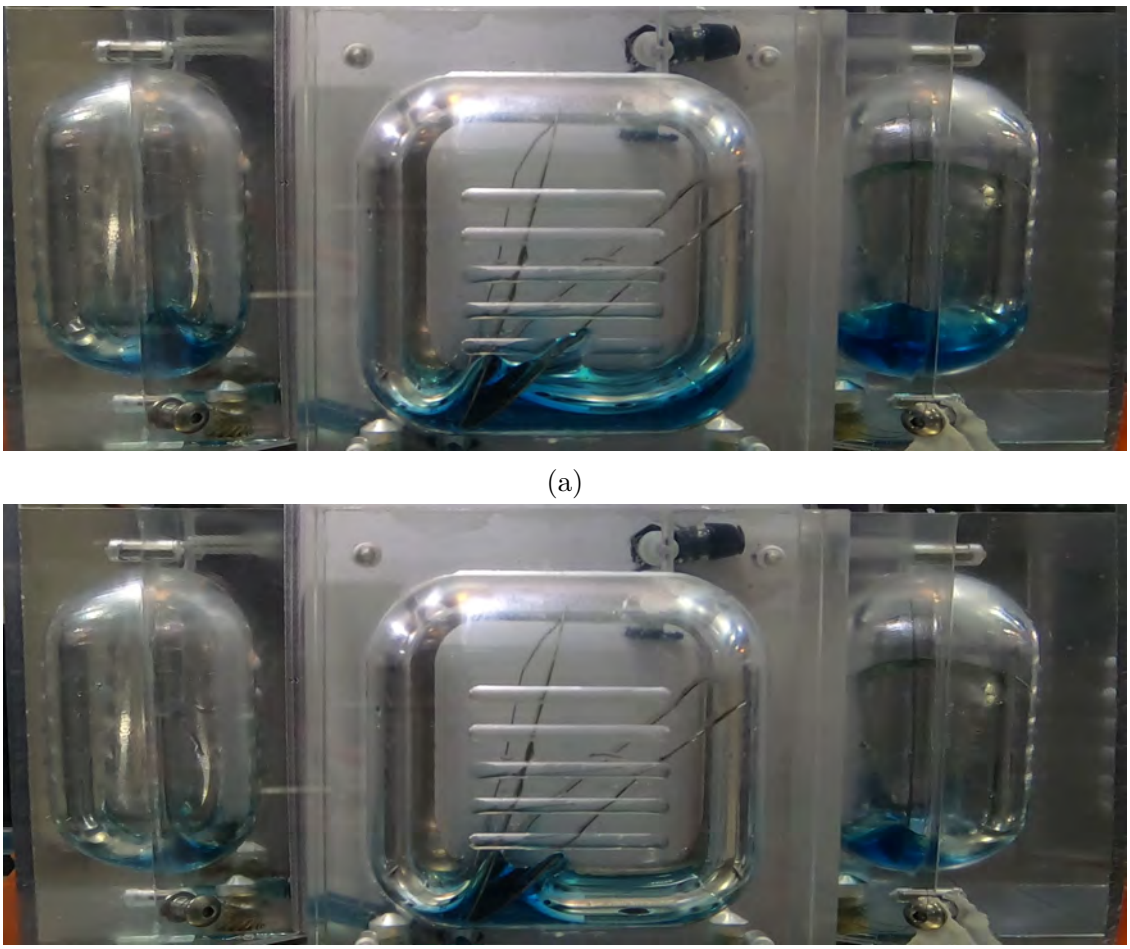

(a)

(b)

Figure 3.12. Stiffened Very Low Fill Fraction at 0±0.01g, Side View Left and Right

Figure 3.12. continued

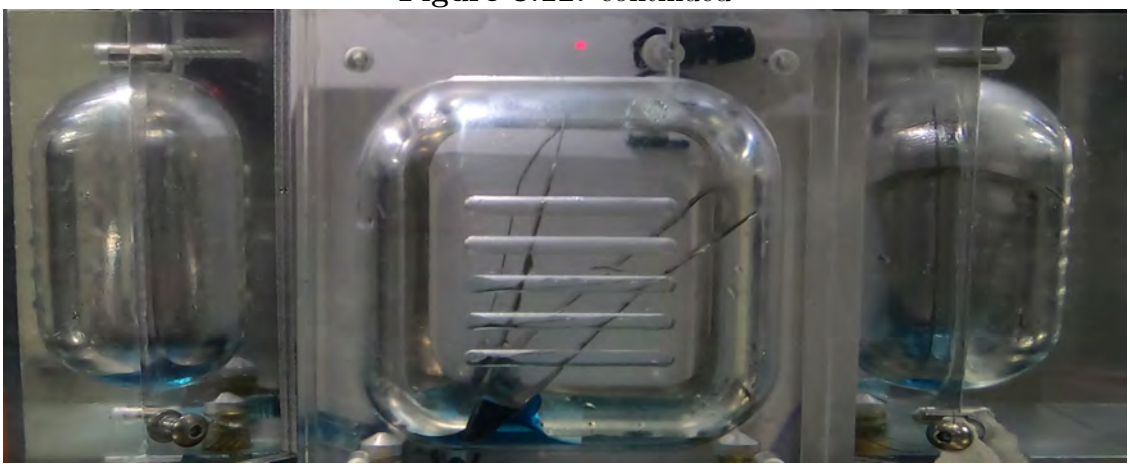

(c)

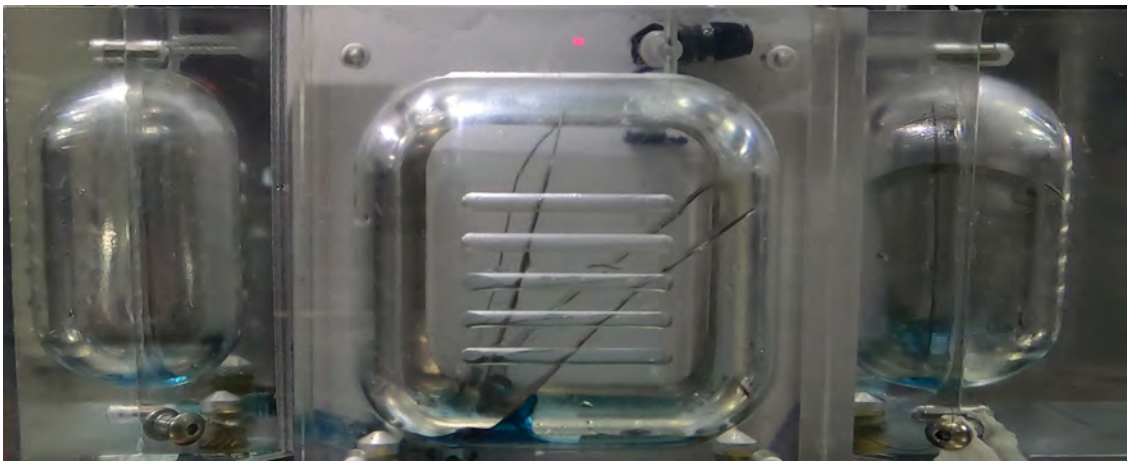

(d)

3.1.5 Arcs V1 Results

The Arc tank with V1 vane design have one lateral vane extending the length of the tank and a transverse vane near the outlet. For figures of the arc V1 tank when filled with blue liquid the tank outlet is on the right, and for green liquid the outlet is on the left. At high fill fractions three phenomenon were observed. The first image in 3.13 shows the liquid taking up all of the volume between the transverse vane and the close tank wall. There is also a fillet extending from the transverse vane to the far end of the tank wall.

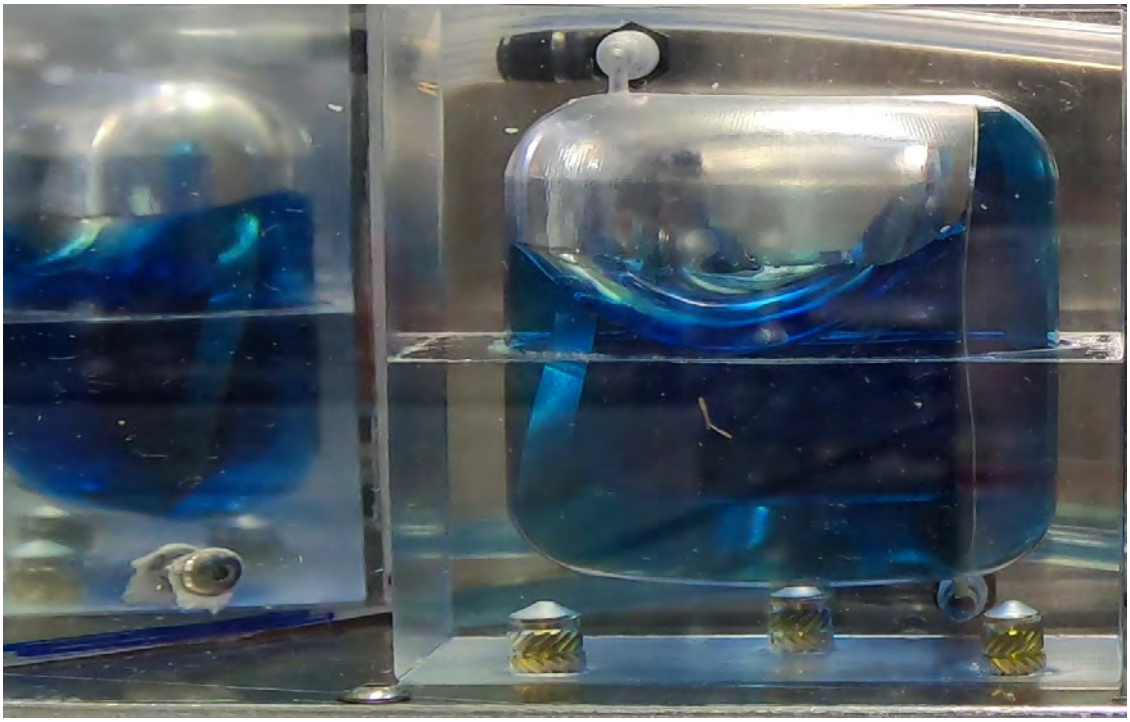

Figure 3.13. Arc V1 High Fill Fraction Phenomenon 1 at 0±0.01g, Side View Left

The second phenomenon is similar to the case discussed above for this vane geometry, except the liquid does not completely fill the volume between the transverse vane and the close tank wall. Across the transverse vane there is also a small discontinuity in liquid height. Figure 3.14 shows this phenomenon.

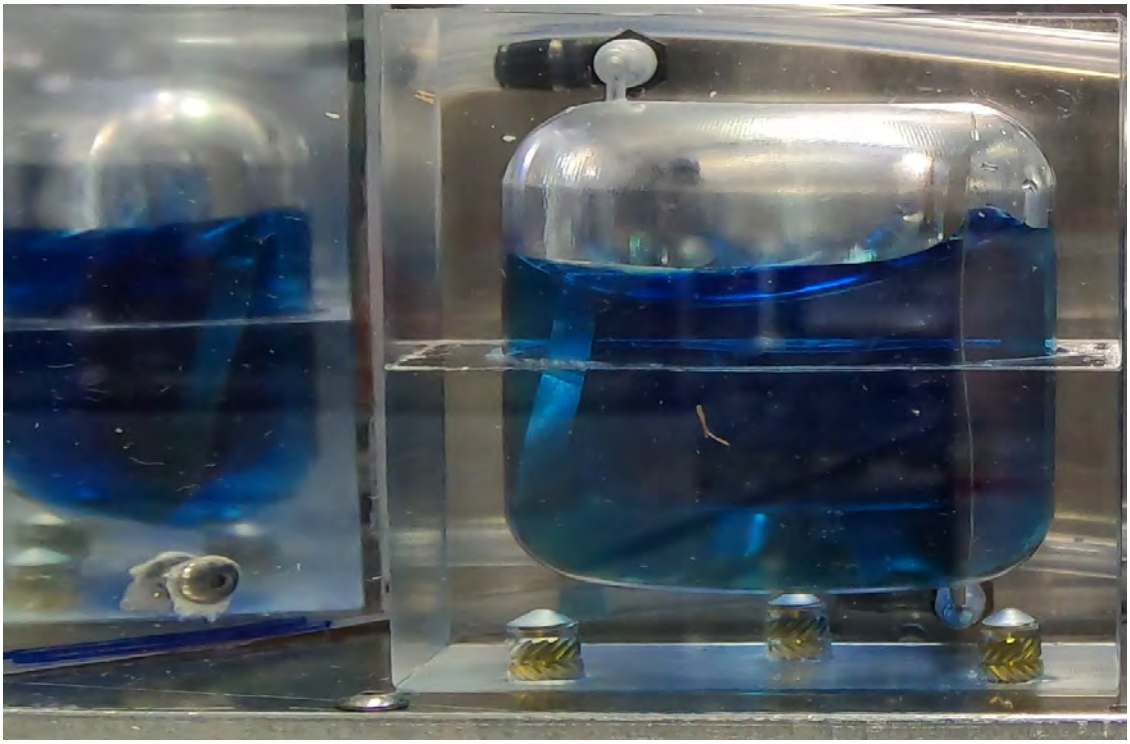

Figure 3.14. Arc V1 High Fill Fraction Phenomenon 2 at 0±0.01g, Side View Left

The final observed phenomenon for the V1 vane geometry at a high fill fraction is a bubble attached to the ceiling of the tank that extends past the the transverse vane, and only intersects the lateral vane near the ceiling of the tank. Figure 3.15 shows the bubble position for this case.

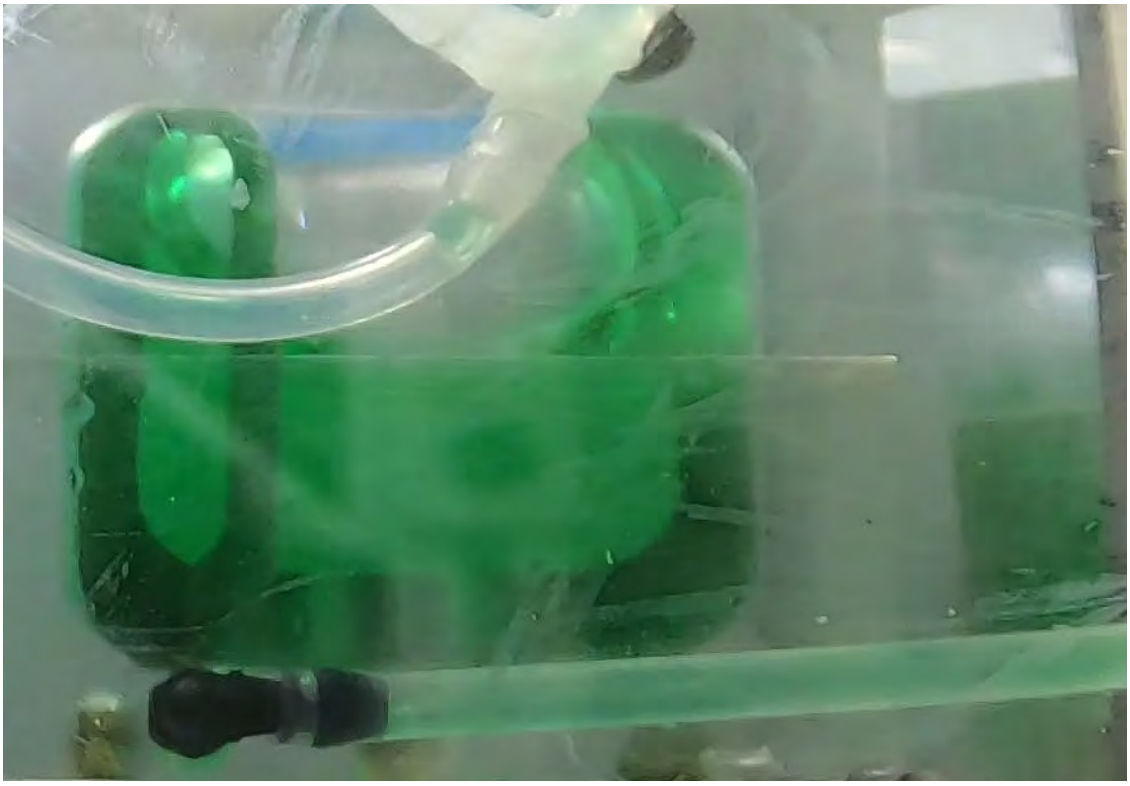

Figure 3.15. Arc V1 High Fill Fraction Phenomenon 3 at 0±0.01g, Side View Right

At medium fill fractions the liquid behaves close to the case shown in figure 3.14. Here the liquid wicks between the transverse vane and the close tank wall once again with a fillet extending from the transverse vane to the lateral vane on the far side. Figure 3.16 shows two examples of this case at differing fill fractions.

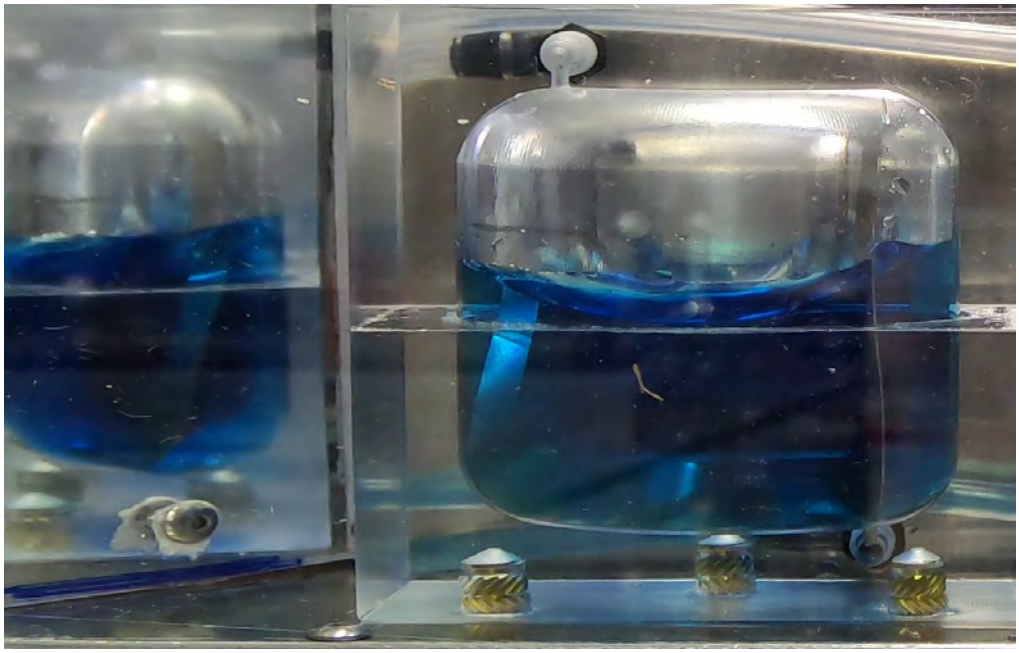

(a)

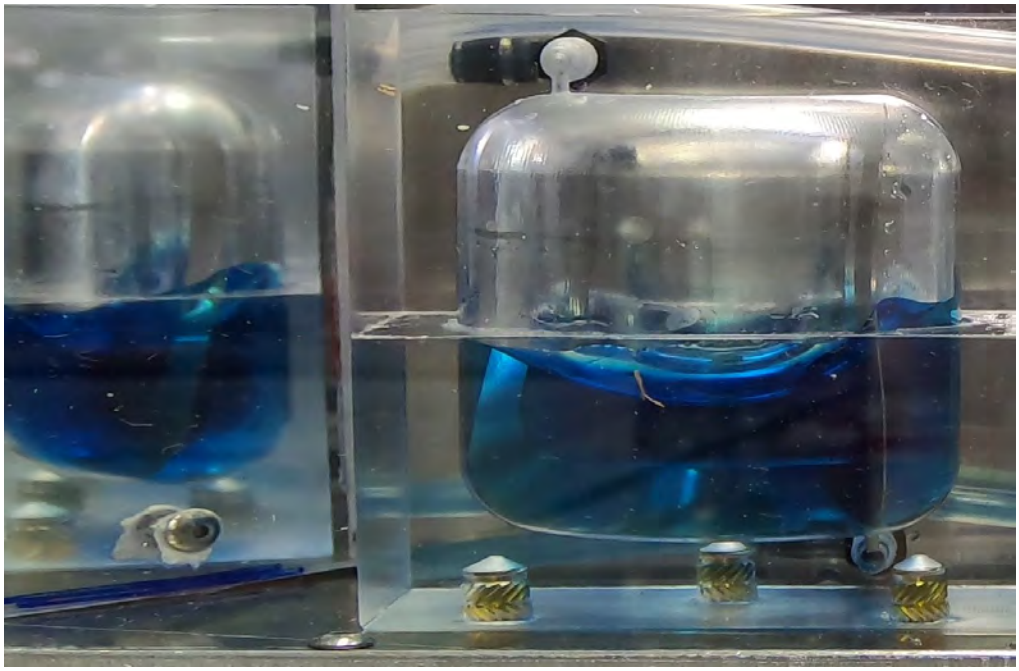

(b)

Figure 3.16. Arcs V1 Medium Fill Fraction at 0±0.01g, Side View Left

The liquid positioning at low fill fractions are again an extension of the high fill fraction positioning, like that shown in 3.14. For all fill fractions examined there is a fillet of roughly the same radius between the transverse vane and far tank wall. There is also a higher liquid

height between the transverse vane and the near tank wall. Figure 3.17 shows the case for low fill fraction behaving as an extension of the high fill fraction liquid positioning.

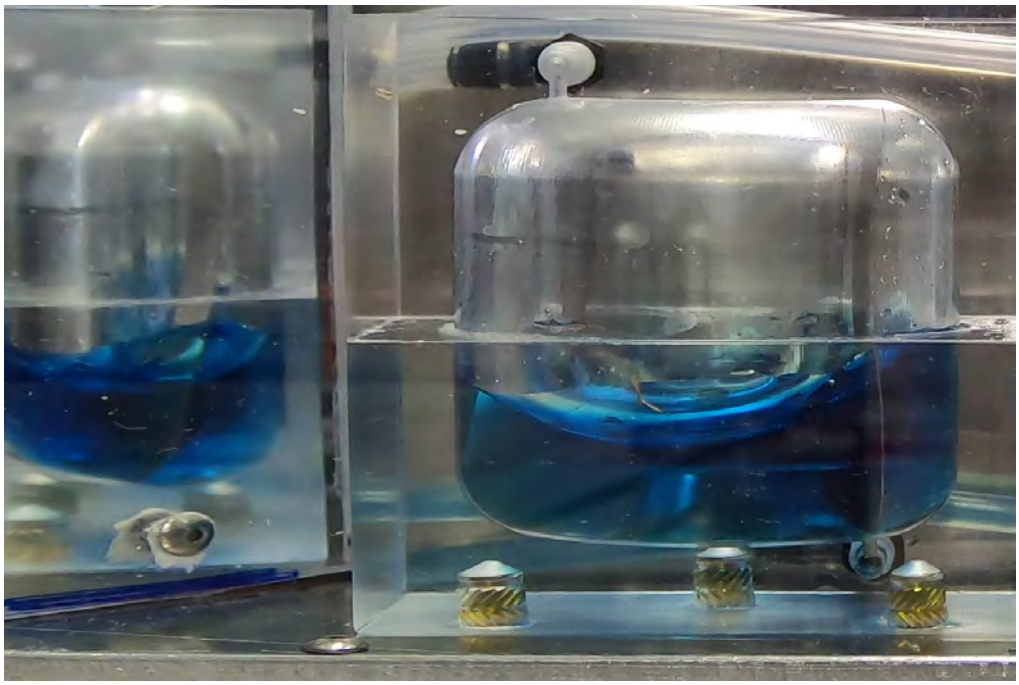

(a)

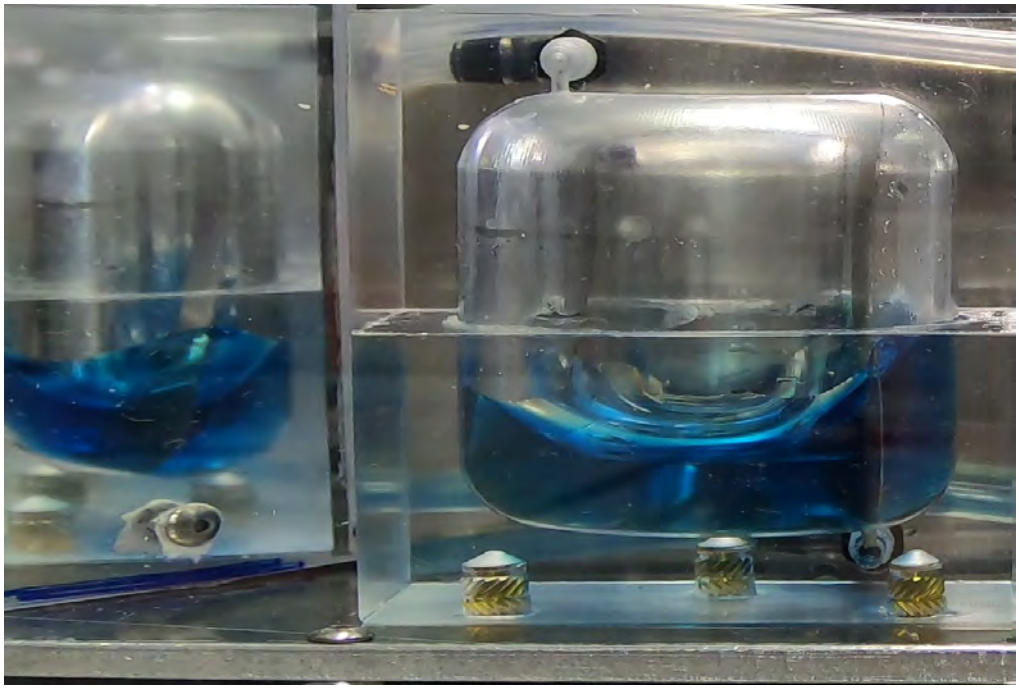

(b)

Figure 3.17. Arcs V1 Low Fill Fraction at 0±0.01g, Side View Left

A second case for the low fill fraction position is shown in 3.18. Here there is a more dramatic fillet between the transverse vane and far tank wall. There is also a higher liquid height between the transverse vane and the near tank wall than that shown in 3.17. This seems to be an extension of the positioning shown in 3.13, with more liquid between transverse vane and near tank wall, but with a less dramatic fillet from the transverse vane to the far tank wall.

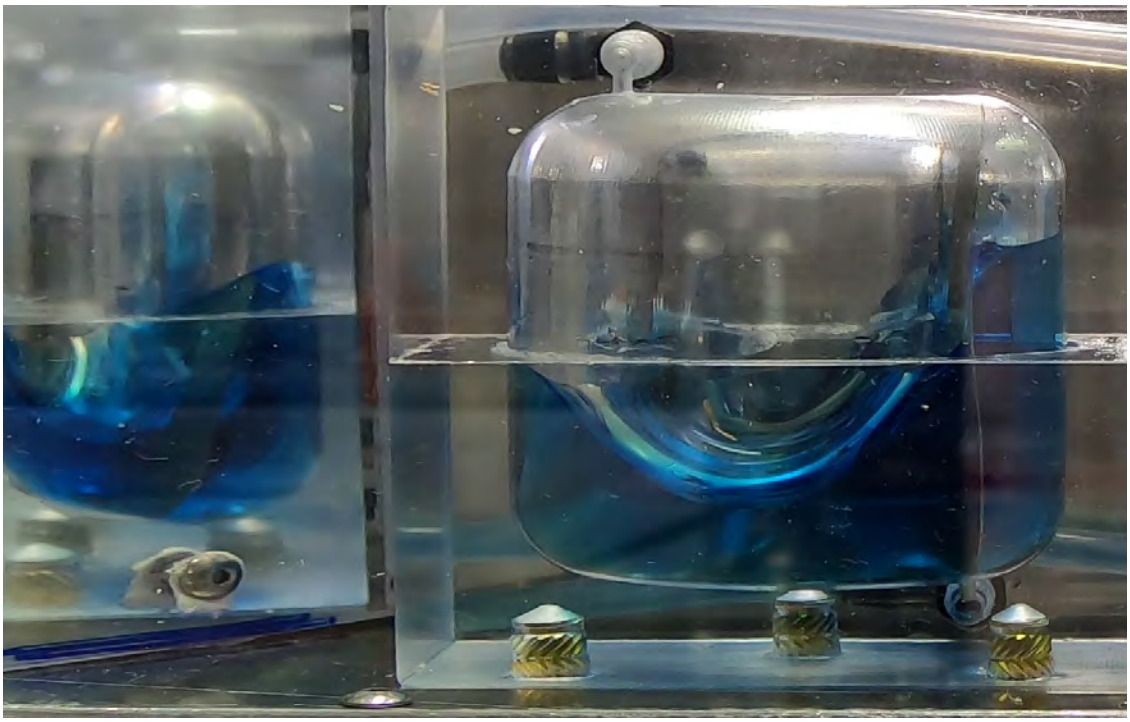

Figure 3.18. Arcs V1 Low Fill Fraction Outlier at 0±0.01g, Side View Left

3.1.6 Arcs V2 Results

The Arc tank with V2 vane design has one lateral vane extending from the corner with the tank outlet to the the next corner in the tank. For figures of the arc V2 tank the tank outlet is on the right for the blue liquid and is on the left for the green and red liquid. There is a short transverse vane at each corner of the tank the lateral vane reaches. This design results in 3 X shapes in the corners of the tank conjoined by the lateral vane. At a high fill fraction the bubble moves into the corner without any vanes. This positions the bubble near the top of the tank, and furthest away from the tank outlet. It is difficult to determine what

the liquids position is near the sides of the tank because of condensation inside of second containment and refraction from the tank body. Figure 3.19 shows two cases of the Arc V2 tank with high fill fraction.

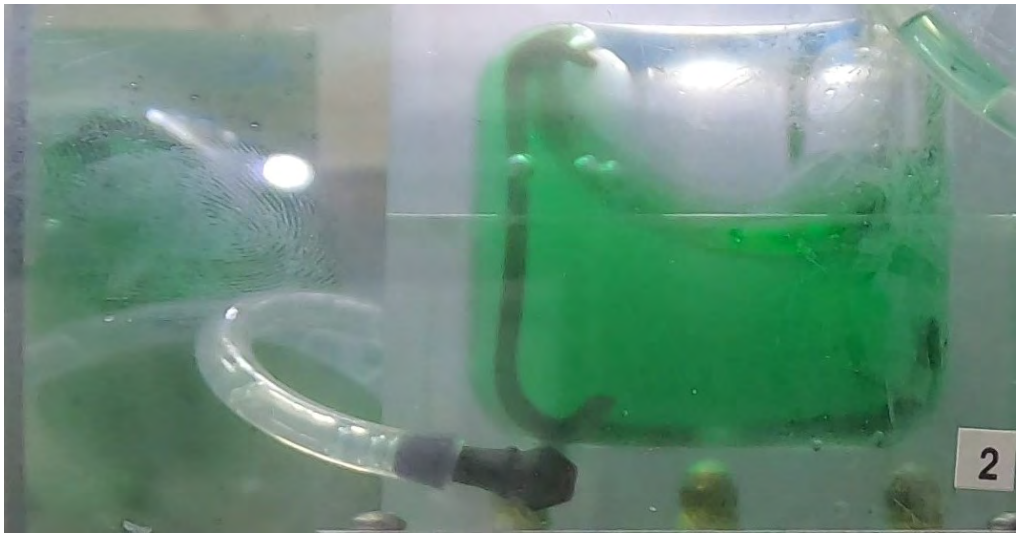

(a)

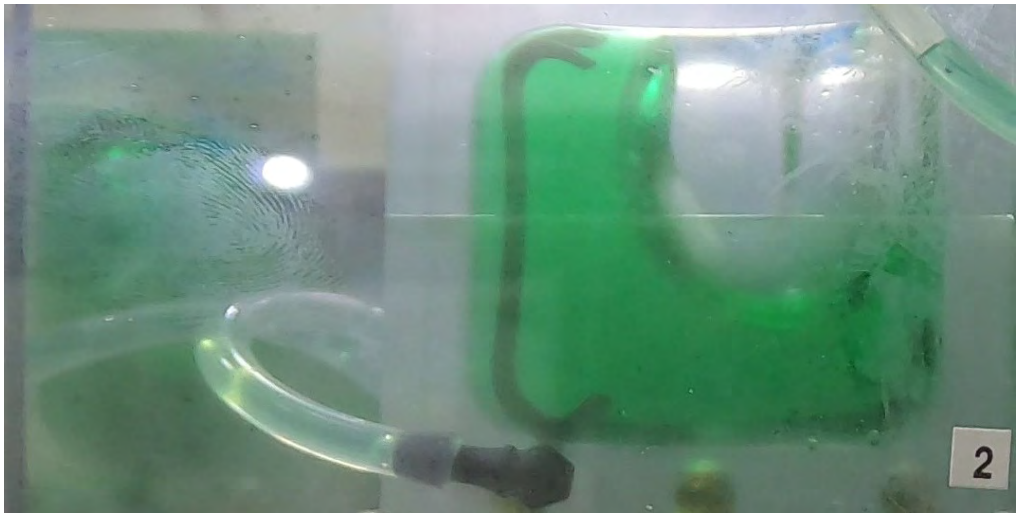

(b)

Figure 3.19. Arcs V2 High Fill Fraction at 0±0.01g, Side View Left

At a medium to high fill fraction the liquid wicks very little in the Arcs V2 tank. At this point the only section of the vane that is touching the tank is the lateral vane's vertical section on one one tank wall. At this fill fraction there is a minimum of the vanes width near the contact line. Since the vanes are small they do not dominate the liquid position,

but the tanks geometry does. Figure 3.20 shows three examples of the liquid position at a medium fill fraction.

(a)

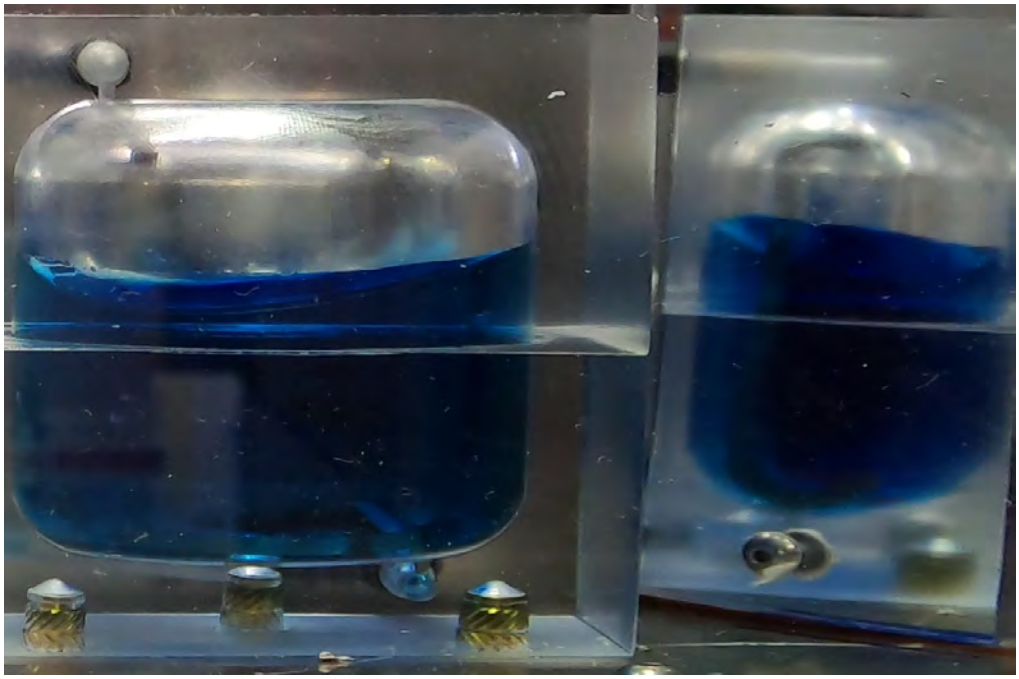

(b)

Figure 3.20. Arcs V2 Medium Fill Fraction at 0±0.01g, Side View Right

Figure 3.20. continued

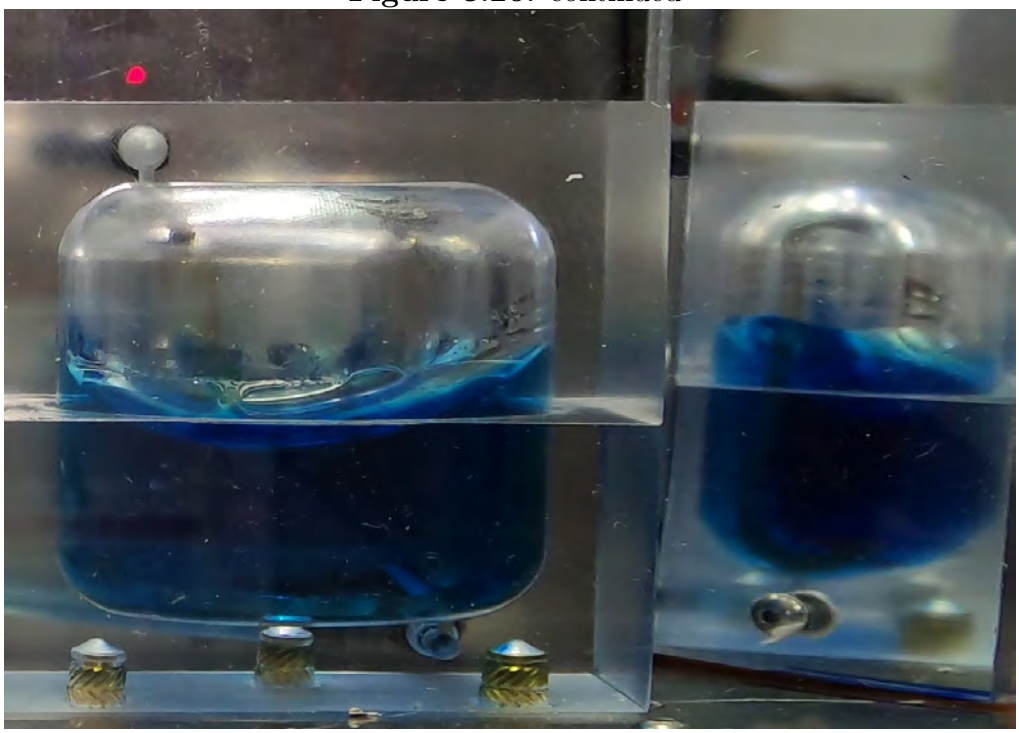

(c)

At a low fill fraction the Arcs V2 tanks have the same features as at medium fill fraction, but with a higher wicking height. In figure 3.21 the liquid wicks up the lateral vane from the bottom right corner of the tank, near the outlet. In the center of the tank is a liquid fillet between the two sides of the tank, which sweeps up into the left side of the tank.

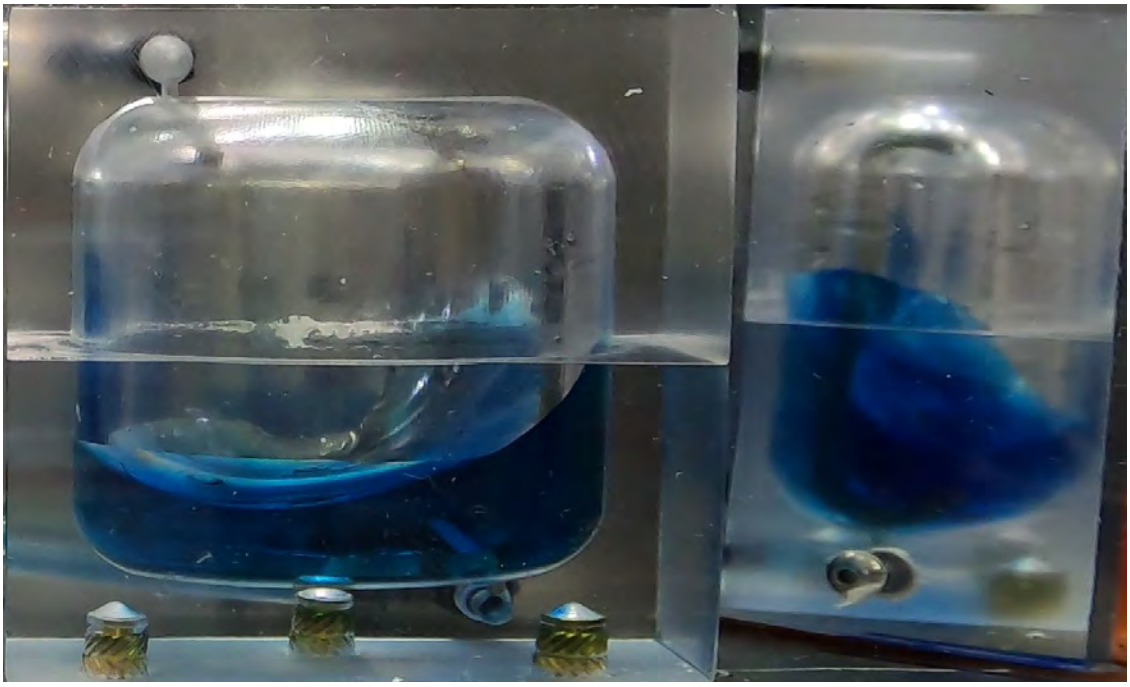

Figure 3.21. Arcs V2 Low Fill Fraction at 0±0.01g, Side View Right

An interesting feature at low fill fraction can be seen in figure 3.22. Here the liquid wicks almost all of the way up into the top right corner of the tank. In the center of the tank there is a steep drop off in liquid height, which is then slowly recovered as the liquid reaches the left side of the tank. This image was taken at the same time as figure 3.18, which shows a similar phenomenon in the Arcs V1 tank, which says that the liquid position is most likely due to light turbulence experienced on the airplane.

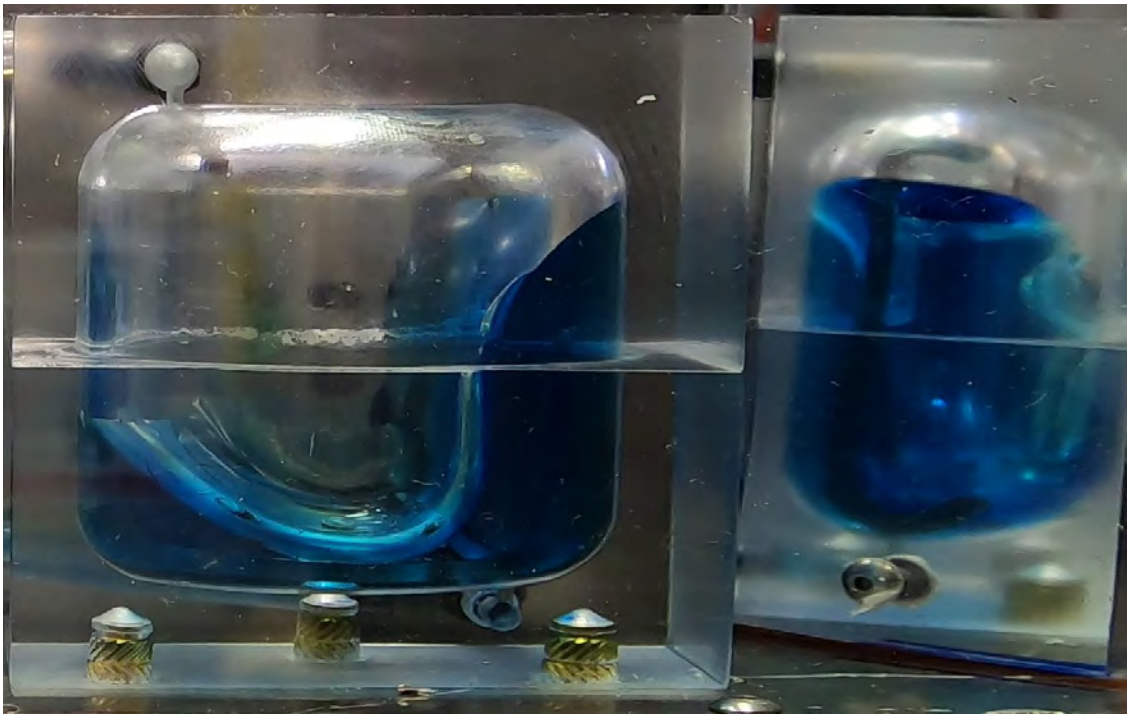

Figure 3.22. Arcs V2 Low Fill Fraction Outlier at 0±0.01g, Side View Right

Arcs V2 Results With Silicon Oil

The arcs V2 tank was also tested with Silicon Oil as the propellant simulant. At medium fill fractions the bubble oscillated up and down rapidly, which makes it extremely difficult to determine the liquids static position. This phenomenon was not seen in the propylene glycol case and implies that Silicon Oil and thus low contact angle liquids are more sensitive to the airplanes motion. At medium fill fractions the bubble would be concentrated at the center of the tank, with liquid along the lateral faces of the tank. When the bubble was at the top of the oscillation the liquid would be in contact with the top of the vane and bubble occupies the opposite corner of the tank. Figure 3.23 shows some examples of the liquid position at medium fill fractions. Additional figures of selected tanks and fill fraction can found in section F of the appendix.

(a) Top of the Bubble's Oscillation

(b) Bottom of the Bubble's Oscillation

Figure 3.23. Arcs V2 Silicon Oil Medium Fill Fraction at 0±0.01g, Side View Right

3.2 Lessons Learned

Throughout the duration of the experiment, several lessons were learned regarding experiment design and testing. The areas where lessons were learned include payload rack feet hole size, second containment design, pump speeds, and the human interface.

While installing the payload rack to the ZeroG airplane for the May 2021 flight, the holes in the feet did not line up with the installation points on the airplane. In an effort to make installation easier for the next flight in December 2021 the holes in the payload rack feet were increased to 1/2 an inch in diameter from .397 inch diameter. Installation of the experiment onto the ZeroG airplane in December took much less time, and 1/2 inch mounting holes are now standard in ZeroG's Payload User Guide.

As the pods were being designed in the spring of 2021, the team had few physical parts and attempted to design the pods with computer aided design. The resulting design had enough room in second containment for the tanks, pumps, mirrors, one media bag, and one air bag. The design goal was to have four tanks per pod which require two media bags, and two air bags to run properly. The design goal was not achieved because the media and air bags are difficult to model using computer aided design. A majority of the pod design and hardware was to be reused for the December 2021 flight, and during the summer AAE 418 course a physical mock up of second containment was produced. The new physical model had the lid of second containment sitting atop a 2 inch U channel base, and instead of using hex stand offs to mount the pumps 3D printed pump stands were used. The design changes ensured that all required media and air bags could fit in second containment while also reducing tubing kinking as a result of the new pump positions. The physical model also allowed for media and air bag positioning to be improved upon.

One difficulty that remains unsolved through the life of the experiment is the Welco WPM EA series maximum pump speed. The WPM EA series pump is a peristaltic stepper motor with 150 RPM as the specified maximum. With the setup described in the Electrical System section with Arduino Leonardo micro controllers and Polulu A4988 stepper motor drivers only 46 revolutions per minute could be achieved. Using an oscilloscope the pulse train coming from the Arduino Leonardo was determined to be adequate to run the pumps at a

higher speed. Testing with the oscilloscope between the Polulu motor driver and the motors was not accomplished, since the power supply would be shorted out through a common ground with the oscilloscope. However, according to Polulu documentation the selected motor driver is adequate for the EA pump series. In lieu of the custom built boards and for faster pumping speeds, a transition to brushed direct current motor powered pumps in the future is recommended. For a new experiment in May 2022 the Adafruit Motorshield was tested with brushed direct current motor pumps from US Solar Pumps and Welco. Using these combinations 8 ml/s flow rate was achieved, while the EA series pump could only achieve 0.13 ml/s. The build time is faster for brushed DC pumps since it relies only on commercially available boards and is more flexible in the flow rates needed for different experiments. The combination of hardware for the DC brushed motors is also less expensive than the hardware for the stepper motors.

Improvements that could be made to the human interface include feedback on the electrical system and ease of use. The buttons that run the pumps have an internal LED. It would be helpful to wire the LED so that it turns on when the pumps are running on a pod. During the flight it is difficult to check if the pumps are on because looking in different directions quickly can result in motion sickness in weightlessness. Researchers are already looking at the buttons and feedback through the LED would be an easy way to check if the pumps are running. Another way to improve the human interface of the experiment is to replace the sliding switch that changes the pumping direction with a toggle switch. The toggle switch would function in the same way as the sliding switch, but would be much easier to use in weightlessness. In weightlessness it is very challenging to brace your body and find the groove in the switch to change the pumping direction. Using the toggle switch would be as simple as turning the lights on in a room.

4. CONCLUSION

Conformal tanks that optimize tank volume are a driving factor in design for many small satellites. Conformal propellant tanks introduce new challenges in propellant management with increasingly complex geometry compared to traditional large satellite propellant tank designs. Further, the transition to new green propellants with a large contact angle makes the performance of conformal tanks unknown. To test various designs, a payload rack with 11 pods was flown on the Zero G airplane. Using the Zero G airplane for the experiment is particularly useful for this research because of its flexibility and many periods of weightlessness throughout a flight.

During the four flights, multiple tank geometries were tested including: traditional, blended, stamped, stiffened, arc V1 and arc V2. The traditional tank is a cylinder with hemispherical end caps and symmetric oval vanes that go from the top to the bottom of the tank. The blended, stamped, and stiffened tanks have increasingly complex geometry. The stiffened tank is the most complex and models a stamped propellant tank with ridges added for increased stiffness. The arc tanks have the same interior tank geometry but have different vanes inside. The arc tanks are meant to model a propellant tank wrapped around a satellite structure in an effort to optimize volume. Each tank design was evaluated at all possible fill fractions.

At all fill fractions in the traditional tank silicon oil wicked to the top of the tank and into the tank air outlet. At high fill fractions the liquid would encapsulate the bubble, and as fill fraction was reduced the liquid would surround the gas in the tank less. In the blended tanks at a high fill fraction of propylene glycol the bubble stayed near the top of the tank or between the radial vanes. At a medium fill fraction there was a large discontinuity in liquid height across the lateral vane and some wicking to the lower radial vane. As the fill fraction was lowered the discontinuity across the lateral vane decreased and the bulk of the liquid was positioned closer to the radial vanes. The stamped tanks behaved similarly to the blended tanks at a low fill fraction with most of the liquid around the radial vanes. At very low fill fractions stamped tanks had the bulk of the propylene glycol centered around the radial vanes and near the tank outlet. For the stiffened tanks at a medium to high fill

fraction, the contact line would not go above the fourth ridge in the tank. At this fill fraction there was a discontinuity in liquid height across the lateral vane on the left side of the tank and liquid wicking up the shallower radial vane. At low fill fractions liquid would wick into the nearest ridge and along both radial vanes. Very low fill fractions behave the same as the stamped tank, with no discontinuity in height across the lateral vane and the bulk of the liquid around the radial vanes.

Three phenomenon were seen at a high fill fraction for the arc V1 tank. The first being the liquid taking up all of the volume between the transverse vane and the wall of the tank. The next being liquid not completely filling the space between the transverse vane and the tank wall. The last phenomenon being a bubble attached to the top of the tank. Medium fill fractions exhibit similar phenomenon to the second case covered at a high fill fraction. The low fill fraction also exhibits the same behavior except for one parabola where the liquid almost wicked all the way to the top of the tank between the transverse vane and the near wall of the tank. At a high fill fraction in the arc V2 tank the bubble was attached to the top of the tank, like one of the V1 cases. The liquid would wick up the lateral vane at a medium fill fraction. In some cases, the liquid would wick up the lateral vane much higher than was seen in other parabolas. This occurred at the same time the arc V1 tank had increased wicking height and in the same location. When the liquid was changed to Silicon Oil in the arc V2 tank, the bubble would oscillate up and down, and would be at the center of the tank or attached to the top of the tank.

Further modeling work includes investigating the seams between stamped tanks and other generalized tank shapes. Unfortunately a conclusion on the effect of the seams on liquid positioning for the stiffened and stamped tanks could not be made. A conclusion could not be drawn because the seam was small compared to the tank and visual distortions at the tank ends because of the rounded interior. An alternative method to model the seam would use two vertical halves that comprise a tank, like the last design. Instead of the tank being rectangular in shape each tank could be more square with the tank seam facing the camera. Reducing the tank width would allow for more cases per pod, and each tank could have a different sized seam. Other generalized tank shapes that may be of interest could be a 60° arc and a right-angled trapezium. The 60° arc tank is a natural extension of the arc

tanks discussed in detail above. Since the proposed tank is wider and shallower than the arc tank previously examined, different PMDs may be needed. This tank shape could be used to predict performance of a satellite tank built from an ESPA ring. In this scenario, each payload adapter would house a different module of the satellite bus, with the propellant tank as a single module. The proposed arc tank can be found in figure 4.1. The right-angled trapezium tank is also a natural step in conformal tank research from the blended tank design. The proposed tank design attempts to use the interior tank geometry as an advantage. If the outlet is placed in the tightest corner of the tank, shown as the bottom left corner in figure 4.2 propellant may wick naturally to the tank outlet. Further, this tank design is of interest to satellite bus designers looking to optimize satellite volume. It is not a stretch to assume in an effort to optimize satellite volume one corner of a tank may be made smaller than the rest.

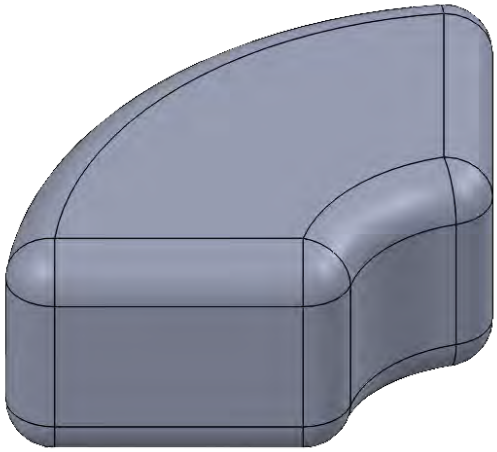

Figure 4.1. 60° Arc Tank Interior Tank Geometry

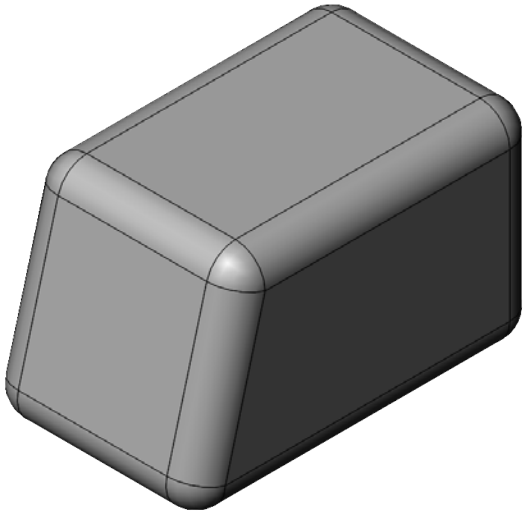

Figure 4.2. Right-Angled Trapezium Interior Tank Geometry

Although parabolic flight provides some advantages over suborbital research, this experiment could benefit from suborbital flight. Parabolic flight disturbs the fluid in the tanks more than suborbital flight. In parabolic flight, light turbulence can slosh the liquid around the tank and variations in body effects across different parabolas. Suborbital flight offers a definitive answer to the position of liquids at any fill fraction because it is closer to true weightlessness and is not significantly impacted by turbulence. Suborbital flight also allows for liquid trapping analysis of conformal tanks since they can be drained from a high fill fraction in a single period of weightlessness.

A. VANE DRAWINGS

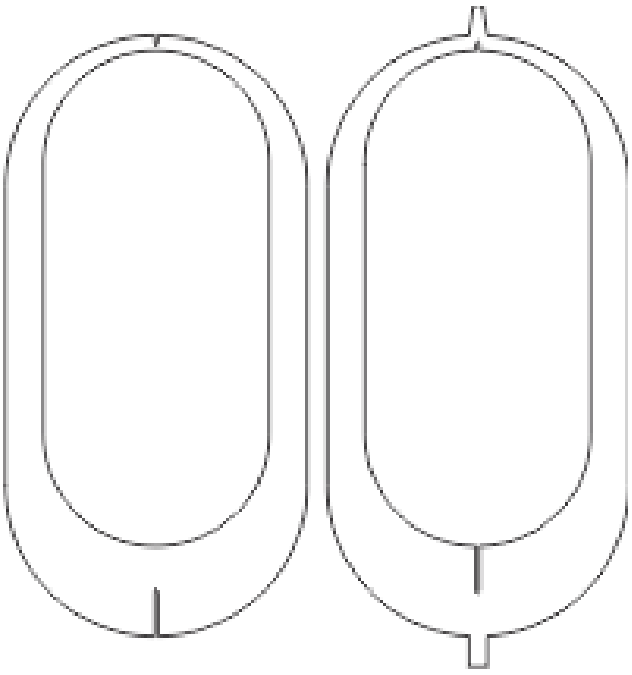

Figure A.1. Traditional Vanes

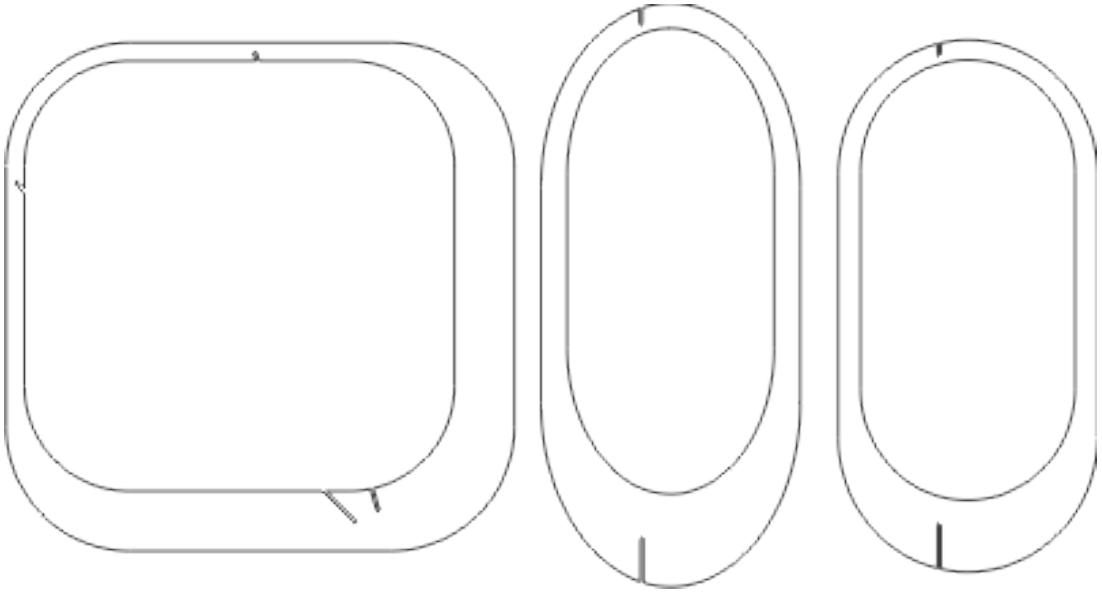

Figure A.2. Blended, Stamped, and Stiffened Vanes

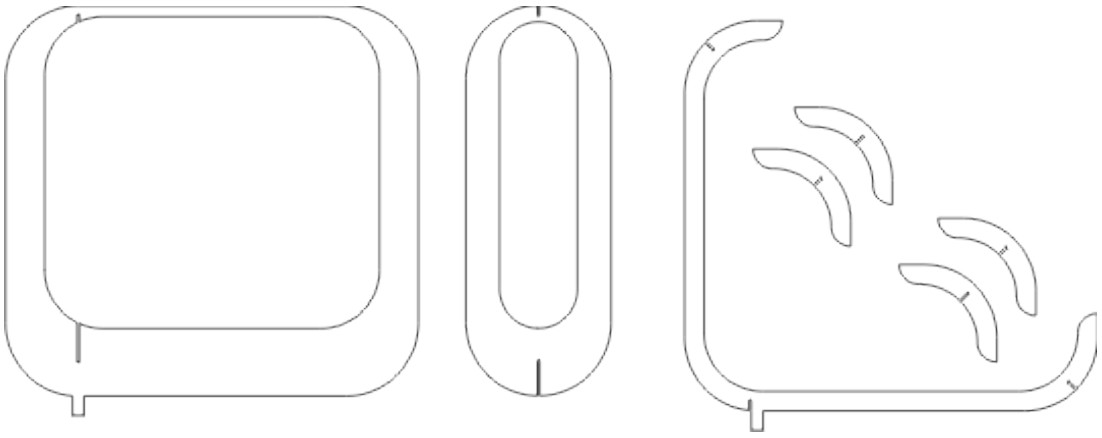

Figure A.3. Arc V1 & V2 Vanes

B. TANK DRAWINGS

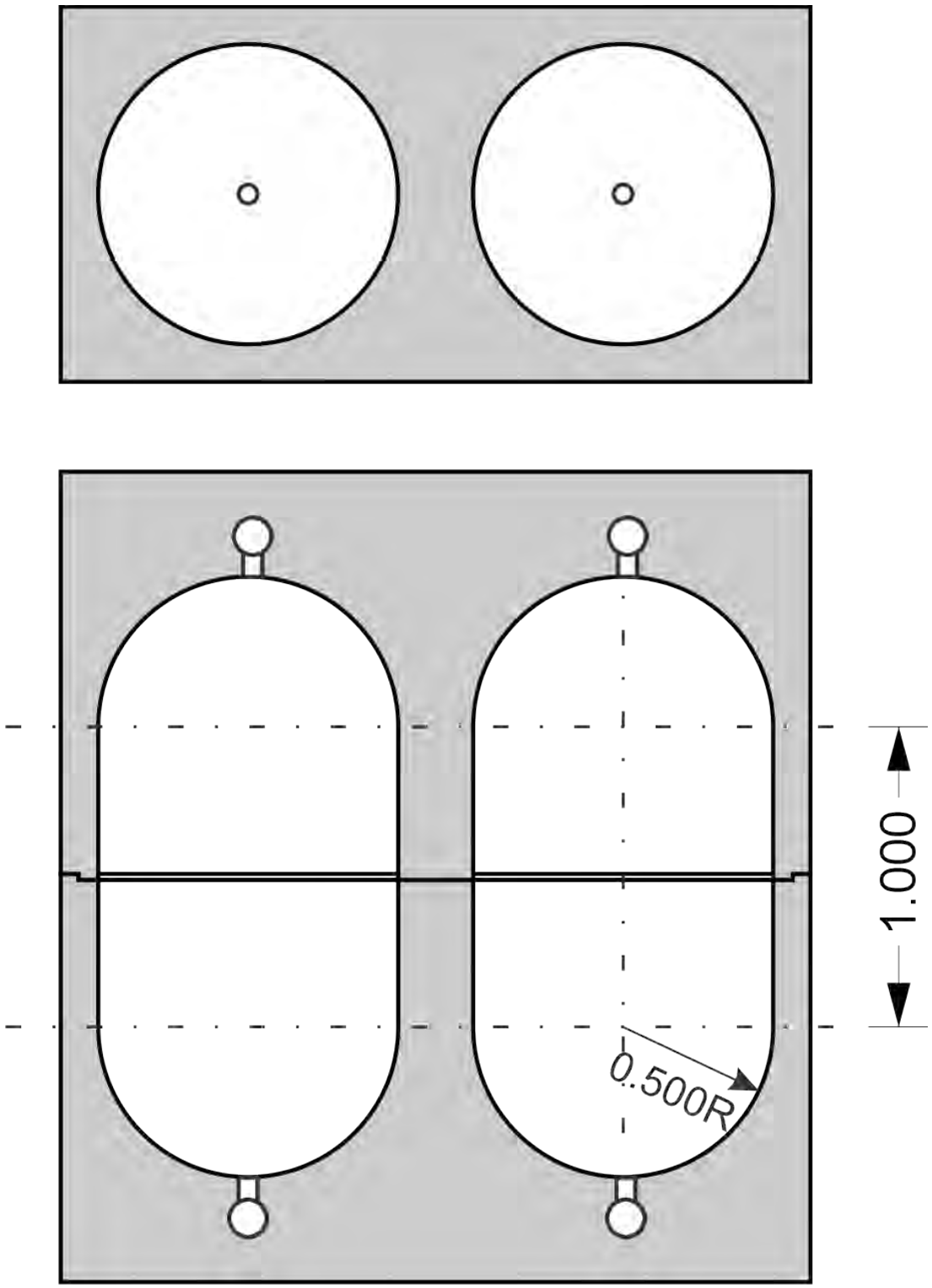

Figure B.1. Traditional Tank Drawing

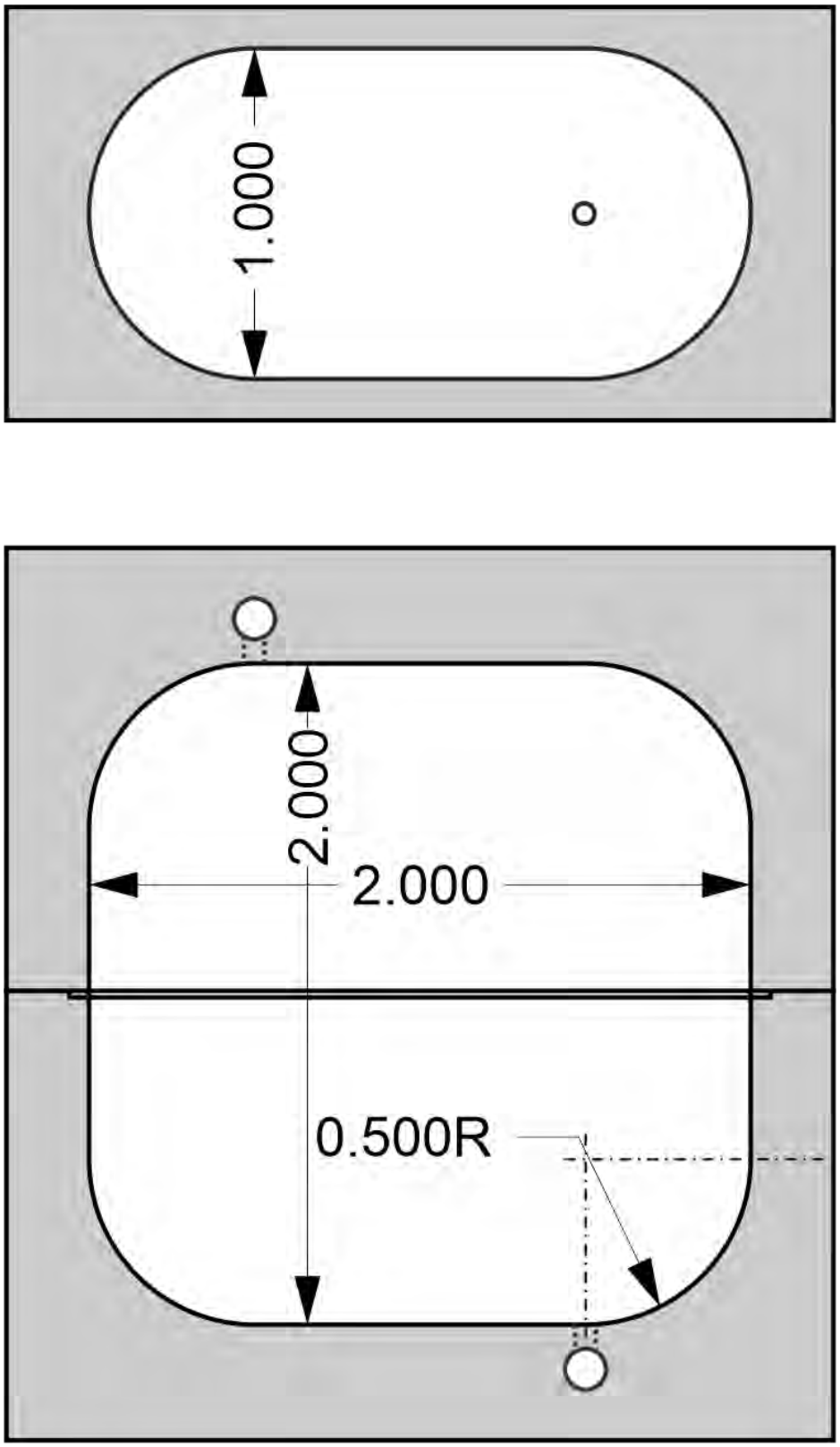

Figure B.2. Blended Tank Drawing

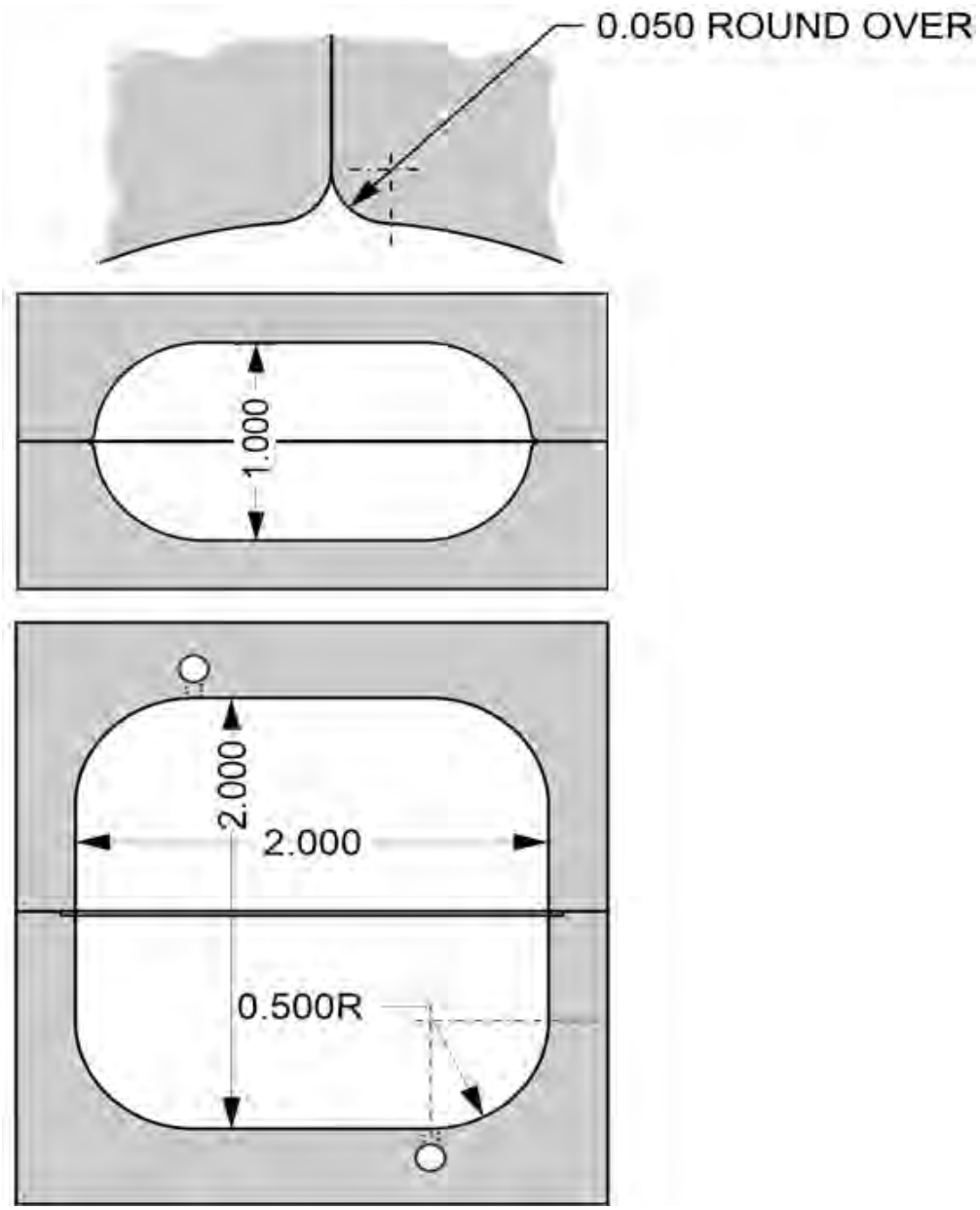

Figure B.3. Stamped Tank Drawing

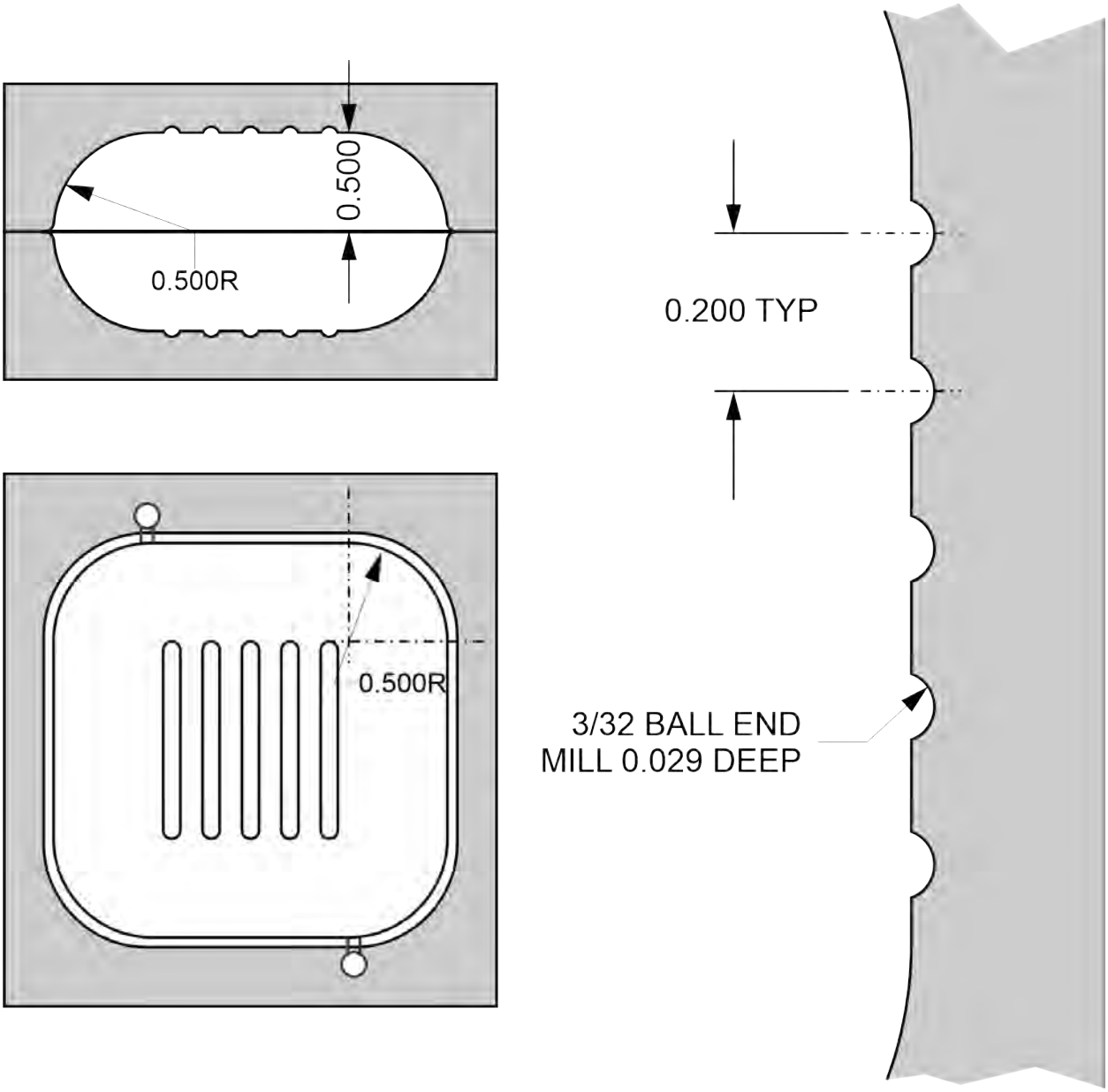

Figure B.4. Stiffened Tank Drawing

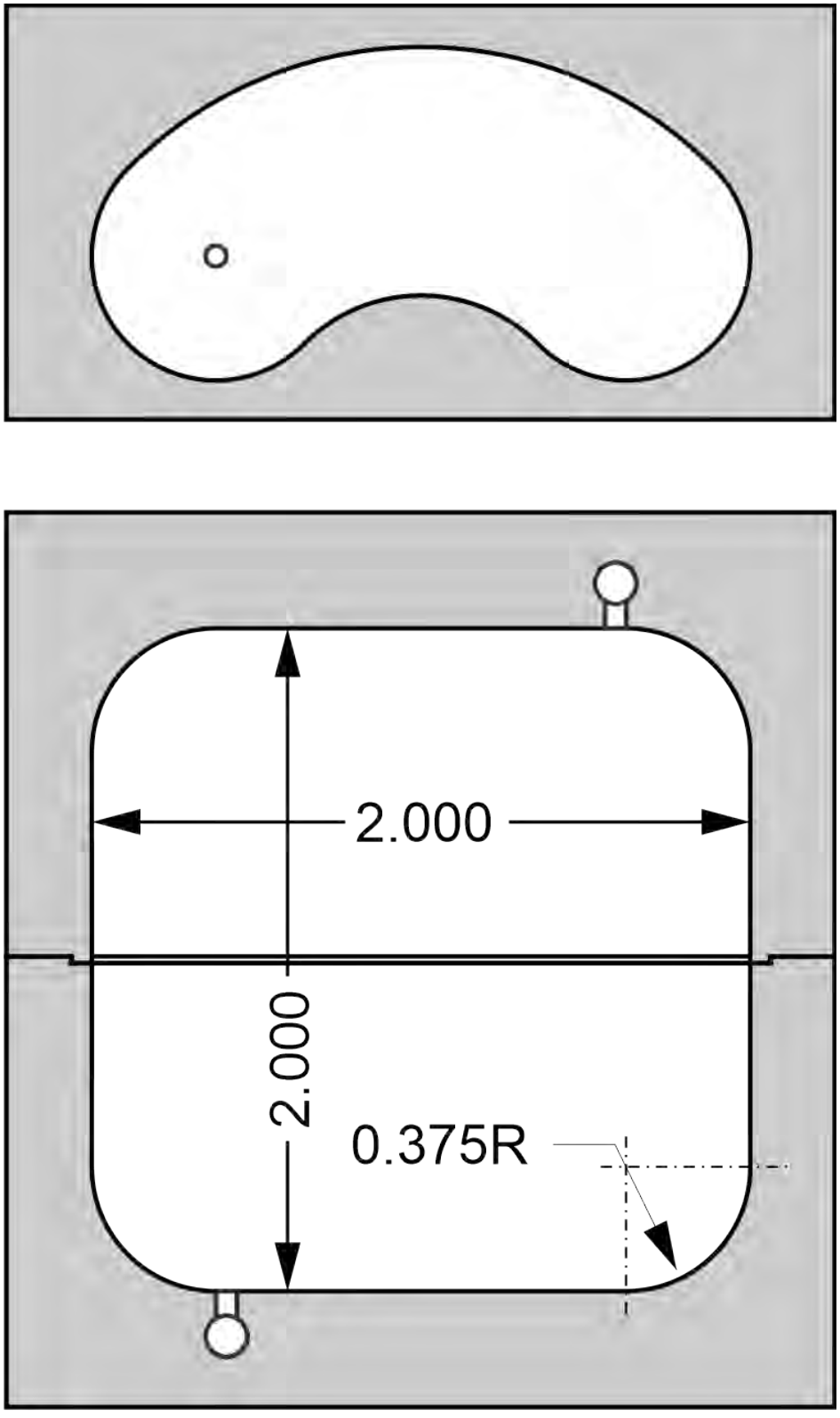

Figure B.5. Arc Tank Drawing

C. EXPERIMENTAL POD CODE

```
#include<Stepper.h>
//stepper motor initialization
const int stepsPerRev = 2800; //steps per rev of stepper motor
Stepper myStepper1(stepsPerRev, 0,4); //initializes motor in pin 0,4
Stepper myStepper2(stepsPerRev, 1,4); //initializes motor in pin 1,4
Stepper myStepper3(stepsPerRev, 2,4); //initializes motor in pin 2,4
Stepper myStepper4(stepsPerRev, 3,4); //initializes motor in pin 3,4

//Button initialization
int val = 0; //reads voltage across pins
int var = 0; //switches pump direction
int inPin = 6; //initializes the input pin
int tog_switch = 5; //input to arduino from toggle switch
int RPM = 46; //pump RPM

float step_num = (2800*RPM*15)/60; //Run time of 15 seconds

void setup() {
  pinMode(inPin, INPUT_PULLUP); // pin 6 as input from push button
  pinMode(tog_switch, INPUT_PULLUP);
}

void loopdrain() {

  if (digitalRead(tog_switch) == true) {
  var = 1; //if toggle switch is set to high, pumps rotate clockwise
  }

  if (digitalRead(tog_switch) == false) {
  var = -1; //if switch is set to low, pumps  rotate counter-clockwise
  }

  val = digitalRead(inPin); //reads input value from button
```

```
  if (val == LOW) //checks if button is pushed
  {

  //Output to motor controllers
  myStepper1.setSpeed(RPM);
  myStepper2.setSpeed(RPM);
  myStepper3.setSpeed(RPM);
  myStepper4.setSpeed(RPM);
    for(int s=0; s<step_num; s=s+1)
    {
      myStepper1.step(var);
      myStepper2.step(var);
      myStepper3.step(var);
      myStepper4.step(var);
    }
  }
}

void loop() {
  loopdrain();
}
```

D. PUMP FLOW RATE CALIBRATION

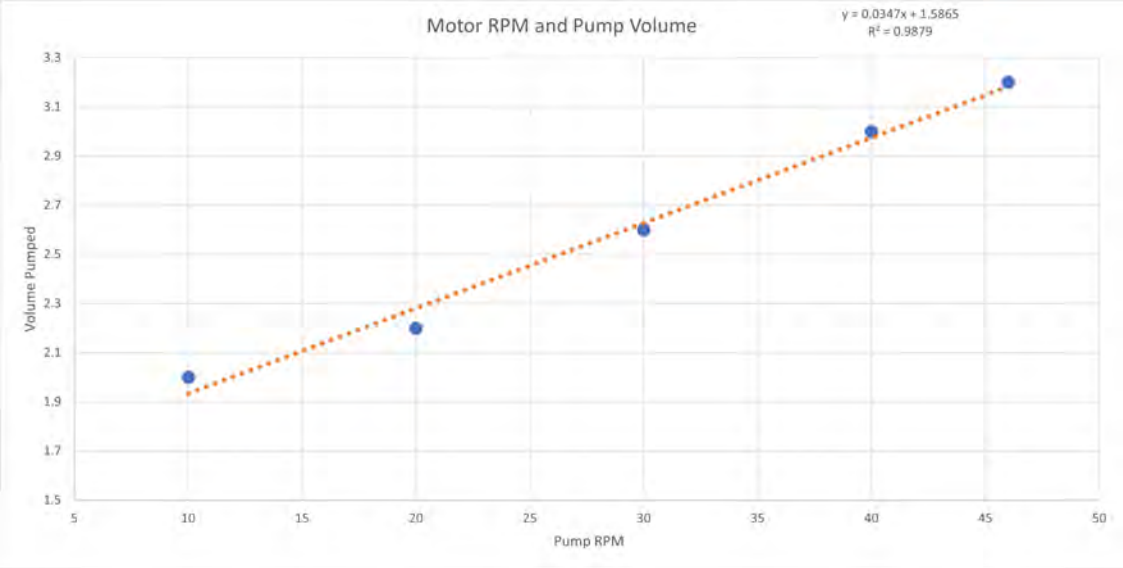

Figure D.1. Pump RPM vs. Flow Rate

E. EXPERIMENTAL POD ELECTRICAL SCHEMATIC

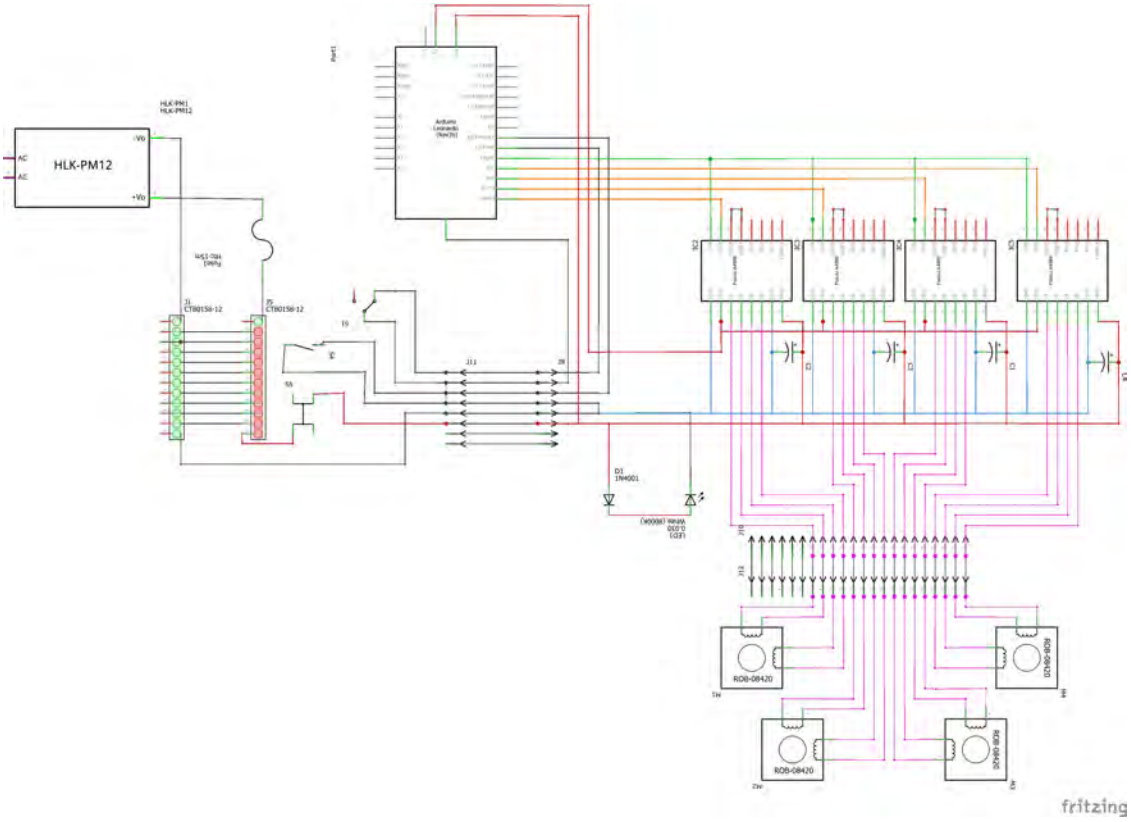

Figure E.1. Experimental Pod Electrical Schematic

F. ADDITIONAL FIGURES

F.1 Stamped Tank Additional Figures

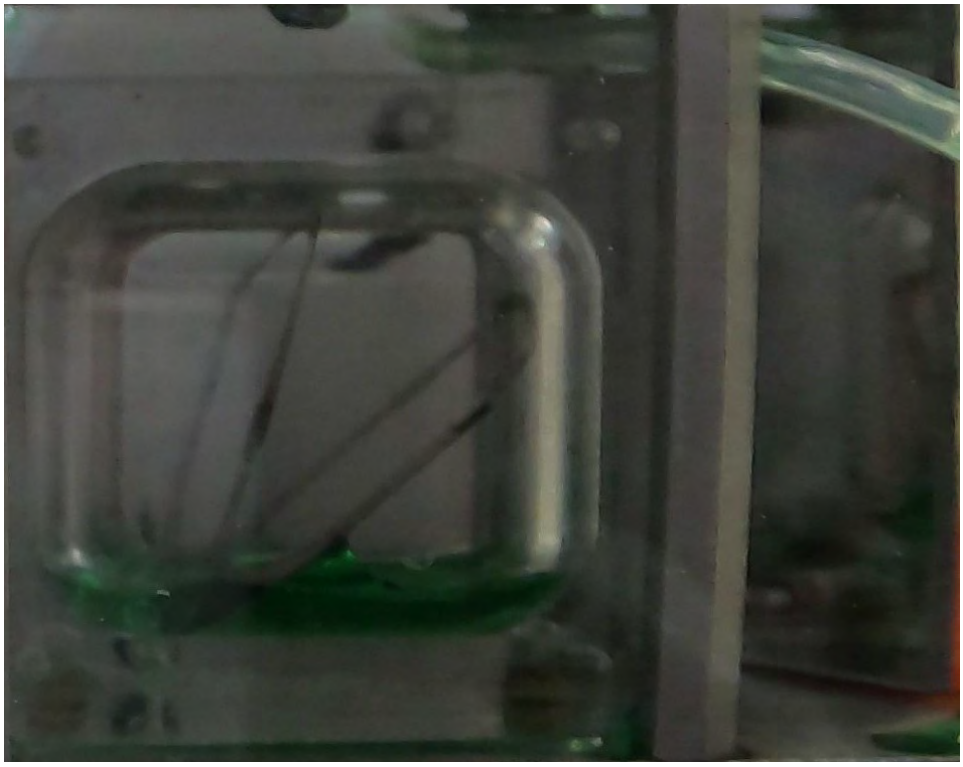

(a)

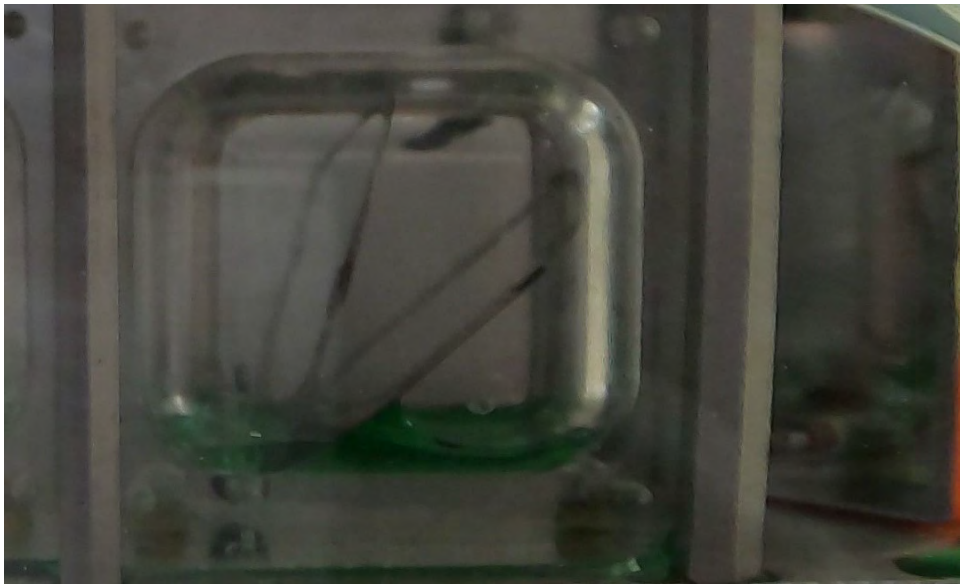

(b)

Figure F.1. Stamped Tank Low Fill Fraction

Figure F.1. continued

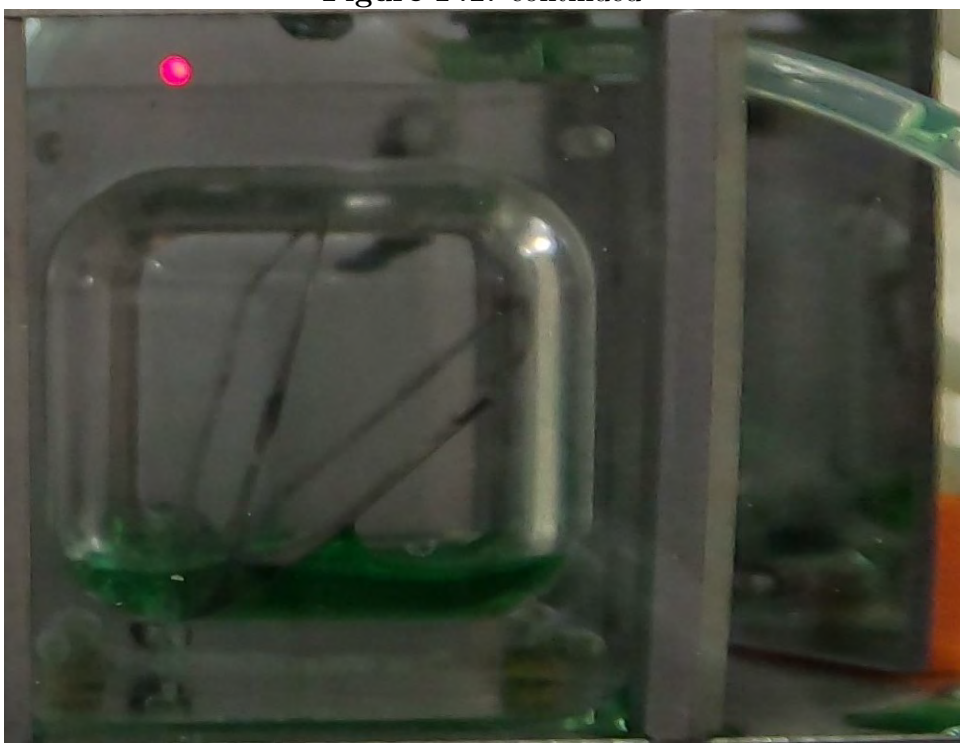

(a)

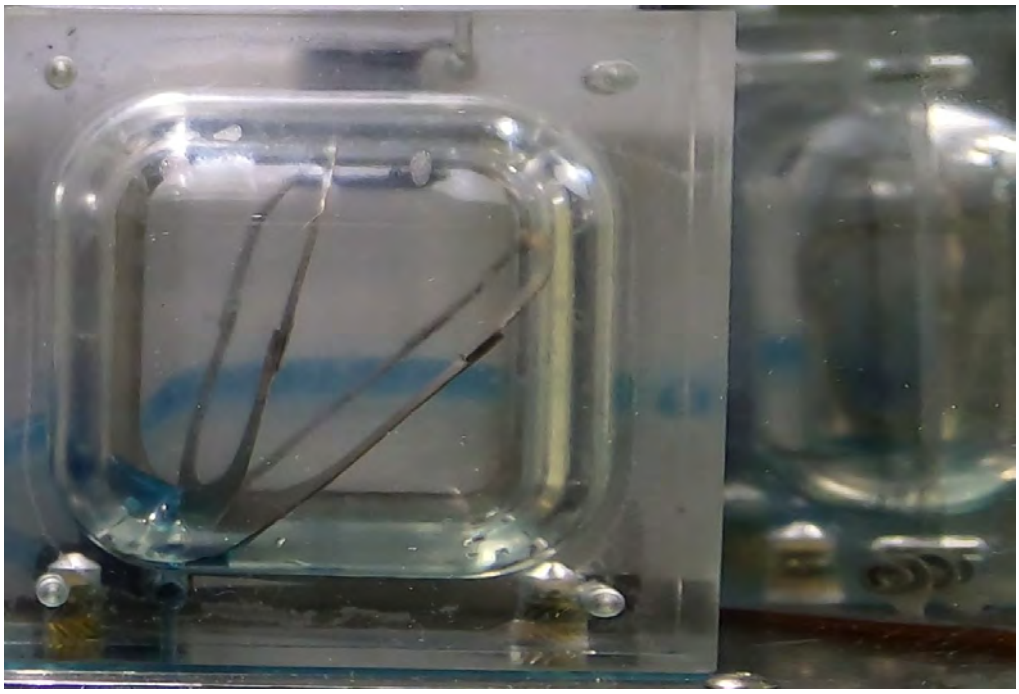

(a)

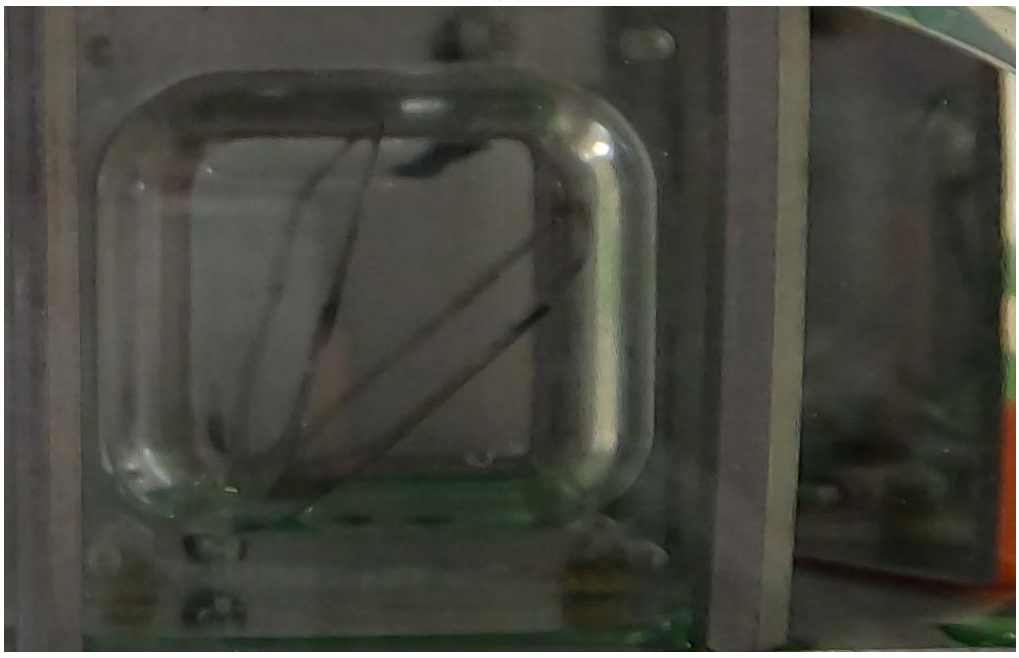

(b)

Figure F.3. Stamped Tank Very Low Fill Fraction

F.2 Stiffened Tank Additional Figures

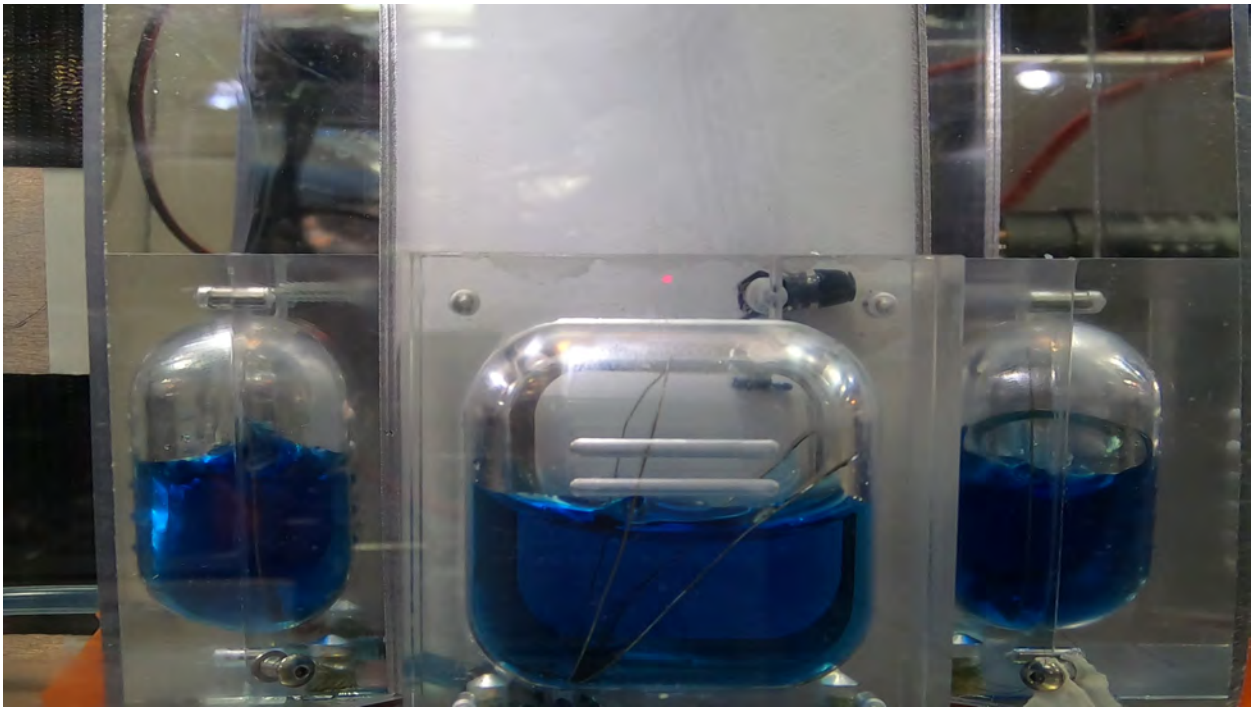

(a)

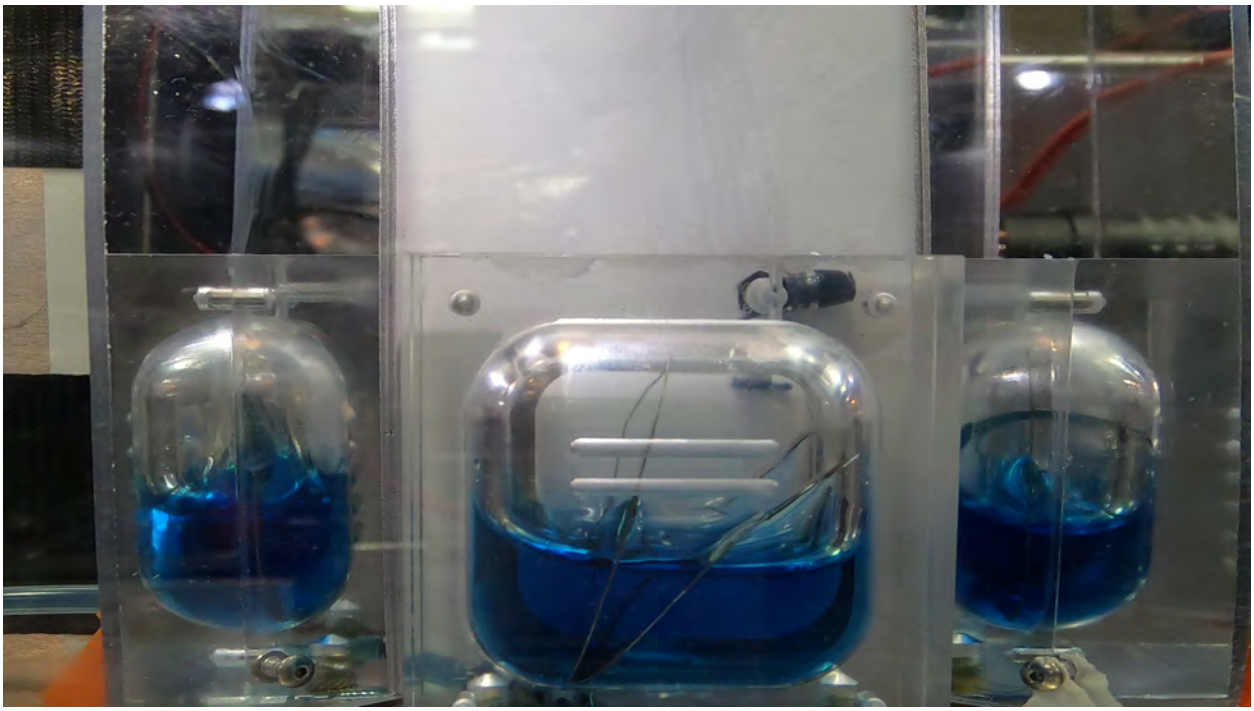

(b)

Figure F.4. Stiffened Tank Medium Fill Fraction

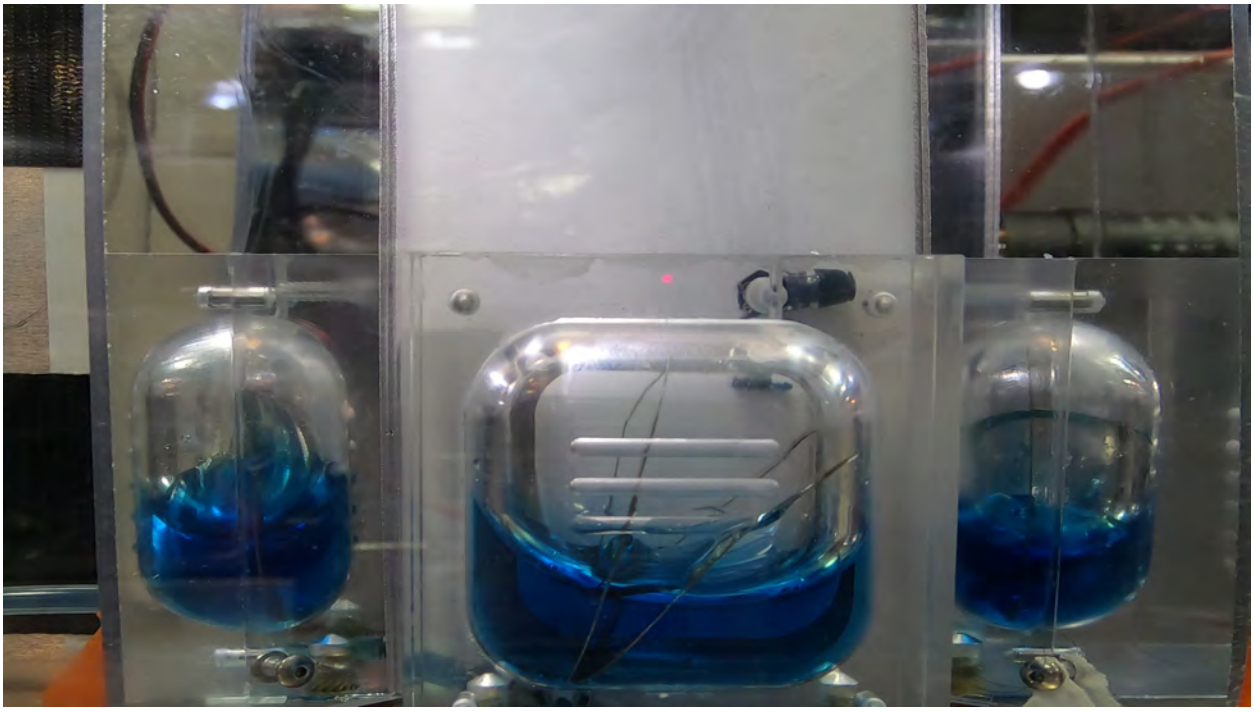

Figure F.5. Stiffened Tank Low Fill Fraction

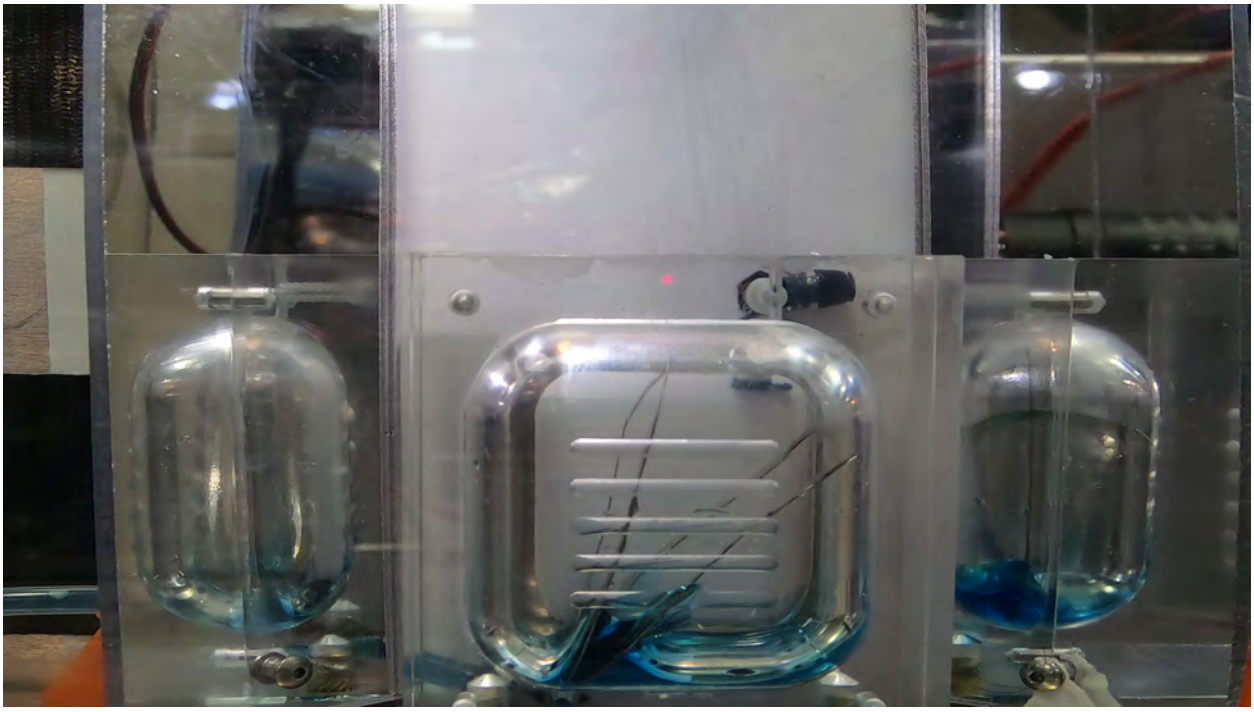

(a)

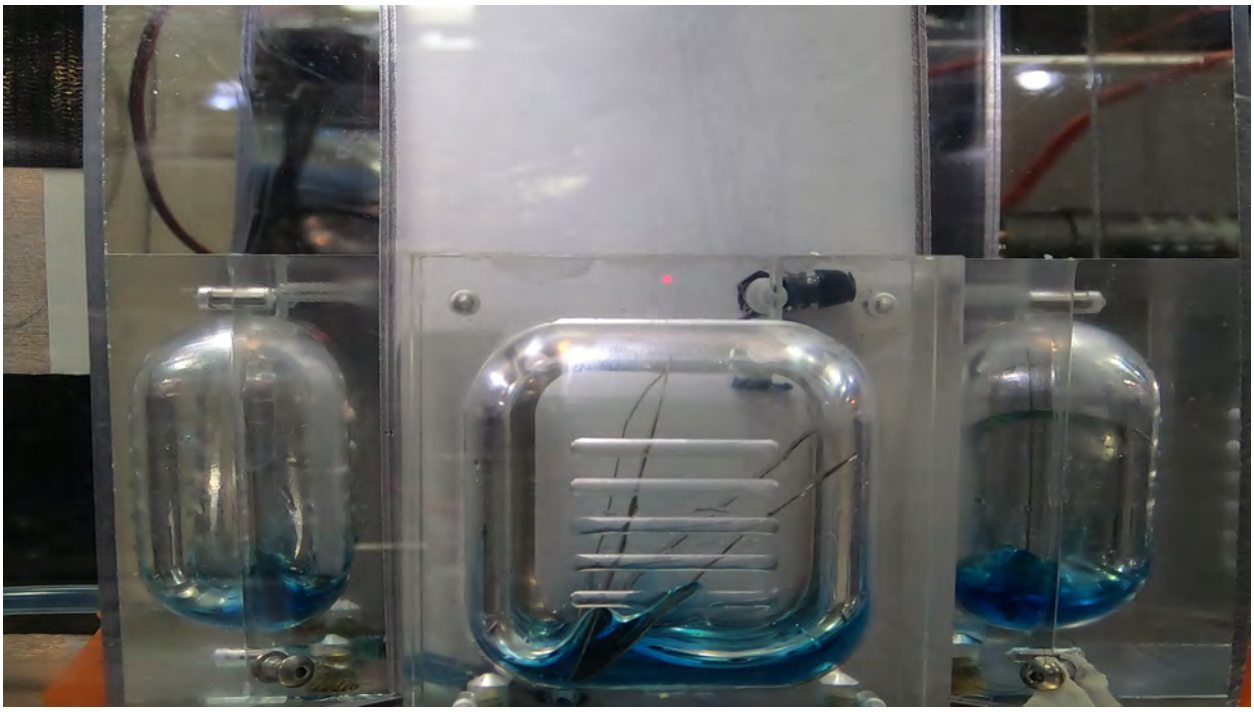

(b)

Figure F.6. Stiffened Tank Very Low Fill Fraction

F.3 Arc Tank Additional Figures

F.3.1 Arc V1

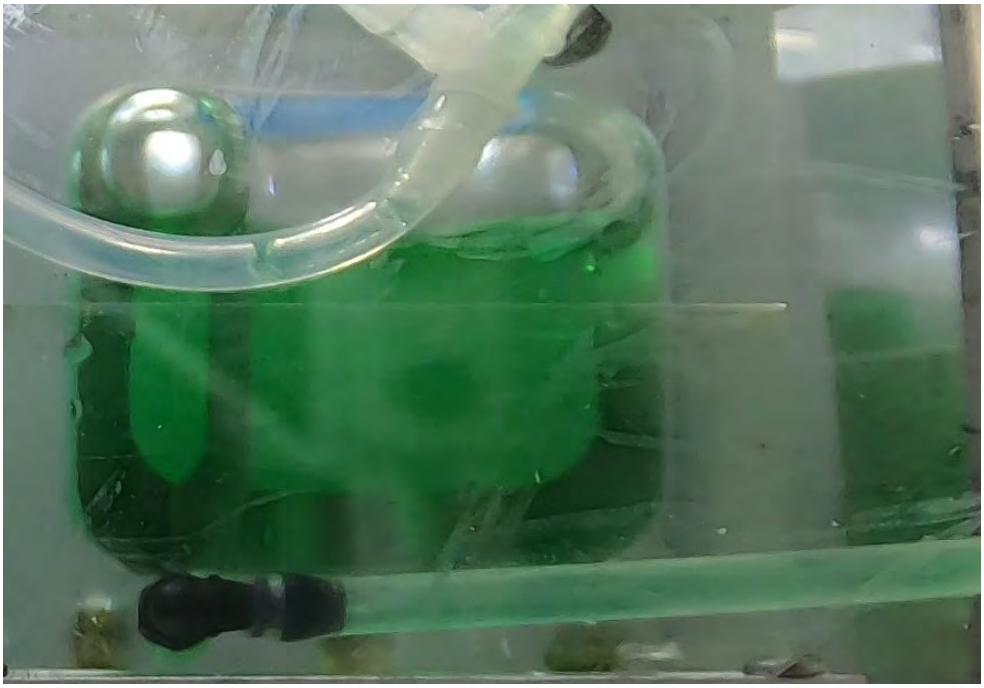

(a)

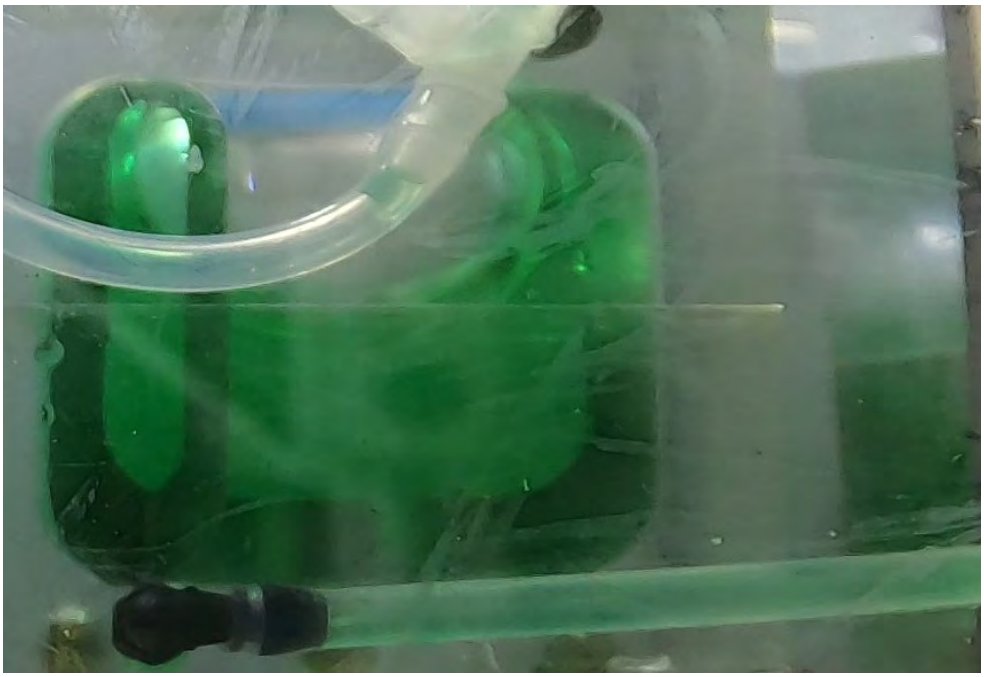

(b)

Figure F.7. Arc V1 Tank High Fill Fraction

Figure F.7. continued

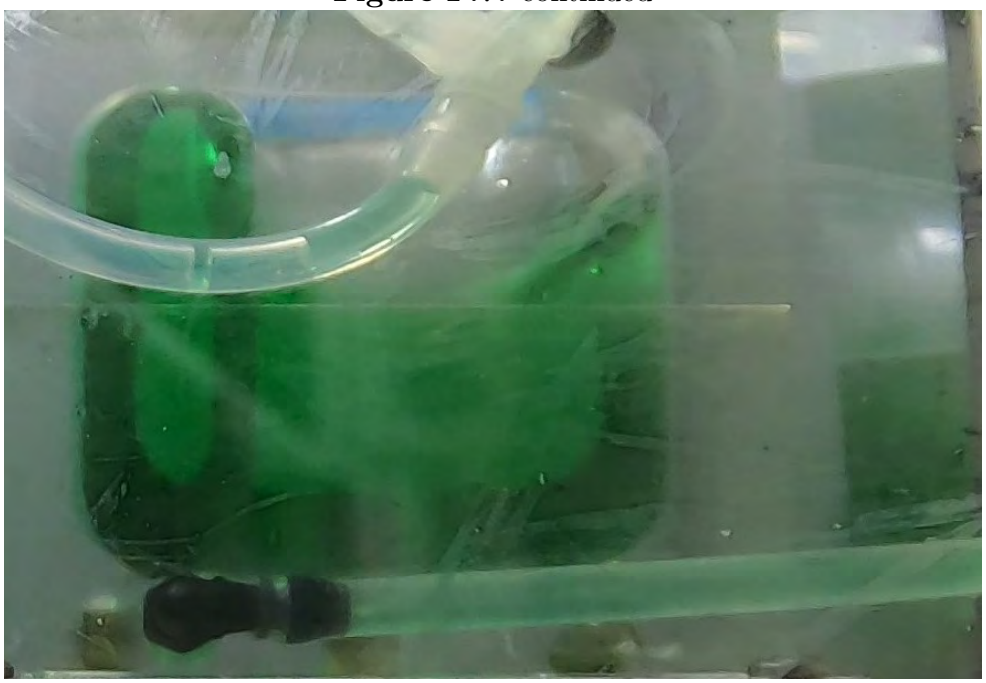

(c)

F.3.2 Arc V2

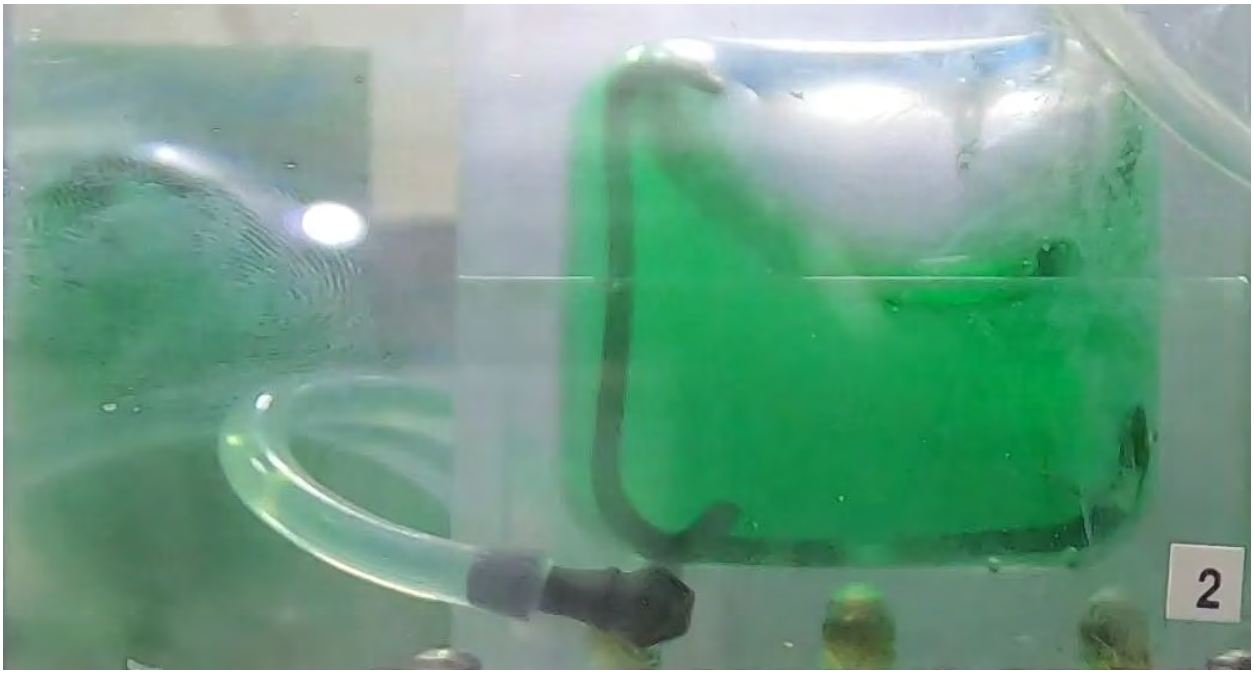

(a)

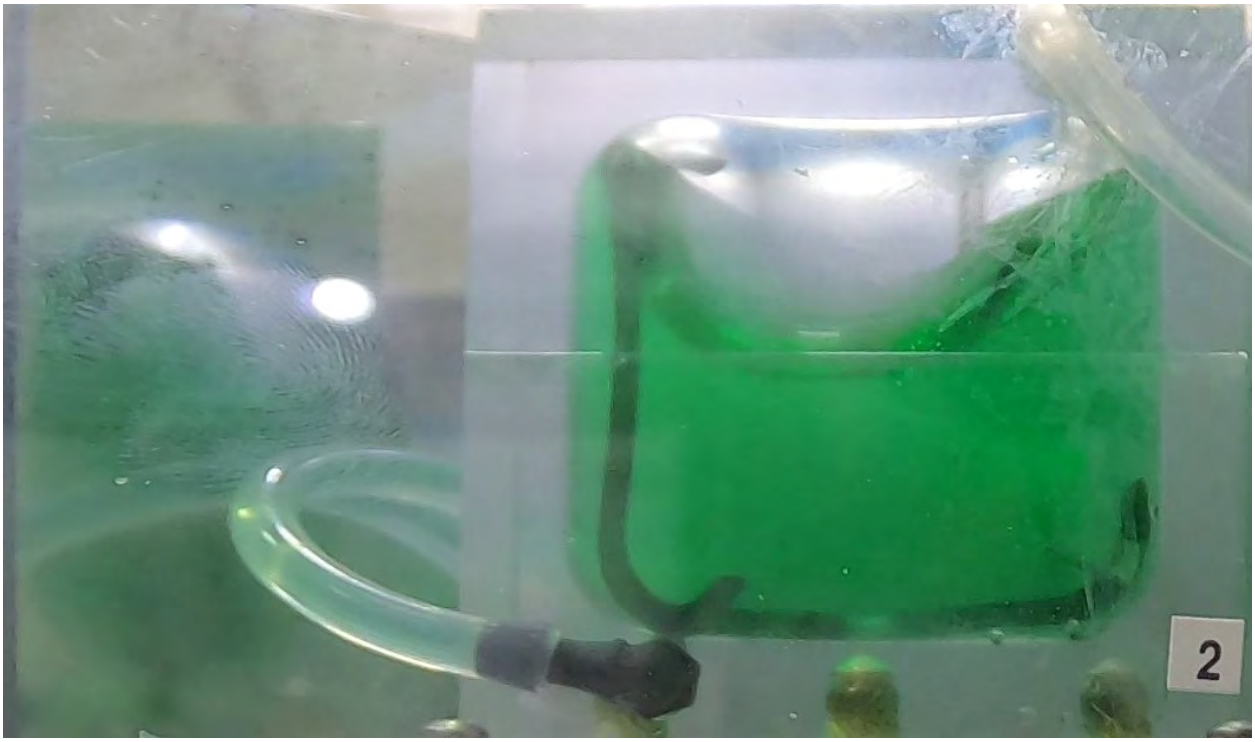

(b)

Figure F.8. Arc V2 Tank High Fill Fraction

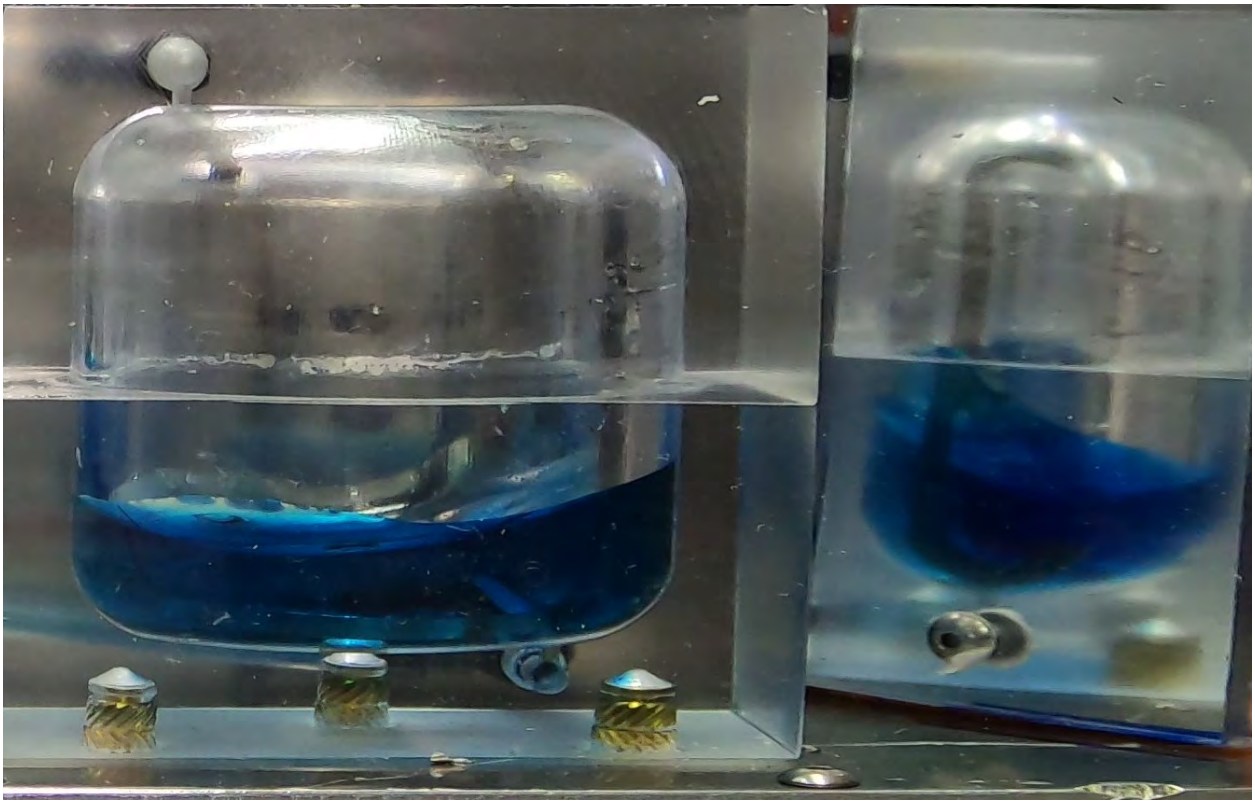

Figure F.9. Arc V2 Tank Low Fill Fraction

Arc V2 With Silicon Oil

(a)

(b)

Figure F.10. Arc V2 Tank Medium Fill Fraction With Silicon Oil

Figure F.10. continued

(c)

(d)

G. CONFORMAL TANKS MISSION PATCH

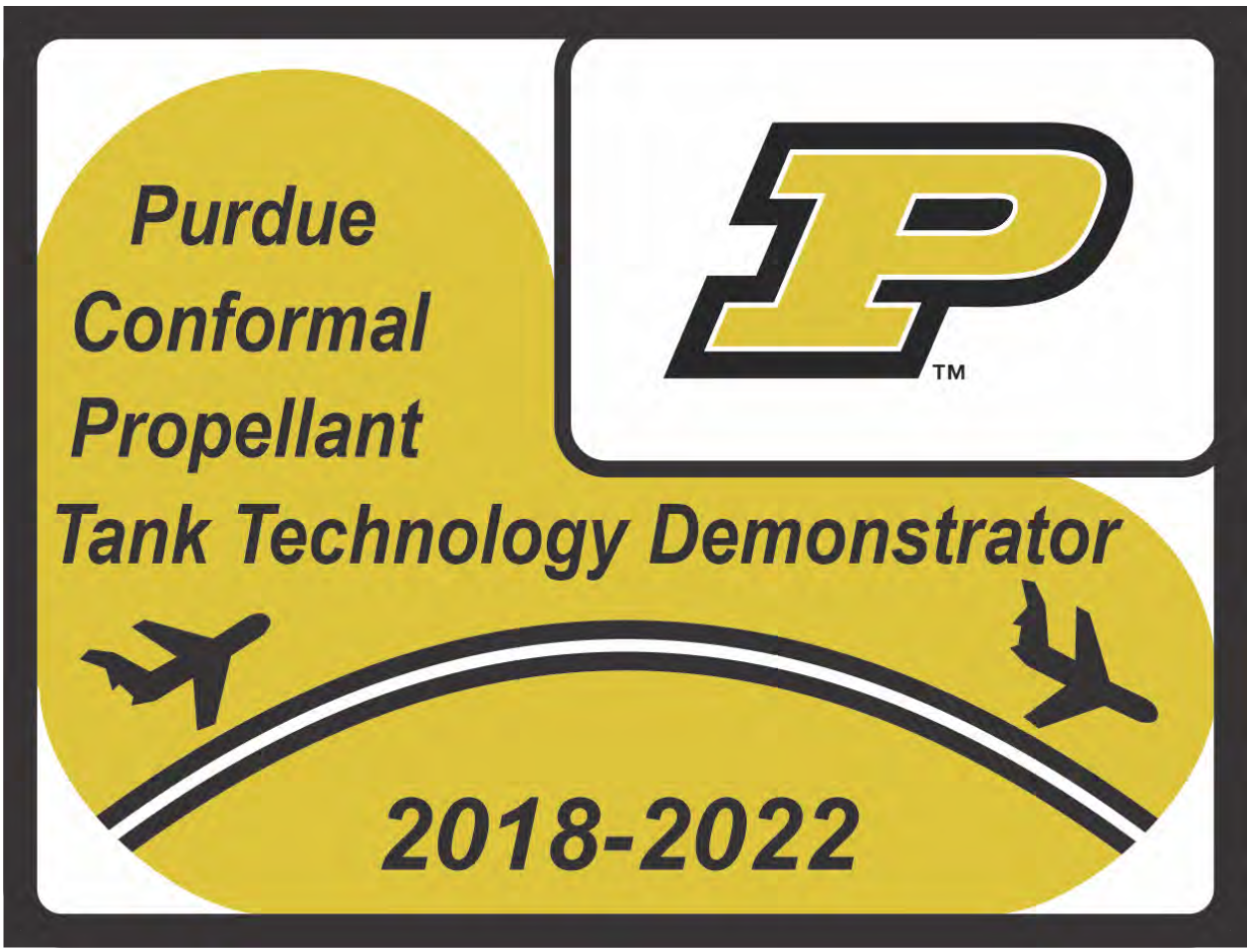

Figure G.1. Conformal Tanks Mission Patch

REFERENCES

[1] S. M. Dominick and J. R. Tegart, "Propellant management in toroidal tanks," eng, in *AIAA, SAE, ASME, and ASEE, Joint Propulsion Conference, 21st, Monterey, CA; United States; 8-10 July 1985*, 1985.

[2] D. Jaekle Jr., "Propellant management device conceptual design and analysis – vanes," *27th Joint Propulsion Conference*, 1991. [Online]. Available: https://doi.org/10.2514/6.1991-2172.

[3] D. Jaekle Jr., "Propellant management device conceptual design and analysis - traps and troughs," *31st Joint Propulsion Conference and Exhibit*, 1995. [Online]. Available: https://doi.org/10.2514/6.1995-2531.

[4] D. Jaekle Jr., "Propellant management device conceptual design and analysis – sponges," *29th Joint Propulsion Conference and Exhibit, Monterey*, 1993. [Online]. Available: https://doi.org/10.2514/6.1993-1970.

[5] D. Jaekle Jr., "Propellant management device conceptual design and analysis – galleries," *33rd Joint Propulsion Conference and Exhibit*, 1997. [Online]. Available: https://doi.org/10.2514/6.1997-2811.

[6] W. C. Reynolds and H. M. Satterlee, "Liquid propellant behavior at low and zero g," in *NASA/SP-106*, ch. 11. [Online]. Available: https://ntrs.nasa.gov/citations/19670006555.

[7] Zero Gravity Corporation, "Zero-g research payload user guide," 2021.

[8] Zero Gravity Corporation. (2022). "Zero-g research programs," [Online]. Available: https://www.gozerog.com/zero-g-research-programs/.